AD-A033 571 BENDIX RESEARCH LABS SOUTHFIELD MICH F/G 1/3
ACOUSTIC EMISSION INVESTIGATION - HELICOPTER ROTOR SYSTEM.(U)
NOV 76 R M RUSNAK, H C YEE, J K SEN DAAJ02-73-C-0066
UNCLASSIFIED RLD-7980 USAAMRDL-TR-76-11 NL

1 OF 2
AD A
033 571

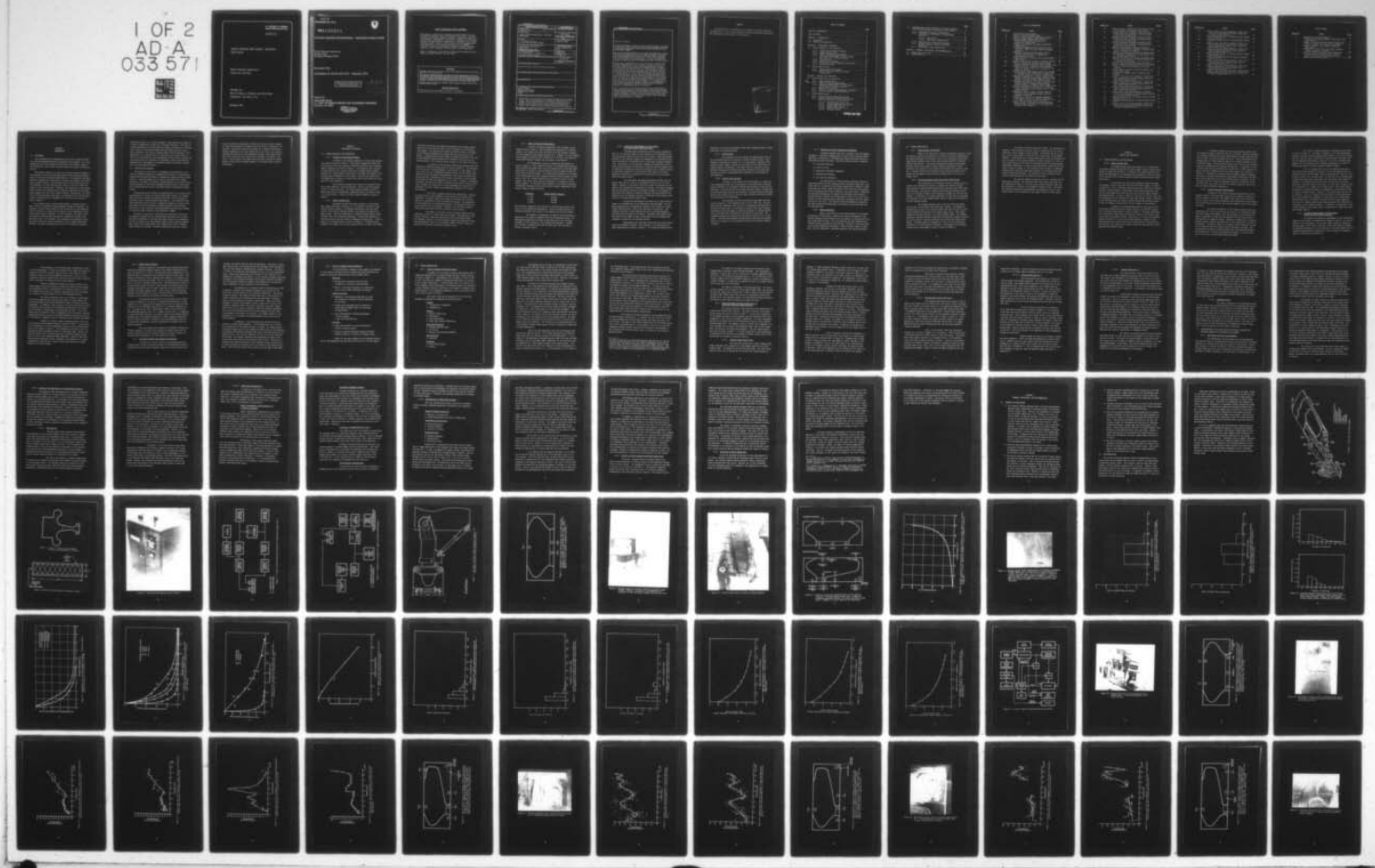

# ACOUSTIC EMISSION INVESTIGATION - HELICOPTER ROTOR SYSTEM

BENDIX RESEARCH LABORATORIES
SOUTHFIELD, MICHIGAN

PREPARED FOR
ARMY AIR MOBILITY RESEARCH AND DEVELOPMENT
LABORATORY, FORT EUSTIS, VA.

NOVEMBER 1976

USAAMRDL-TR-76-11



# ACOUSTIC EMISSION INVESTIGATION - HELICOPTER ROTOR SYSTEM

Bendix Research Laboratories
Bendix Center
Southfield, Michigan 48076

November 1976

Final Report for Period April 1973 - December 1975





Prepared for

EUSTIS DIRECTORATE
U. S. ARMY AIR MOBILITY RESEARCH AND DEVELOPMENT LABORATORY
Fort Eustis, Va. 23604

## EUSTIS DIRECTORATE POSITION STATEMENT

This report is considered to provide a possible solution to the problem of detecting cracks in helicopter rotor blades. The lack of sufficient testing, however, precludes a complete evaluation of the technique; consequently, the reader is cautioned to avoid overlooking the complexities of applying this technique as an on-board detection system. Results of this effort will be integrated with other R&D efforts at the Eustis Directorate and at AVSCOM to establish research and development programs to improve the applicability of this technique to future Army aircraft subsystems.

Roger J. Hunthausen of the Military Operations Technology Division served as project engineer for this effort.

UNCLASSIFIED
SECURITY CLASSIFICATION OF THIS PAGE (When Data Entered)

| REPORT DOCUMENTATION PAGE | | READ INSTRUCTIONS BEFORE COMPLETING FORM |
|---|---|---|
| 1. REPORT NUMBER<br>USAAMRDL-TR-76-11 | 2. GOVT ACCESSION NO. | 3. RECIPIENT'S CATALOG NUMBER |
| 4. TITLE (and Subtitle)<br>ACOUSTIC EMISSION INVESTIGATION - HELICOPTER ROTOR SYSTEM | | 5. TYPE OF REPORT & PERIOD COVERED<br>Final Report<br>April 1973 - December 1975<br>6. PERFORMING ORG. REPORT NUMBER<br>7980 |
| 7. AUTHOR(s)<br>R. M. Rusnak, H. C. Yee<br>J. K. Sen (Bell Helicopter Company) | | 8. CONTRACT OR GRANT NUMBER(s)<br>DAAJ02-73-C-0066 |
| 9. PERFORMING ORGANIZATION NAME AND ADDRESS<br>Bendix Research Laboratories<br>Bendix Center<br>Southfield, Michigan 48076 | | 10. PROGRAM ELEMENT, PROJECT, TASK AREA & WORK UNIT NUMBERS<br>62205A 1F162205A119 08<br>005 EK |
| 11. CONTROLLING OFFICE NAME AND ADDRESS<br>Eustis Directorate<br>U.S. Army Air Mobility R&D Laboratory<br>Fort Eustis, Virginia 23604 | | 12. REPORT DATE<br>November 1976<br>13. NUMBER OF PAGES<br>110 |
| 14. MONITORING AGENCY NAME & ADDRESS(if different from Controlling Office) | | 15. SECURITY CLASS. (of this report)<br>Unclassified<br>15a. DECLASSIFICATION/DOWNGRADING SCHEDULE |

16. DISTRIBUTION STATEMENT (of this Report)

Approved for public release; distribution unlimited

17. DISTRIBUTION STATEMENT (of the abstract entered in Block 20, if different from Report)

18. SUPPLEMENTARY NOTES

19. KEY WORDS (Continue on reverse side if necessary and identify by block number)

Acoustic emission
Helicopter rotor system
Nondestructive testing
Fatigue

20. ABSTRACT (Continue on reverse side if necessary and identify by block number)

An investigation was carried out to determine the feasibility of detecting fatigue crack initiation and growth in dynamically loaded helicopter rotor systems. This was accomplished by first conducting laboratory tests to determine fatigue emission characteristics, signal attenuation, ambient extraneous noise characteristics, and potential noise discrimination methods. The information procured from the laboratory tests was employed

DD FORM 1 JAN 73 1473 EDITION OF 1 NOV 65 IS OBSOLETE

UNCLASSIFIED
SECURITY CLASSIFICATION OF THIS PAGE (When Data Entered)

Block 20 - Continued

to design and assemble an acoustic emission monitoring system. The utility of this system in detecting fatigue crack initiation and growth was demonstrated during fatigue tests of full-scale blade sections carried out at Bell Helicopter Company.

The acoustic emission monitoring system included the capability of sequentially processing information from up to eight transducers. Three noise discrimination methods were built into the system: load cycle gating, rise-time discrimiation, and spatial gating. Only the rise-time method was used effectively in this investigation. The other two methods were limited by either the nature of the extraneous noise or the crack location.

Fatigue tests, to demonstrate the utility of the acoustic emission monitoring system, were carried out on outboard and inboard full-scale blade sections. Generally, the acoustic emission technique with rise-time discrimination provided an indication of impending failure as evidenced by an increase in the acoustic count rate. This increase in count rate occurred at from 50 to 80% of the fatigue life of the blade. However, in two tests the acoustic emission monitoring did not give an indication of impending failure. In one of these the rise-time discrimination was set at too high a value and crack emission as well as extraneous noise signals were rejected. This was not a serious problem in that resetting at a lower value for subsequent tests proved successful. In the second test, a 3.5-inch crack formed in the abrasion strip of the blade and was not detected by the acoustic emission equipment. It is assumed that the crack was not of sufficient severity to produce detectable emissions or that emission amplitude and activity was small because the crack was located in a non-loadbearing portion of the blade.

In all blade section tests the crack initiated in areas inaccessible for direct viewing and therefore crack growth could not be visually followed. Therefore, exact physical cause of the increase in acoustic activity which provided a warning of impending failure could not be ascertained. For this reason and because of the negative results obtained on one of the blade section tests, additional full-scale blade testing in which crack growth can be followed visually is recommended.

## PREFACE

The efforts of R. H. Thompson in the analysis of acoustic data and in suggestions for the acoustic emission monitoring system are appreciated, and contributed to the success of this project.

TABLE OF CONTENTS

## LIST OF ILLUSTRATIONS

LIST OF TABLES

# SECTION 1
# INTRODUCTION

## 1.1 BACKGROUND

This investigation was spawned by the need for an onboard system for detecting impending failure in helicopter rotor systems. As a step toward this end, this program was initiated in April 1973 to explore the feasibility of the acoustic emission method as a means of detecting failure.

The approach taken was to apply the acoustic emission technique to the detection of crack initiation and growth during laboratory fatigue tests of full-scale helicopter blade sections. To accomplish this, Bell Helicopter Company was subcontracted to provide the facility for fatigue tests on blade sections. Since fatigue tests of full-scale blades are very expensive, it would have been too costly to carry out these tests solely for this investigation. Therefore, the evaluation of the acoustic emission method was combined with the testing program for the Bell Helicopter Company 214A (HU-1 type system) program. Consequently, the schedule for this investigation was tied to the schedule for the 214A program. A sketch showing the basic components of a 214A type rotor system is given in Figure 1.

As a fatigue crack is initiated and grows, it produces elastic waves ("acoustic emissions") which propagate through the material. The detection of these elastic waves and the correlation of these emissions with the existence of cracks are the essence of the nondestructive test method called acoustic emission. In this technique, the elastic waves are generally detected with piezoelectric transducers coupled to the material or part to be examined. The transducers and band-pass filters are usually selected to detect emissions in the frequency range above 100 kHz. The higher frequencies are selected to eliminate extraneous

noise which tends to be of lower frequency. The initiation or growth of a crack is reflected by a high rate of acoustic emissions. This rate is usually quantified by counting either the number of emissions or the number of times the oscillating signal from the transducers goes above a given threshold. The acoustic emission method offers advantages in the application to an onboard system for detecting rotor system cracks in that it is very sensitive, can simultaneously scan the entire system, and can function while the helicopter is operating. Other crack detection methods such as radiography or ultrasonics would be difficult to implement in an operating helicopter.

## 1.2 OBJECTIVE AND APPROACH

The purpose of this work is to determine the feasibility of the acoustic emission technique as a nondestructive method for detecting fatigue crack initiation and growth in dynamically loaded helicopter blade sections. This information will be used to help answer the ultimate question as to whether the acoustic emission method can be used as an onboard instrument for detecting impending fatigue failures in helicopter rotor systems and thus serve to warn pilots before catastrophic failure occurs.

The approach used to assess the applicability of the acoustic emission method was to define the factors which might inhibit its intended function and then measure the potential influence of these factors in laboratory tests at Bendix Research Laboratories. The information from these laboratory tests was used to design and assemble an acoustic emission system for use on dynamically loaded helicopter blade sections. The utility of this system was then demonstrated during fatigue testing of full-scale blade sections at Bell Helicopter Company.

The basic factors which could limit the usefulness of the acoustic emission technique are (a) low-amplitude emissions from the crack, (b) severe attenuation of the emissions before they reach a transducer, and (c) the inability to discriminate between acoustic emission signals from cracks and the high ambient noise signals which exist in dynamically loaded rotor systems. Therefore, laboratory tests were carried

out to determine the amplitude of emissions from small fatigue samples of blade skin materials to establish the lower level of emissions to be expected. Attenuation tests were carried out on samples representing various components of the rotor system and on an actual rotor system to determine the severity of the attenuation problem. Noise monitoring of full-scale blade tests was carried out to establish the ambient noise level. The information from these tests was used to design an acoustic emission system which was deemed capable of overcoming these potential limitations.

## SECTION 2
## EXPERIMENTAL PROCEDURE

### 2.1 SYSTEM FEASIBILITY AND DEFINITION

#### 2.1.1 Fatigue and Attenuation Samples

A summary of the samples prepared for fatigue and attenuation testing is given in Table 1. The fatigue samples were made from two different rotor skin materials, 2024-T3 and S-Glass epoxy composite. Sample dimensions are shown in Figure 2. The dimensions were selected to coincide with those normally employed for bending fatigue samples. However, the rounded wings on each side of the sample were added to permit mounting of transducers on the sample. The hole was drilled into the sample body to serve as a stress riser which would provide the location for crack initiation.

The attenuation samples were selected to represent blade skin, blade composite, and grip materials. The skin and grip samples consist of single materials. The blade composite samples consist of blade skin materials sandwiching a honeycomb support as would be found in an actual blade. A sketch of these composite samples is given in Figure 3.

#### 2.1.2 Sample Fatigue Tests

Laboratory fatigue tests were carried out on the blade skin samples described in section 2.1.1 to determine the level of the acoustic emission signal, its frequency distribution, and the sensitivity of the acoustic emission method in detecting the formation of small cracks. Tests were performed on a Sonntag fatigue machine (model SF-01-U) under reverse bending conditions. The load was applied by a rotating eccentric and was constant throughout any given test. A photograph of the fatigue machine is given in Figure 4. Transducers were coupled to the sample with silicone grease and held in place with clamps.

A binocular microscope and lights were mounted on the fatigue machine table as an aid in the detection of crack formation and in following crack growth. The samples were tested at different loads to determine if the emission characteristics change with the stress level on the sample. A maximum bending stress range of 30,000 to 50,000 psi was used for the 2024-T3 aluminum samples and of 15,000 to 28,000 psi for the S-Glass samples. The loading rate was constant at 30 cycles per second.

A schematic of the acoustic emission monitoring system used during the laboratory fatigue tests is shown in Figure 5. The band-pass filters were set to accept signals in the 100 kHz to 2 MHz range. The lower limit was set to eliminate extraneous noise, and the rather broad band was selected to permit determination of the acoustic emission frequency spectrum. Transducers with resonant frequencies of 150 (D 140B) and 750 kHz (D 750B) were employed for all tests. Initially a broad-band transducer was used in an effort to obtain an undistorted frequency spectrum. However, the sensitivity of this transducer was found to be insufficient to detect fatigue crack emissions; therefore, its use was discontinued.

The acoustic emission activity was quantified by counting the oscillations of the transducer signal above the electronic noise background. An abrupt change in the acoustic emission count rate was taken as an indication of crack initiation and growth. The observation of crack growth with the microscope proved to be inaccurate because the crack tip could not be discerned. Therefore, no correlation between crack growth and acoustic emission acitivity could be made.

Recording of the actual acoustic emission signal was performed with a Sony (AV 3650) video tape recorder. The amplitude of the acoustic emission signal was measured from the oscilloscope screen. The frequency content of acoustic emission signal was determined by setting the band-pass filter to successively smaller frequency bands and measuring the decrease in acoustic emission counts.

### 2.1.3 Sample Attenuation Measurements

Acoustic attenuation measurements were performed on the samples listed in Table 1. The attenuation was measured for a 150-kHz signal on all samples since this was found to be the dominant frequency of crack emissions during sample fatigue tests. However, for some samples, several signal frequencies were measured up to 750 kHz to ascertain the relationship between frequency and the degree of attenuation.

The experimental setup for attenuation measurements is shown in Figure 6. This consists basically of a transmitting transducer which provides the signal which will be attenuated and a receiving transducer which is located at various distances from the signal source and detects the attenuated signal. The transmitting transducer is activated by the combination pulse and frequency generator, which provides a pulse train of $20 \times 10^{-3}$ seconds duration with a repetition rate of 10 per second. This pulse train causes the transducer to resonate at the desired frequency. To facilitate the attainment of the desired frequency, transmitting transducers were selected with resonant frequencies in the desired range as identified below.

| Transducer | Desired Signal Frequency |
|---|---|
| D 140B | 150 kHz |
| D 140B | 450 kHz |
| D 750B | 750 kHz |

The receiving transducers were selected to have the same resonant frequency as the transmitting transducers. Both the transmitting and receiving transducers were coupled to the samples with silicone grease.

The degree of attenuation was taken to be the decrease in amplitude of the signal as measured from the oscilloscope screen. The nonattenuated amplitude was taken as that detected by the receiving transducer located adjacent to the transmitting transducer. Signals were recorded on magnetic tape with the Sony video tape recorder to provide a permanent record.

### 2.1.4 Attenuation Measurements in Rotor Blades and Across Rotor System Interfaces

Although sample measurements provided basic attenuation data for the materials found in rotor systems, it was desirable to obtain attenuation data from the actual rotor system. These measurements provided a more realistic measure of attenuation to be expected in the rotor system since the materials were in the actual hardware configuration. In addition, it was desired to measure the attenuation across rotor system interfaces to determine if acoustic emission signals could be effectively transmitted across the interfaces and to permit location of detecting transducers in the hub area rather than on the blade. Therefore, attenuation measurements were performed on an actual Bell model 214A blade assembly.

The measurement and signal generating procedure was the same as that used for samples as described in section 2.1.3 of this report. However, in the case of the rotor system the frequency of the signal to be attenuated was maintained at 150 kHz. The single frequency was selected because this was the dominant frequency in the sample fatigue tests (as revealed by spectral analysis) and would therefore be expected to be the dominant frequency of emissions during fatigue crack growth in full-scale blade fatigue tests.

Attenuation measurements were made in the blade along its length at the midspan and at the leading and trailing edges. For all these measurements the transmitting transducer was located in a longitudinal position about 2 inches from the edge of the doubler. The transducer was kept in this position while the receiving transducer was moved down the length of the blade. Attenuation measurements were also made on the doubler portion of the blade, with the transmitting transducer located near the gripping fixture.

Measurements were also made across the rotor system interfaces and attachment hardware. The locations of the transducers for these measurements are shown in Figure 7. The interfaces measured were

blade/grip, across grip, grip/yoke, across yoke, blade/drag brace, across drag brace, and drag brace/grip.

### 2.1.5 Flaw Location

The potential for flaw location was demonstrated with the use of hardware which was developed to reject extraneous noise. This hardware is described in section 3.2.1 of this report. Basically this hardware rejects signals coming from one section of the blade while accepting signals from another. Thus flaws could be located by having different transducers monitoring different sections of the blade, and locating the flaw by identifying which transducers are receiving the flaw emissions.

### 2.1.6 Ambient Noise Analysis

A measure of the ambient noise environment in a blade section undergoing fatigue test was necessary to determine what techniques would be necessary to discriminate between the extraneous noise and flaw emissions. To accomplish this, the noise generated during a fatigue test of an outboard blade section was monitored. The monitoring was performed early in the fatigue test so that the noise recorded represented extraneous noise and not flaw emissions.

The transducer locations during the noise monitoring are shown in Figure 8. The transducers were of the D 104B type. The signals from the transducers were fed into a preamplifier and amplifier to provide the proper gain for recording on the Sony video tape recorder. Following the test the magnetic tapes were analyzed to provide information on the amplitude and frequency distribution of the noise. The frequency analysis was performed as described in section 2.1.2 of this report. The amplitude analysis was performed by measuring the acoustic counts as a function of the threshold setting on the acoustic emission totalizer.

### 2.1.7 Evaluation of Noise Suppression Techniques

Extraneous ambient noise was considered to be the biggest detriment to successful implementation of the acoustic emission method. Therefore, techniques for discriminating between extraneous noise and flaw emissions were evaluated. Five basic techniques were considered:

- electronic filtering
- window in noise
- gating with secondary transducers
- correlation techniques
- rise time discrimination

The applicability of these various techniques depends on the characteristics of the extraneous noise (frequency, amplitude, rise time), when it is emitted in the fatigue loading cycle relative to emissions from the cracks, signal distortion in the structure, and location of the extraneous noise source relative to the crack source. Therefore, the procedure employed was to examine the extraneous noise emissions recorded during a fatigue test as described in section 2.1.6 and to ascertain the most promising noise suppression techniques from the characteristics of the noise. The selected noise discrimination procedures were then evaluated experimentally to determine if they were effective in rejecting noise.

### 2.1.8 System Definition

Based on the results of the work described in the preceding sections of this report, a decision was made to determine if the acoustic emission method showed sufficient promise to continue with full-scale blade section tests. Once this decision was made affirmatively, the basic system requirements were defined. Foremost of these was selection of noise suppression techniques. Others included number of channels, type of transducers, recording intervals, and recording methods.

## 2.2 SYSTEM DEMONSTRATION

### 2.2.1 System Design and Assembly

Based on the definition of system requirements (section 2.1.8), the hardware required was selected and a method for overall integration of the system components was designed. Some of the components required were commercially available, while others were designed and built at Bendix Research Laboratories. All capital equipment procurement and hardware building efforts were funded by Bendix Research Laboratories (BRL). Integration and checkout of the system was performed under contract funding. A system checkout was performed at BRL following assembly of the system and then again at Bell Helicopter Company prior to its use on fatigue tests.

### 2.2.2 System Evaluation During Full-Scale Fatigue Tests

The feasibility of the acoustic emission technique for detecting crack formation and growth in dynamically loaded helicopter rotor systems was demonstrated during fatigue testing of Bell model 214A blade sections. The acoustic emission monitoring was performed according to the schedule defined by Bell Helicopter Company for the 214A test program. In addition, the loading conditions for each test were defined by the needs of the 214A program rather than for purposes of testing the acoustic emission system.

The fatigue machines used to test the full-scale blade sections were custom made at Bell Helicopter Company. One machine is hydraulically actuated (for outboard blade tests) and the other is actuated by mechanical eccentrics (for inboard blade tests). Both permit loading of the blade section in the three separate modes. The loading duplicates loading conditions experienced by helicopter blades in service and can be varied to provide conditions more severe than normal level flight. The blade sample is fatigued at a rate of 5.4 cycles/second (inboard) or 10 cycles/second (outboard). A photograph of the fatigue machine with a blade sample in place is shown in Figure 9.

Two types of blade sections were tested: an inboard and an outboard. These sections are about 9 feet in length and are cut from a blade with a total length of about 20 feet. The inboard section is that part of the blade adjacent to the hub and is tested with the attachment hardware. A photograph of an inboard blade section with the gripping fixture as inserted in the fatigue machine is shown in Figure 10. The outboard blade section is that part of the blade located at the approximate longitudinal midsection. A sketch of the inboard and outboard blade sections is given in Figure 11. The doubler sections consist of laminated aluminum sheet, while the blade body consists of an aluminum sheet supported by aluminum honeycomb. The position at which transducers were located during testing are also shown on this sketch.

The acoustic emission system was tested on outboard and inboard blade sections. The conditions under which these tests were run are summarized in Table 2. For each test, acoustic emission count rate was recorded as a function of the number of fatigue cycles. The acoustic emission monitoring system employed was developed as part of this project effort and is described in the results section of this report.

# SECTION 3
# RESULTS AND DISCUSSION

## 3.1 SYSTEM FEASIBILITY AND DEFINITION

### 3.1.1 Sample Fatigue Tests

The sample fatigue tests were carried out to determine if the acoustic emission method was sensitive enough to detect fatigue crack growth in blade skin materials. In addition, the characteristics (frequency and amplitude) of the emissions were determined to provide a basis for the design of the acoustic emission system for monitoring full-scale blade tests.

It was found that the acoustic emission method was sensitive enough to detect very fine cracks in the fatigue sample. As shown in Figure 12, a plot of acoustic emission counts as a function of fatigue cycles is characterized by a sharp rise in the acoustic emission count. The test was stopped after this rise was noted and the sample examined metallographically. As seen in Figure 13, the rise in acoustic count rate was associated with the formation of very small fatigue cracks. Therefore, it was concluded that the acoustic emission method had sufficient sensitivity for fatigue crack detection in rotor blades of like material.

A summary of the maximum amplitudes of the acoustic emission signals emanating from the fatigue cracks in the 2024-T3 aluminum and the S-Glass epoxy samples is given in Table 3. The pulse amplitudes were considerably higher than the electronic noise in the acoustic emission system, with signal-to-noise ratios from 7.5 to 19 for the aluminum samples and from 3.1 to 13 for the S-Glass samples. Signals of this amplitude should be readily detected in fatigue tests on full-scale systems provided that they are not severely attenuated and that they can be separated from ambient noise.

A frequency analysis of the crack emissions revealed that the dominant frequency range was from 100 to 300 kHz. Several representative frequency distributions taken under different fatigue loads and number of cycles are shown in Figures 14 and 15. These distributions were obtained with a D 140B transducer which has a resonant frequency in the 100-300 kHz range. There was some question as to how much the transducer itself was influencing the frequency distribution. A comparison of the frequency distribution obtained with a D 140B and a D 750B (resonant frequency ∿740 kHz) transducer during the same fatigue test is shown in Figure 16. Although the transducer with the higher resonant frequency did bias the frequency distribution toward higher frequencies, the major part of the signal was in the 100 to 300 kHz range. Therefore, it was concluded that the D 140B type transducer would be the best for use in the full-scale rotor tests, in that its resonant frequency lies in the band of expected emission frequencies.

### 3.1.2 Sample Attenuation Measurements

A summary of the sample attenuation measurements is presented in Table 4 and attenuation curves for the composite samples are given in Figures 17 and 18. The summary table shows that attenuation is very severe in the composite samples, with progressively less attenuation in the S-Glass sheet, the 7075 aluminum samples, and the 2024 aluminum sheet.

The severe attenuation in the composite samples which are representative of the blade body was attributed to the honeycomb attachment which dampens the signal. This was reflected by the fact that the signal transmission through the skin samples alone was more efficient than through the composite samples. Therefore, transmission of acoustic emission signals through the blade body is the limiting path in terms of attenuation. As shown in Figure 17, composite signal dampening is least in the composite mode with S-Glass skin and aluminum honeycomb. The attenuations in composites having aluminum skin with aluminum honeycomb and aluminum skin with nomex honeycomb are comparable to or lower than that of the S-Glass skin/aluminum honeycomb sample.

The effect of signal frequency on transmission efficiency is shown in Figure 18. The degree of damping in the aluminum/aluminum composite increases with increasing signal frequency from 110 to 750 kHz. The facts that the higher frequencies are more severely attenuated and that the emissions from fatigue cracks are in the 100 to 300 kHz range suggest that the transducers with resonant frequencies in the 100 to 300 kHz range should be used to optimize signal strength.

If it is assumed that the ratio of signal-to-electronic noise from fatigue emissions is about 10 to 1 as was measured with the fatigue samples, then the signal would be completely lost when it is attenuated to 10% of its original value. In the case of the aluminum skin/aluminum honeycomb sample (represents 214A type blade), the signal (if assumed to be 150 kHz) would be lost about 5 inches from the source. Therefore, transducer spacing would have to be less than 5 inches to prevent nondetection of a signal from a crack source. This would require an apparently prohibitive number of transducers on the helicopter blade to monitor the entire blade. However, in the actual blade this may not be required. First it is expected that much better sound transmission will occur through other components of the blade (e.g., leading edge, trailing edge, spar, and doubler sections) and that these components will serve to transmit emission much greater distance than indicated by attenuation in the composite samples. In addition, the amplitude of the acoustic emission from fatigue cracks in blades may be larger than those from fatigue samples.

### 3.1.3 Attenuation Measurements in Rotor Blades and Across Rotor System Interfaces

The results of attenuation measurements of 150 kHz acoustic pulses in rotor blades are summarized in Figures 19 and 20. As shown in Figure 19, the attenuation of an acoustic signal along the leading and trailing edges of the blade is much less severe than along the midspan. The midspan measurements are on the portion of the blade supported by the aluminum honeycomb and are comparable to those obtained for composite samples as described in section 3.1.2.

The attenuation in the leading edge is comparable to that in the trailing edge. In these two sections of the blade, the signal is reduced to 10% of its original value at about 5 feet from the source. Therefore, based on an initial signal-to-noise ratio of 10 to 1, the transducers could be located about 5 feet from the crack source and still detect the signal if cracking occurs in these regions.

Acoustic transmission through the doubler section of the blade (Figure 20) was also found to be much more efficient than through the honeycombed section. Attenuation of the acoustic signal to 10% of its original value occurs at a distance exceeding four feet as compared to a distance of about one-half foot in the honeycombed section.

The lower attenuation values in the doubler, leading edge, and trailing edge sections indicate that failure in these regions can be detected without requiring a prohibitive number of acoustic emission transducers. In addition, these portions of the blade can serve to transmit emission from failures in the honeycomb sections which are located near the doubler, leading edge or trailing edge sections. It was concluded that for purposes of this investigation that the acoustic emission transducers would be located on the high transmission efficiency portions of the blades to maximize chances of detecting crack formation and growth.

A summary of acoustic signal attenuation across rotor system interfaces and attachment hardware is given in Table 5. The location of the transducers for these measurements was given in the procedure section of this report in Figure 7. The transmission efficiency across the yoke and the drag brace/grip interface is relatively good. However, attenuation across other interfaces and other attachment hardware varies from 6 to 34% of the transmitted signal amplitude. Based on these relatively severe attenuation values it appears to be impractical to locate transducers in the hub area to detect cracks which occur in the blade section of the rotor system.

### 3.1.4 Ambient Noise Analysis

Frequency analysis of the ambient noise obtained from three transducers during the fatigue testing of an outboard blade section are given in Figures 21, 22 and 23. The locations of the transducers on the blade are shown in Figure 8 of the procedure section of this report. The frequency distribution varies somewhat from transducer to transducer, but all basically show the same thing. That is, the bulk of the noise signal lies in the 100 to 300 kHz frequency band. The extraneous noise which is present during fatigue testing of blade sections has basically the same frequency spectrum as that of acoustic emission from crack emissions (as obtained from sample fatigue tests). These results indicate, then, that band-pass filtering would not be an effective method for discriminating between acoustic emissions and ambient extraneous noise.

The amplitude distribution of the extraneous noise signal is shown in Figures 24, 25 and 26. The amplitude distribution in these figures is not the maximum pulse amplitude but rather the amplitude distribution for the individual oscillations of the acoustic emission signal. The figures show that a large number ($\sim$20%) of the oscillations have amplitudes greater than 10 to 1 signal-to-noise ratio. A comparison of these amplitudes found for the acoustic emission from fatigue samples indicates that the background noise has at least comparable amplitude to that of acoustic emissions. Therefore, noise discrimination could not be effectively implemented by merely adjusting the threshold level for signal acceptance.

The noise signals were examined to determine if there were periodic windows of low noise level during the loading cycle such that acoustic emissions could be recorded during this interval without extraneous noise interference. No such windows were found.

### 3.1.5 Selection of Noise Discrimination Techniques

A review of the results given in the preceding sections indicated that the most promising techniques for discrimination between extraneous noise and acoustic emission signals were spatial gating with

secondary transducers and rise time discrimination. Electronic or band-pass filtering was not selected because the extraneous noise appeared to have the same frequency distribution as acoustic emissions. The lack of a "window" in the ambient noise prevented the use of a cycle gating technique. Correlation techniques were reviewed but were found to be too complicated to implement and subject to error because of signal distortion. Adjustment of the threshold setting on the acoustic emission instrumentation was rejected because the ambient noise appeared to have amplitude levels comparable to those produced by crack emissions.

The gating out of extraneous noise by determining the time of arrival at primary and secondary transducers was selected as the method with the most potential for successful application. This method is spatial gating. The region in which cracks are to form contains the primary transducer and is separated from the region where extraneous noise is being generated by secondary transducers. Signal processing equipment is used in this method to reject signals which arrive at the secondary transducer before the primary transducer and accept signals which arrive at the primary transducer before the secondary transducer. In this way the emissions from the crack are accepted and those from the extraneous noise source are rejected. The primary drawback to the technique is if the fatigue crack and extraneous noise source are in close proximity.

In addition, a rise time method was selected as having potential for noise discrimination. In this method the rate of rise of the voltage level of the acoustic signal is sensed. All signals below a selected voltage rise rate are rejected and those above it are accepted. This assumes that acoustic emissions have faster rise times than does extraneous noise. This would be expected to be the case in the helicopter rotor blade. The sensing transducer would generally be located closer to the crack source than to the extraneous noise source. Therefore, extraneous noise would be expected to have undergone greater distortion as it travels through the structure prior to arriving at the sensing transducer. This distortion would tend to reduce the rise time of the signal.

### 3.1.6 Acoustic Emission System Definition

The following basic components were judged to be required for the acoustic emission system for monitoring crack initiation and growth in helicopter blade sections during fatigue tests:

Detection

- Piezoelectric transducers with resonant frequencies in the 100 to 300 kHz range
- Method of attaching transducers to blade which will be secure under vibrations encountered

Signal Processing

- Capability of processing signal from at least five transducers located at various positions on the blade
- Preamplifiers and amplifiers as required to obtain desired signal levels for recording and quantifying
- Noise discrimination processing equipment
  - Spatial gating
  - Rise time discrimination

Recording

- Video tape recorder to provide recording of acoustic emission signals
- Printer to provide hard-copy record of acoustic emission counts as a function of fatigue cycles

Details of the exact design of the system and description of the components used are given in Section 3.2.1 of this report.

## 3.2 SYSTEM DEMONSTRATION

### 3.2.1 Acoustic Emission Monitoring System

A schematic of the acoustic emission system which was designed and assembled for use during fatigue testing of blade sections is shown in Figure 27. A photograph of the equipment is shown in Figure 28. The system is capable of monitoring sequentially the outputs of up to eight transducers. It provides hard copy of the data in the form of magnetic tape recordings of the emission signals and printout of acoustic emission counts as a function of the number of fatigue cycles. Identification of the individual components of the system and the function of each is given in Table 6.

The entire system may be divided into five functional groupings containing the components as indicated below.

Sensing

- Piezoelectric transducers
- Preamplifiers

Control

- Digital control unit
- Multiplexer
- Load synchronizer
- Video tape recorder (VTR) drive

Noise Discrimination

- Voltage controlled gate
- M-S gating
- Envelope rise-time discriminator

Quantification

- Totalizer

Recording

- Video tape recorder
- Printer

The sensing section consists of transducers of the D 140B or D 450B type (D 450B were found to perform like D 140B transducers). The transducers were bonded to the blade section with Eastman 910 adhesive. The preamplifiers were commercially purchased and are Dunegan model 801 P, which provides for signal amplification in the 100 kHz to 2 MHz frequency range with a total gain of 40 dB. Generally, five transducers were employed on each blade section fatigue test.

The heart of the control system is the digital control unit (DCU). As the name implies, the DCU controls the operation of the acoustic emission monitoring system. It dictates the operating sequence for the transducers, the selection of the noise discrimination technique, the time intervals between data collection, the duration of the data collection intervals, and data transfer functions. The time interval between data collections could be varied from 1 min to 99 min, while the duration of the data collection intervals could be varied from 1 sec to 99 sec. The multiplexer is the interface between the signals from the transducer (via the preamplifiers) and the signal processing equipment. It steers the signals sequentially to the processing equipment. The load synchronizer consists of a magnetic pickup and amplifier which provides a signal to the digital control unit and which permits the DCU to synchronize with the loading cycles of the fatigue machine. The gates in the system are controlled by the DCU and are used to control which signal enters the totalizer. The VTR drive is an electromechanical device designed by Bendix which permits the DCU to operate the video tape recorder mechanically.

Three noise discrimination units were incorporated into the acoustic emission system. The voltage controlled gate permitted signal monitoring on selected portions of the loading cycle. It consisted of a Dunegan/Endevco voltage-controlled gate (with some BRL modifications) and a strain gage signal conditioner so that the gate could be interfaced with strain gages attached to the blade section. This unit was not used during the tests conducted in this investigation because, as discussed in Section 3.1.4, there appeared to be no window in

the extraneous noise. It was incorporated into the system to provide this capability should future tests on the rotor system show more periodic extraneous noise variation.

The spatial gating or spatial discrimination was used to accept signals from the portion of the blade where crack initiation was expected and to reject signals emanating from extraneous noise sources. As discussed in Section 3.1.5, the method is based on the time of arrival of signals at primary and secondary transducers. For this system the unit was set up to operate with one primary and two secondary transducers. The primary transducer was located at the leading edge of the blade section approximately at the longitudinal center. The secondary transducers were located on the leading edge between the primary transducer and the ends of the blade. This arrangement was employed since most of the extraneous noise was generated in the fatigue machine and interfacing fixture and thus transmitted through the blade section ends.* The hardware for the spatial gating consisted of two Dunegan/Endevco model 902 flaw locator units (BRL modified) integrated with a processing unit designed and built by Bendix Research Laboratories.

The envelope rise-time discriminator was designed and built by Bendix Research Laboratories. It measures the rise time of the acoustic pulse envelope and rejects pulses having rise times less than a selected value. The range of rise times covered with this instrument varies from 0 to 10 volts/millisecond. As discussed in Section 3.1.5, the discrimination between acoustic emissions and extraneous noise depends on the extraneous noise pulses having slower rise times than the acoustic emission pulses.

---

*It would be expected in an operating aircraft that most of the extraneous noise would be generated at the inboard attachment fixture and at the hub area. Therefore, extraneous noise transmission into the blade would be similar to that occurring during blade fatigue testing. However, it is not known how noise generated by the transmission and rotor in an aircraft compares with that generated by the fatigue machine.

The quantity of acoustic emissions was determined with a Dunegan/Endevco totalizer model 301 (BRL modified). This instrument is basically a counter with a 1-volt threshold and includes amplifiers which provide up to 60 dB gain and band-pass filters. The oscillations of the acoustic signals above the threshold voltage are counted and displayed on a digital readout. In addition, the counts are fed to the digital control unit so that they can be recorded.

Two types of recordings of the data were made. The actual acoustic signals were recorded on a Sony model AV-3650 video tape recorder. The acoustic counts were recorded with a printer (Hewlett-Packard digital recorder, model 5055A) which also printed out information denoting the fatigue cycle, the transducer number, the discrimination method employed, and whether a video tape recording of the signal was made.

### 3.2.2 System Evaluation During Fatigue Tests of Full-Scale Helicopter Blade Sections

The acoustic emission monitoring system was demonstrated on outboard and inboard blade sections. The exact locations of the transducers during each test are given in Table 7. In all cases transducer 1 is the primary transducer in the spatial noise discrimination mode while transducers 2 and 3 are the secondary transducers. All three transducers operate in the normal mode and rise-time mode as well as in the spatial discrimination mode. For example, acoustic activity from transducer 1 is first recorded for the spatial discrimination mode, then for the normal mode, and then with rise-time discrimination. The test conditions for each test are given in Table 2. The basic objective of this testing was to determine if the initiation and growth of fatigue cracks could be correlated with an increase in acoustic activity.

#### 3.2.2.1 Outboard Blade Section Test

This test was carried out at 230% of normal level flight load with three transducers on the leading edge and two on the trailing edge. The sample failed after 853,500 cycles. The crack originated at a burr on the tooling tab of the spar 18.5 inches inboard of

midspan. It then progressed through the upper blade skin, the spar, and the leading edge abrasion strip. A secondary crack was found 2.5 inches inboard of midspan in the center of the spar's upper aft edge at a pit 0.003-inch deep. The location of the cracks relative to transducer location is shown in the sketch of Figure 29. The appearance of the crack is shown in the photograph of Figure 30. No cracking was observed prior to failure of the specimen.

Because the crack was located closer to the secondary transducer than it was to the primary transducer, spatial noise discrimination rejected acoustic emission noise from the crack as well as extraneous noise. Therefore this technique was not effective and only rise-time noise discrimination was useful during this test. A plot of acoustic count rate (with rise-time discrimination) for transducer 2, which was located nearest the crack, is shown in Figure 31. A sudden rise in the count rate is observed at about 450,000 cycles. This rise in acoustic activity is also seen in the output from transducer 1 (Figure 32), which is the next closest to the crack. Unfortunately, crack initiation and growth were not detected visually prior to failure because the cracks initiated and propagated internally during most of the blade life. Therefore, correlation cannot be established with the acoustic count rate. However, the sudden rise in acoustic activity at 450,000 cycles is interpreted to represent crack formation and the continuing rise to represent crack growth. Therefore, an indication of impending failure appears to occur at about 50% of the fatigue life of the blade section.

A plot of acoustic activity from transducer 4, which is located on the trailing edge of the blade at a location most removed from the crack, is shown in Figure 33. Although there is high acoustic activity at about the same number of cycles (450,000) as was found for transducers 1 and 2, this high level is not sustained and, in fact, the acoustic activity becomes relatively low toward the end of the test. Since this transducer was far removed from the crack, it is not surprising that it would not track the fatigue crack growth;

therefore, it is not certain that the high activity at 450,000 to 500,000 cycles is associated with fatigue crack formation.

The acoustic activity from transducer 2 without rise-time discrimination is shown in Figure 34. This does show a jump in acoustic activity at 500,000 cycles, but this level of activity decreases with increased cycles until just prior to failure, where a sharp rise in activity is noted. In a comparison of the output of this transducer with and without rise-time discrimination, the most striking difference appears to be the disappearance of the steady rise in acoustic activity from 450,000 cycles to failure when rise-time discrimination was not employed.

#### 3.2.2.2 Inboard Blade Section Test No. 1

This inboard blade section was loaded at 150% of normal level flight load and failed after 1.87 million cycles of fatigue. The crack formed on the bottom surface of the blade and originated at the edge of the grip plate (about 50 inches from rotor system center line). It propagated toward the trailing edge about 5 inches before being detected. The crack location relative to the transducer location is shown in Figure 35. A photograph of the crack is shown in Figure 36. Since the crack originated outside the signal acceptance region for spatial gating, this noise discrimination technique was not able to be implemented and the rise-time technique was the sole noise discrimination technique employed.

A plot of the acoustic count rate during the fatigue test is shown in Figure 37 for transducer 1 (with rise-time discrimination), which was located closest to the crack source. This graph shows high acoustic activity in two regions from 0.4 to 0.8 million cycles and from 1.3 million cycles to failure. Since the crack growth could not be followed visually, the physical meaning of these two high-activity areas is not clear. One or both could be associated with the fatigue of the sample. Similar results are shown in Figure 38 for the

signal from transducer 5 (with rise-time discrimination), which, although located on the trailing edge, is reasonably close to the crack.

3.2.2.3 Inboard Blade Test No. 2

This blade section was tested at a loading of 175% of normal level-flight conditions. The specimen failed after 2.2 million cycles. The fatigue crack originated on the grip plate at the retention bolt hole. This crack progressed to the leading edge and through to the spar before being visually detected. The crack location relative to the transducer position is shown in a sketch in Figure 39. The appearance of the crack is shown in the photograph of Figure 40. Because of the crack location, the spatial discrimination mode rejected signals from the crack as well as extraneous noise. Therefore, the rise-time technique was the only noise discrimination method effective during this test.

A plot of acoustic activity from transducer 2 (with rise-time discrimination) is shown in Figure 41. The gap shown in the data plot was the result of faulty cables, which were repaired during the test. This transducer was located closest to the crack source. A definite rise in acoustic activity is noted at about 1.7 million cycles, which is interpreted to represent crack formation and growth. Visual observation of the crack was not made until failure occurred. The indication of failure by acoustic activity occurs at about 80% of the blade section life. There is some drop-off of acoustic activity near the end of the test. This is attributed to the completion of crack propagation through the grip plate.

Similar trends are noted in the acoustic activity plot from transducer 1 (with rise-time discrimination) as shown in Figure 42. However, this plot more clearly shows an indication of crack formation at 1.7 million cycles with a sharp rise in acoustic counts than did that of transducer 2. This is because less data was lost from this transducer because its cable was repaired sooner than that of transducer 2.

### 3.2.2.4 Inboard Blade Test No. 3

The inboard blade section was loaded at 175% of normal level flight conditions and failed after 4.7 million cycles. The fatigue crack initiated on the underside of the blade in the abrasive strip under the first doubler and propagated into the first doubler. The crack was approximately 3.5 inches long and propagated perpendicular to the longitudinal axis of the blade. It was located relatively close to transducer 1, as shown in Figure 43. A photograph of the fatigue crack is shown in Figure 44.

Indications of impending failure should have been evident in outputs from transducers 1 and 3, which were located closest to the crack. Plots of acoustic activity from these transducers (with rise-time discrimination) are shown in Figures 45 and 46. (The lack of data prior to one million cycles is because the acoustic emission monitoring system had been hooked up to a different blade test when this test was initiated and subsequently transferred to this test after one million cycles had been accumulated.) These results show no indication of impending failure. The sudden rise in acoustic activity at 4.3 million cycles is attributed to a failure in one of the machine components. A plot of the acoustic activity as processed through spatial gating is shown in Figure 47. (The lack of data between 1 and 1.5 million cycles is because transducer 2 had a bad coupling to the blade during this portion of the test and this transducer is required for spatial gating.) This plot also gives no indications of impending failure.

The lack of correlation between acoustic activity and blade failure for this test may be attributable to the size or location of the crack. The crack was located primarily in the steel abrasion strip (only 0.2 in. length in doubler) which is designed to be a non-load bearing member of the blade. The acoustic emissions from crack propagation in this portion of the blade may not be as strong or as copious as from sections designed for load bearing.

The extent of crack propagation was somewhat less than in the preceding tests in which acoustic activity did rise prior to failure. This implies that there may be a threshold of crack severity required before detection with the acoustic emission system can be made under these conditions. Although much finer cracks were detected by acoustic emission in the sample fatigue test, the high ambient noise level of the blade tests did not exist during these tests. Consequently, extraneous noise may be masking the emissions from fine cracks in the blade tests. Although the noise discrimination techniques do dramatically reduce extraneous noise, neither the spatial gating or rise-time methods can be assumed to be 100% efficient.

#### 3.2.2.5 Additional Tests

The results presented in the preceding sections for four blade tests provide the basic data for evaluating the acoustic emission method. However, in the course of this investigation, additional tests of full-scale blade sections were carried out which did not yield reasonable data for evaluating the acoustic emission method. This was because either (1) the test was carried out for another function (e.g., noise monitoring), (2) the sample did not fail, or (3) technical difficulties prevented the procurement of data. All tests conducted as part of this investigation are summarized in Table 8 along with a brief description of the outcome of each test.

## 3.3 CONSIDERATIONS IN THE APPLICATION OF ACOUSTIC EMISSION FLAW DETECTION METHODS TO HELICOPTER ROTOR SYSTEMS

### 3.3.1 Conclusions From This Investigation

The experimental results obtained in this investigation have answered some of the questions relating to the potential of acoustic emission as an onboard flaw detection concept for helicopters. The primary question, of course, is whether or not the formation and growth of fatigue cracks generate acoustic emissions with sufficient intensity and amplitude to permit detection of the crack prior to blade failure. In

this investigation, most fatigue failures were preceded by an increase in acoustic count rate at 50 to 80% of the fatigue life which provided a warning of impending failures. However, the test in which a 3.5-inch crack formed in the abrasive strip without yielding an increase in the acoustic count rate suggests that additional laboratory fatigue tests on full-scale blade sections are needed to verify the consistency of the results. In addition, because crack growth could not be followed visually in these tests it could not be correlated directly with acoustic activity. This suggests that tests should be conducted in which the crack growth can be monitored by an independent method so that correlation between acoustic activity and growth can be made.

Even though a fatigue crack may be emitting readily detectable acoustic signals in its vicinity, detection by the acoustic emission technique is limited if the acoustic signal is heavily attenuated as it eminates from the crack. The attenuation measurements performed in this work do show that the honeycomb in the blade body does severely attenuate an acoustic signal in the blade skin. This attenuation limits the useful detection range to about 5 inches. This would seem to require a prohibitively large number of transducers to monitor a full size blade. However, the acoustic signal was found to be much less severely attenuated in the doubler, spar, leading edge and trailing edge of the blade. The detectability in these regions is about 5 feet. Consequently, failures which occur in these sections of the blade may be detected without requiring an extremely large number of transducers. Since failure in one of the low attenuation portions of the blade is more likely than in the honeycomb and since these members can serve as sound transmission paths from high attenuation regions, it appears that the high attenuation in the honeycomb section of the blade would not limit the usefulness of the acoustic emission technique.

The attenuation in the blade and across rotor system interfaces does however limit system design. That is, transducers cannot be located in the hub area and still detect failures in the blade. Rather, transducers must be located relatively near (5 feet) the point of failure.

### 3.3.2 Potential for Application in an Operating Helicopter

The purpose of this investigation is to provide information which will help to answer the ultimate question as to whether or not the acoustic emission method can be used as a rotor system flaw detection method on an operating helicopter. As discussed in the preceding section, the experimental work during laboratory fatigue tests does indicate that the acoustic emission method provides a warning of impending failure and that fatigue crack emissions are detectable. However, because of some of the negative results obtained in the testing, it is recommended that additional laboratory tests be carried out to clearly establish the reliability with which fatigue cracks can be detected in this environment prior to testing on an aircraft. Assuming that additional laboratory testing does establish the reliability of the acoustic emission method in this environment, then the potential for application to the operating helicopter is good.

#### 3.3.2.1 Main Factors

The main factors which influence detectability are attenuation of the acoustic signal in the rotor structure, fatigue crack size and location, and extraneous noise level. The laboratory tests have established that, although attenuation does offer an impediment to successful crack detection, it is not prohibitive; proper transducer placement should insure signal detection. The attenuation measurements made in this work are directly translatable to the operating rotor system since these measurements were made on actual hardware. Therefore, attenuation should not be an insurmountable problem in applying the acoustic emission method to an operating rotor system.

The nature and location of fatigue cracks would be expected to be similar in operating rotor systems to that encountered in the laboratory tests. The laboratory tests were conducted on full-scale blade sections and under loads which match the actual operating environment. Therefore, laboratory test results should be directly

translatable to the operating system with respect to this factor. However, laboratory tests completed in this work did bias the failure toward the extremities of the blade sections. Therefore, additional laboratory tests in which fatigue cracks are induced into other sections of the blade should be performed to clearly establish the range of fatigue crack types and locations which may be encountered in the operating rotor system. Once these tests have been carried out, the crack size and location factor should not be of concern in applying the acoustic emission technique to an actual operating system.

The one factor which is not directly translatable between the laboratory tests and an actual operating system is that of extraneous noise. Although the extraneous noise level during laboratory fatigue tests of blade sections is quite high, it is not known whether or not the noise environment in an actual operating system would be greater or less than this. Therefore it is not known at this stage whether or not the noise environment of the operating system could limit the usefulness of the acoustic emission techniques. However, it is likely that the noise discrimination techniques used in the laboratory tests would be successful in reducing the extraneous noise level existing in the operating system. The potential problems with extraneous noise in an operating system cannot be fully evaluated until noise monitoring tests are carried out on an operating system.

In summary: Of the three major factors determining the usefulness of the acoustic emission technique, two of them (attenuation, and crack size and location) can be reasonably evaluated in laboratory tests and should not offer a serious impediment to successful application in an operating system. The third (extraneous noise) is not directly translatable from laboratory tests to the operating system. However, the technique for noise discrimination used in the severe noise environment of the laboratory tests should be applicable in the actual operating system.

### 3.3.2.2 Additional Considerations

In addition to the major factors discussed above, there are several other considerations or problems to be solved before the acoustic emission method can be applied to an operating system. These are: (a) signal transmission from transducer to processing equipment, (b) transducer attachment methods, (c) prediction of remaining useful life, and (d) environmental considerations.

#### Signal Transmission From Transducers to Processing Equipment

Signal transmission considerations are required in two areas, within the rotor system and from the rotor system to stationary equipment. The preamplifier should be located within about 10 feet of the transducer cable to avoid signal loss in the cable. This could require mounting of the preamplifier on the rotating system. If this is the case, the preamplifier would have to be tested and perhaps redesigned in order to ensure that it would withstand the rigors of operation in the rotating environment. Recent work in the acoustic emission field, however, has advanced the state of the art so that it may be possible to increase the 10-foot cable distance so that preamplifiers could be mounted in the stationary part of the system.

Transmission of the acoustic emission signal from the rotating system to stationary signal processing equipment could pose some problems. Strain gage signals of the same magnitude as acoustic emission signals have been successfully transmitted from the rotating section through slip rings by Bell Helicopter Company. However, these signals are of considerably lower frequency than the hundreds of kilohertz encountered in acoustic emissions. Therefore, the impedance offered by slip rings could be prohibitive. It is anticipated that special techniques will have to be developed to reduce attenuation and provide a distortion-free signal.

## Transducer Attachment Methods

Although procedures for attaching transducers to the helicopter rotor system were developed during the feasibility study, the requirements in this case differ from in-flight requirements. During laboratory fatigue testing, the transducers were attached externally to the system in a temporary manner to facilitate their movement to various locations. During in-service monitoring, the transducers must be attached internally (particularly if located on the blade) so as not to create aerodynamic interference and so that the transducer will not be subject to the forces due to airflow. In addition, the transducers should be attached in a permanent manner. It is not anticipated that transducer attachments for in-service use will pose a large problem, in that they could be cemented to internal positions in the blade during manufacture. Transducers could also be cemented into hollows in other rotor system components.

## Prediction of Remaining Useful Life

Some difficulty will be encountered in predicting the remaining life in an operating helicopter rotor system because of the variable and unscheduled loading which it receives. That is, although fatigue life may be predictable during laboratory tests, these tests are conducted under constant load rather than variable load conditions.

Although life predictions may be difficult, the onset and degree of fatigue damage should be determinable. This information could then serve as the basis for removing a rotor system from service. However, to correlate the acoustic emissions with fatigue damage during flight, the acoustic emission signal would have to be correlated with a signal representing the loading on the helicopter blade since the emissions are dependent on the load level.

## Environmental Considerations

State-of-the-art acoustic emission equipment is designed more for the laboratory than for the corrosive and vibratory

conditions existing in a helicopter. Although there is no serious impediment to operating in this environment, the design of the various acoustic emission components should be reviewed to ensure that they are suitable for this application. Ultimately the equipment should also be designed to minimize weight.

### 3.3.3 Applicability to Other Rotor Systems

The rotor design factors which could have a pronounced effect on acoustic emission generation and detection are summarized below.

Acoustic Emission Generation

- Material of Construction
- Stress Distribution and Level in Flawed Area

Attenuation and Distortion

- Blade Construction
- Interface Methods
- Location of Failure

Extraneous Noise

- Rubbing Interfaces
- Bearing Noise
- Drive-Train Noise

The material of construction and stress level are important in signal generation in that together they govern the energy release from the flaw. In turn, the greater the energy release, the greater the potential success of flaw detection through acoustic emission. The primary material factors are the elastic modulus, which governs energy storage, and the characteristic fatigue crack initiation and growth, which defines the energy release. The stress state governs the stored energy and flaw growth rate. The materials used in the blade are not peculiar to the type of rotor system, so this should not be a problem in applying the results obtained from the semirigid system to the rigid

and fully articulated systems. In addition, the two major types of blade skin material (aluminum and fiber-reinforced composite) were tested in this program and provide an adequate indication of their emission characteristics for projection to rotor systems other than the semirigid. The stress level and distribution in the flawed area are impossible to determine without knowing the flaw location for different rotor systems and the design stresses. This information could not be procured in this study. However, it is anticipated that cracks will form in the more highly stressed regions of the rotor system and thus facilitate detection.

The blade construction is another factor which does not appear to be peculiar to the type of rotor system. Attenuation and signal distortion measurements made on blade sections with aluminum and fiber composite skins and reinforced with honeycomb and spars should be projectable to other rotor systems. The length of the rotor blade does vary from system to system and would certainly be important in the acoustic emission system design. However, any length blade should be able to be monitored by placement of transducers in the blade at intervals consistent with the attenuation characteristics.

The location of the flaw dictates the positioning of transducers to prevent severe attenuation of the signal. It was not determined if flaw location could be generalized with respect to a specific type of rotor system. However, it is not expected that variation in flaw location as a consequence of system design will really seriously inhibit the application of acoustic emission detection methods.

It is expected that the greatest detriment to successful use of acoustic emission methods will be the extraneous noise in the rotor system. It is also expected that the source which will be most difficult to eliminate will be that emanating from rubbing interfaces, primarily in the regions connected by bolts. This type of noise should generally increase with the increasing degrees of movement in the rotor system. That is, the rigid should provide the least noise of this type followed by the semirigid, while the fully articulated would generally

provide the greatest noise source. However, techniques for extracting the acoustic emission signal from this type of noise in the semirigid system should prove generally applicable to the other systems.

The bearings employed in rotor systems do not appear to be peculiar to the type of system. Therefore, this noise source should not prove to be an obstacle to projecting results from the semirigid to other rotor systems. The relative noise from the drive train for the three rotor systems could not be determined in this study. However, this noise source is expected to be secondary to the rubbing interface noise in terms of difficulty in extracting the acoustic emission signal.

In summary, it appears that if experimental work proves that acoustic emission flaw detection in the semirigid rotor system is feasible, it should also be applicable to the rigid and fully articulated systems. This is based on the fact that most of the factors which define the feasibility of the technique are not peculiar to the particular type of rotor system. In cases where detriments to application are potentially more severe in systems other than the semirigid (e.g., rubbing noise in the fully articulated systems), it is expected that experimental techniques developed in this program will be applicable to other systems. It should be remembered that, even within a given type of rotor system, the extraneous noise environment can vary significantly. Therefore, extraneous noise monitoring will probably be required for each rotor system design prior to application of acoustic emission flaw detection equipment. However, the application should be relatively routine, once the noise suppression techniques have been developed in this program.

### 3.3.4 Acoustic Emission Design for On-Board Application

An acoustic emission system for onboard application would conform essentially to that developed for the laboratory fatigue tests of blade sections. The components of such a system are described in Section 3.2.1, Figure 27, and Table 6. The specific commercial brands listed would not necessarily have to be used, but components performing the same functions would be required. The onboard acoustic

emission system would deviate from the laboratory system in five major respects: (a) a video tape recorder would not be required, (b) load cycle gating and the voltage controlled gate are not necessary, (c) a display type of readout rather than a printer would be more desirable, (d) additional transducers and transducer channels would be necessary, and (e) hardware for transmitting the signal from the rotating system to the stationary portion of the helicopter would have to be developed.

The load-cycle gating equipment would not be required because the rise time and spatial discrimination modes of noise rejection are the more promising modes. The video tape recorder, although useful in laboratory tests to provide a permanent record, would not be needed in the on-board system. The printer used in laboratory tests provides a hard copy record, but a visual display would be required on-board to provide a convenient warning to the pilot of potential failure.

The number of transducers required along with preamplifiers and channels in the acoustic emission system would depend on the size of the blade and the transducer spacing. The results of this investigation indicate that transducers should be placed no further than 5-feet apart. As described in Section 3.3.2, a method would have to be developed for transmitting the acoustic signals from the rotating blade system to the processing equipment located in the stationary portion of the helicopter. It should be noted that such a system would provide an indication of the location of the failure in that the multiple transducer system could use spatial gating to isolate the origin of failure.

### 3.3.5 Prediction of Rotor System Life

One of the desirable objectives of this investigation is to provide a method of predicting the remaining useful life in a rotor system. The acoustic emission method provides a means of detecting crack initiation and crack growth. However, use of this information to predict remaining useful life depends on the application of a model based on fracture mechanics.

It is beyond the scope of this study to review all of the methods in detail. Rather, it is sufficient to say that there have been successes in predicting fatigue life by a fracture mechanics approach[1] and by a combined fracture mechanics and acoustic emission approach.[2] It should be noted that these and similar results were obtained on laboratory samples and that the fracture mechanics model was based on plane strain or other stress or strain states, simplifying assumptions. These conditions do not generally exist in the helicopter blade; consequently, application of these fracture mechanics models would be somewhat suspect. Alternately, it is suggested that an empirical approach to life prediction would have greater utility. That is, for a given rotor system, the fatigue life should be established experimentally over the potential in-service load range. The acoustic emissions then could be correlated with the extent of fatigue damage and the remaining life. The correlation would not necessarily have to follow fracture mechanics models to be useful.

The major obstacle to application of even the empirical approach is the variable and somewhat unpredictable loading that the rotor system will encounter in service. This in-service loading poses two problems: First, life predictions cannot safely be made in terms of time that a system can remain in service unless worst-case loading conditions are assumed. Second, the extent of fatigue damage may be difficult to correlate with fatigue emissions under variable loading conditions. That is, the amount and characteristics of the emissions for a given increment of crack growth will depend on the stress during

---

[1] R. V. Sanga and T. R. Porter, "Application of Fracture Mechanics for Fatigue Life Prediction," Proceedings of the Air Force Conference on Fatigue and Fracture of Aircraft Structures and Materials, AFFDL TR 70-144, September 1970.

[2] D. O. Harris, H. L. Dunegan, and A. S. Tetelman, "Prediction of Fatigue Lifetime by Combined Mechanics and Acoustic Emission Techniques," Proceedings of the Air Force Conference on Fatigue and Fracture of Aircraft Structures and Materials, AFFDL TR 70-144, September 1970.

this crack extension. Therefore, to correlate damage with emission, either the emissions will have to be correlated with the system loading or a method will have to be established for relating the emissions to crack growth independent of stress. The latter could be established if the character of the acoustic emissions could be related to the particular stress level during crack extension.

## SECTION 4
## SUMMARY, CONCLUSIONS, AND RECOMMENDATIONS

### 4.1 SUMMARY AND CONCLUSIONS

- The acoustic emission technique with rise-time discrimination generally gave indications of impending failure during blade-section fatigue tests. Failures were preceded by an increase in the acoustic signal count rate. However, there were two tests in which no acoustic precursor to failure was evident. In one test the setting on the rise-time discriminator was set at such a high level that all signals were rejected - those from the crack as well as extraneous noise - and no data were obtained. In another test no increase in acoustic activity was obtained (either with rise-time discrimination or spatial gating) although a 3.5-inch crack formed in the leading edge of the blade. It appears that the crack was not sufficiently severe to be detected with the acoustic emission monitoring system or that its emissions were low because it was located in a non-loadbearing member of the blade.

- Rise-time noise discrimination appears to be a viable noise suppression technique, in that it provides a better indication of impending failure than does the signal without any noise discrimination procedure applied.

- The spatial gating technique was not successful in defect detection when the fatigue crack was located near the retention bolt, the spindle, or the grip. This is because the method requires the insertion of slave transducers between the extraneous noise source and the recording transducer. This was not practical for the above locations in that these locations were in themselves sources of extraneous noise. However, it should be noted that this technique should be effective for eliminating extraneous noise when failures occur on the main section of the blade.

- Acoustic emission monitoring should be carried out in the 100-300 kHz frequency range, because emissions from fatigue crack propagation fall predominantly into this frequency band and signal attenuation is less severe in this range than at higher frequencies.
- Frequency band-pass filtering is not an effective noise discrimination technique, in that extraneous noise and fatigue emissions fall into the same frequency band (100-300 kHz).
- One of the potential difficulties in implementing the acoustic emission technique in rotor systems is the high attenuation of the acoustic signal in the honeycomb-supported section of the blade. This problem is somewhat alleviated by the fact that acoustic signals are transmitted with much greater efficiency through the doubler, leading edge, and trailing edge of the blade. These blade sections can serve to transmit signals from failures in the honeycomb which occurs near them. However, a failure exclusively in the honeycomb and removed from one of these high transmission efficiency regions would be difficult to detect.
- The high attenuation of acoustic signals across rotor system interfaces indicates that transducers cannot be located in the hub area to detect failures in the blade section. This procedure is also prohibited by the relatively high attenuation values in the blade section itself.

## 4.2 RECOMMENDATIONS

The acoustic emission technique should be demonstrated in additional blade section fatigue tests in order to verify its effectiveness in detecting fatigue cracks. The testing to date has shown that high acoustic activity generally appears prior to failure. However, since crack growth could not be viewed and correlated with acoustic activity, this relationship can only be assumed. In addition the negative results obtained on one test dictate the need for additional tests to verify the reliability of crack detection.

Additional verification could be accomplished in two ways. First, if the fatigue crack cannot be viewed prior to failure, as was the case in the tests performed to date, then the presence of a high acoustic activity precursor to failure should be established on a fairly large number of samples ($\sim$10). This would be an empirical type approach in which it would be determined if a consistent acoustic pattern was found in these samples. A second and perhaps more desirable approach would be to carry out blade section fatigue tests in which the crack could be detected visually shortly after initiation so that acoustic activity could be correlated directly with fatigue crack growth. This would require less tests than the first approach, in that the correlation with actual crack growth would relieve the doubts about the actual source of the increased activity.

It is also suggested that the effectiveness of spatial gating as a noise discrimination technique be explored in blade section fatigue tests. As described in the text of this report, spatial gating was not properly evaluated because in most cases fatigue cracks initiated outside of the region for which the spatial gating was set up (cracks occurred near blade extremities). Laboratory tests on samples indicated that this technique was effective in rejecting signals which occurred outside a selected region. Therefore, this technique appears to hold promise. Evaluation of the method on blade section tests would require failure to occur away from the blade extremities so that a secondary transducer could be placed between the extraneous noise source and the fatigue crack.

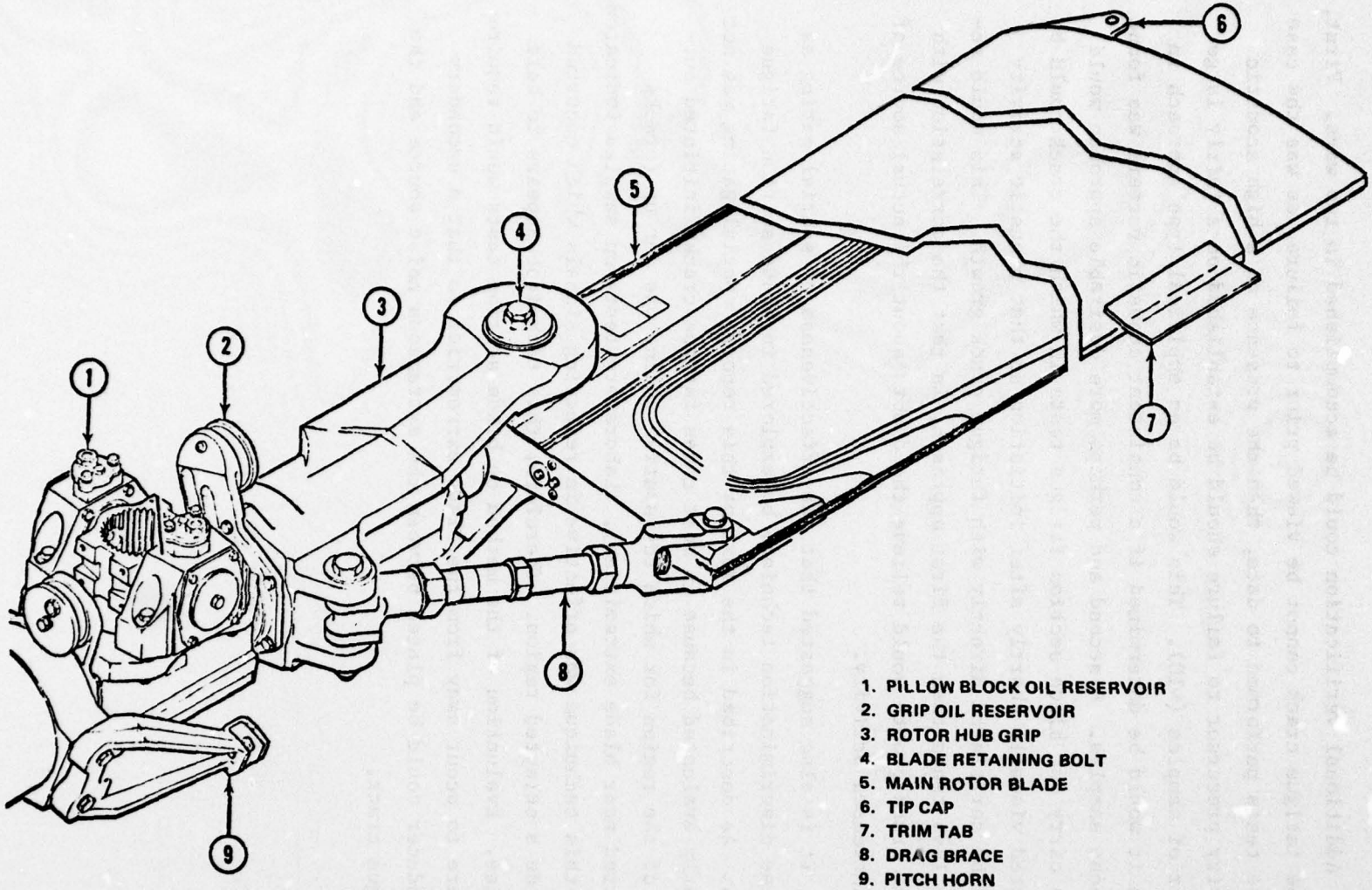


Figure 1 - Rotor hub and blade assembly.

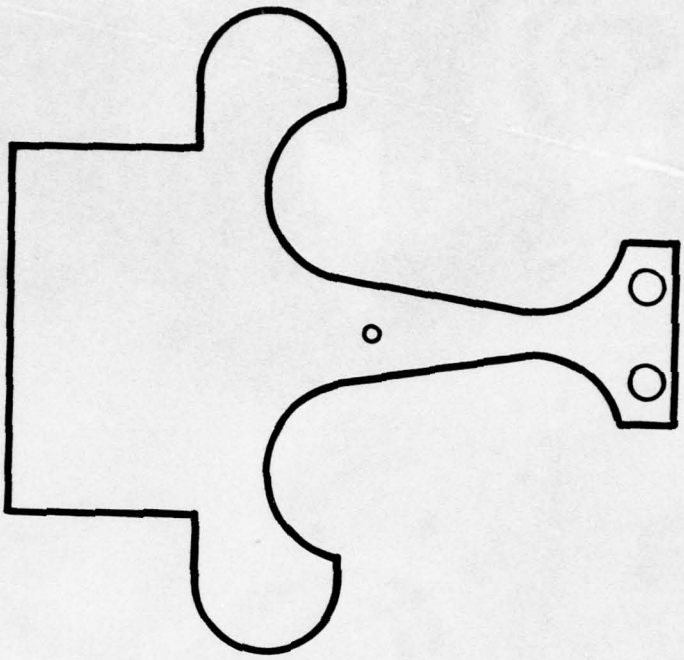

Figure 2 - Sketch of bending fatigue sample.
(Drawing is approximately to scale.)

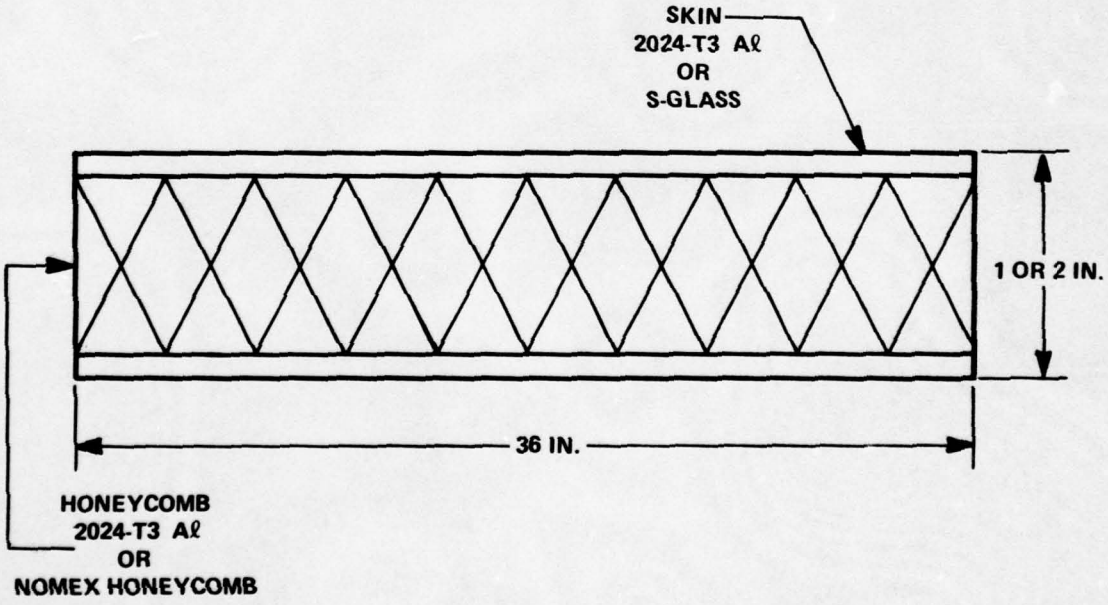


Figure 3 - Sketch of blade composite attenuation sample.

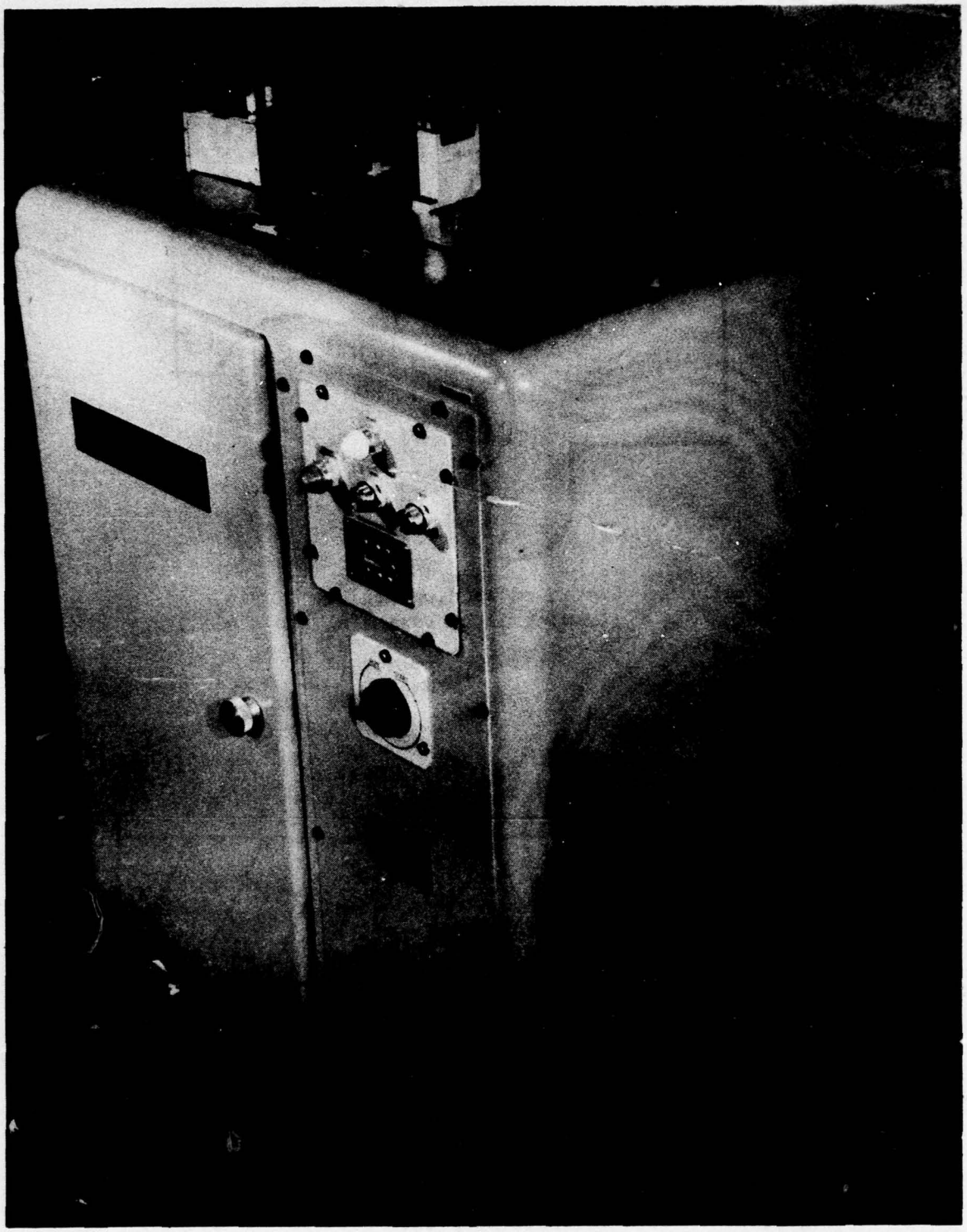

Figure 4 - Sonntag fatigue machine, Model SF-01-U.

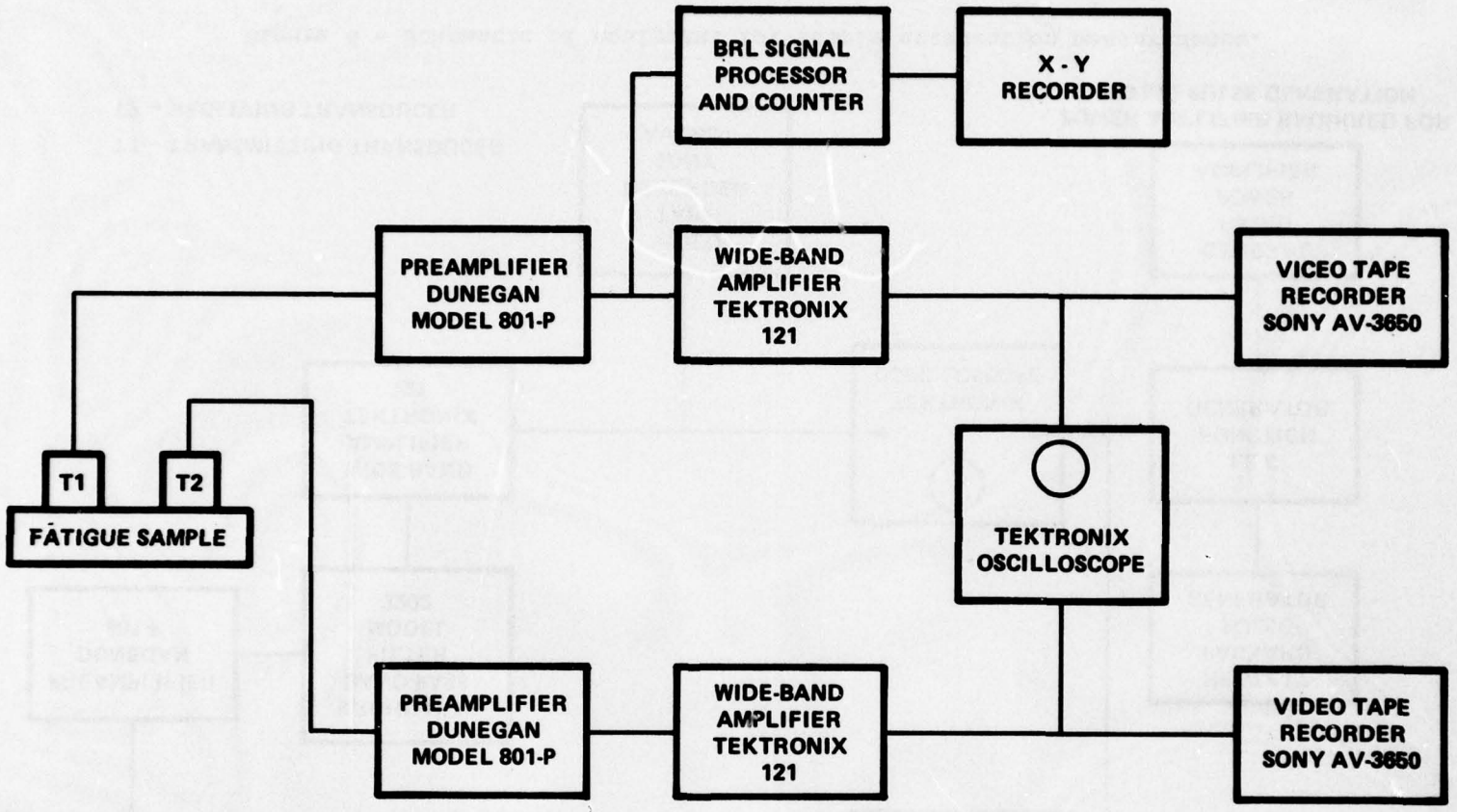


Figure 5 - Acoustic emission monitoring system for laboratory fatigue tests.

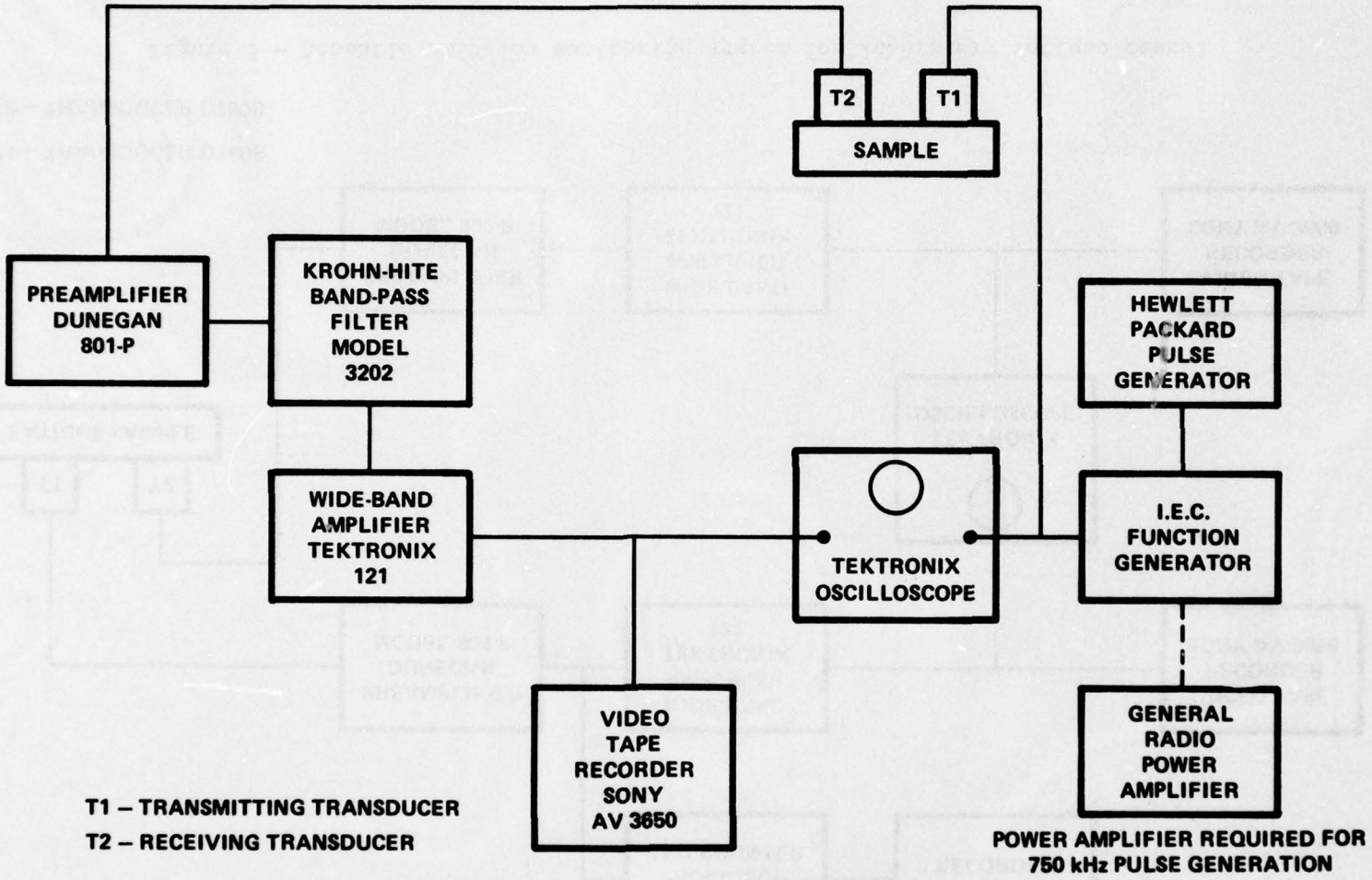


Figure 6 - Schematic of equipment for sample attenuation measurements.

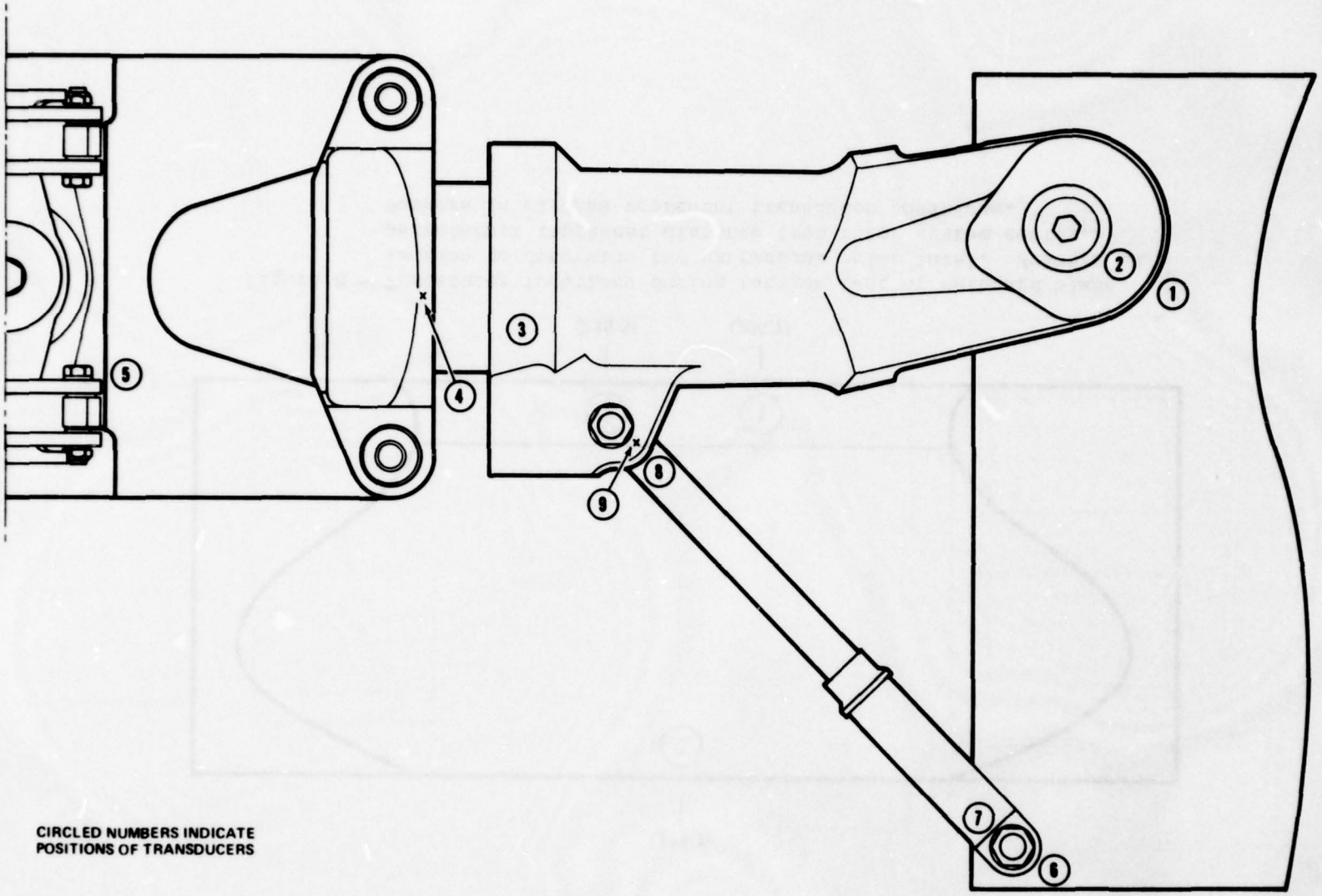


Figure 7 - Transducer placement during attenuation tests on the Bell Model 214 rotor system attachment hardware.

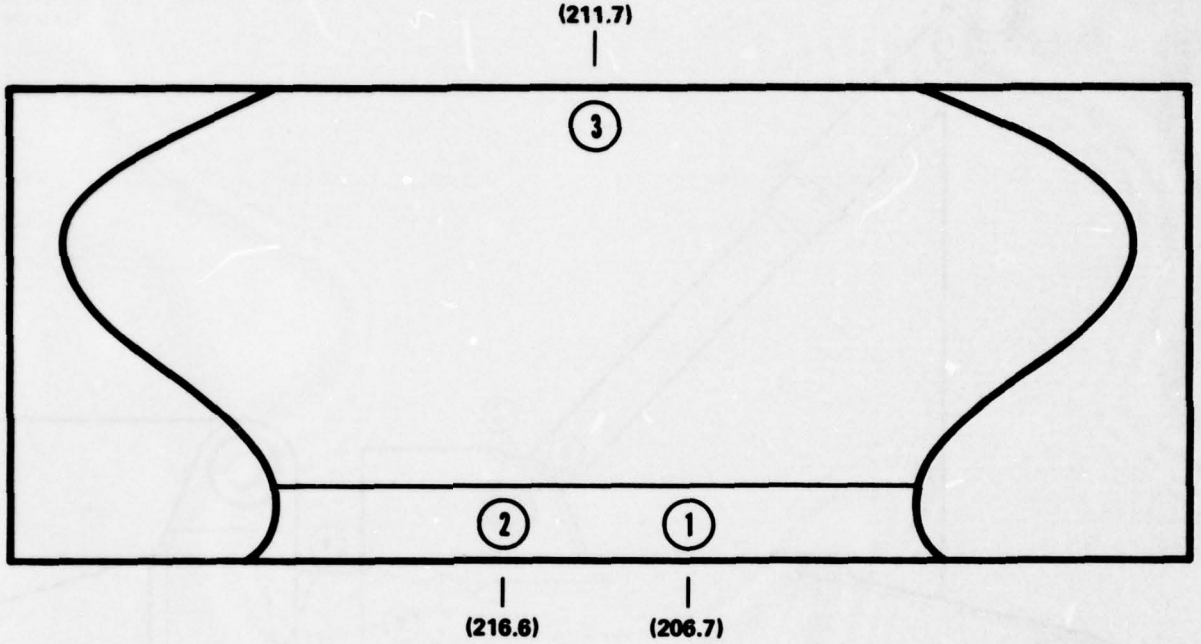


Figure 8 - Transducer locations during fatigue test of outboard blade section to determine the extraneous noise level. Numbers in parentheses represent distance from rotor system center. Numbers in circles represent transducer positions.

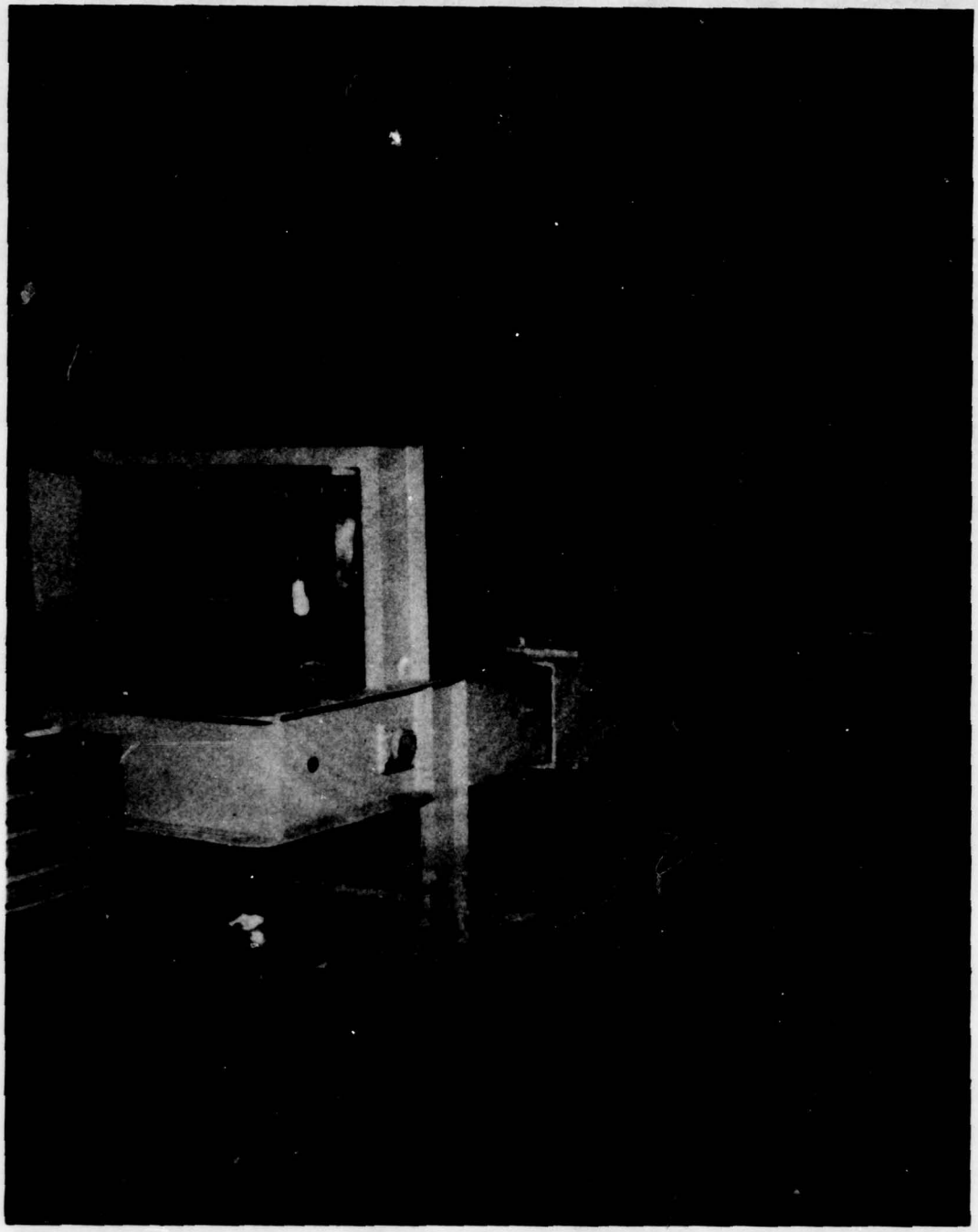

Figure 9 - Fatigue machine for testing full-scale helicopter blade section. Machine is located in the mechanical test laboratory of Bell Helicopter Company, Fort Worth, Texas.

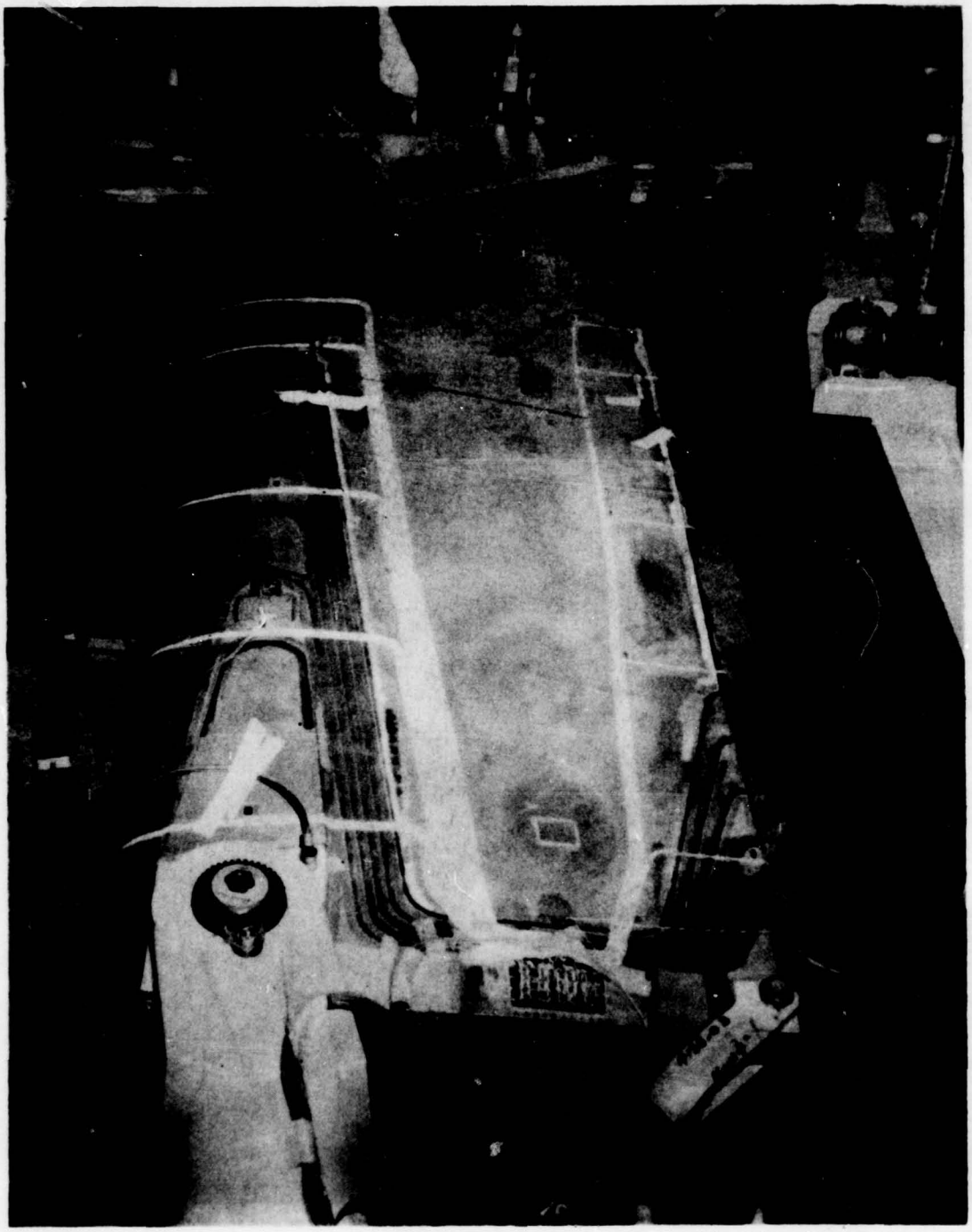

Figure 10 - Inboard blade section in place on fatigue machine.

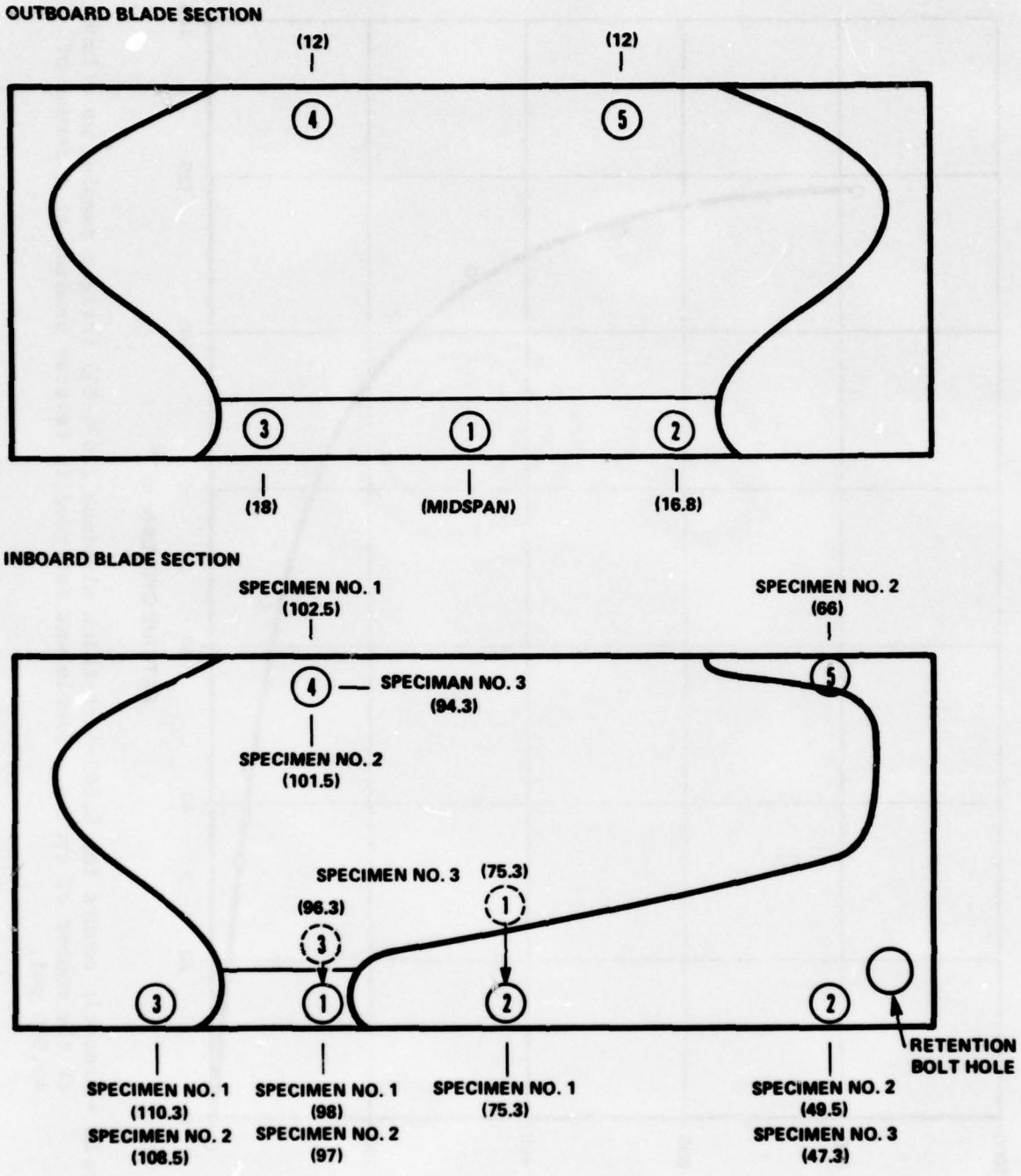


Figure 11 - Sketch of inboard and outboard blade sections showing transducer locations during fatigue tests. Numbers in parentheses represent distance in inches from rotor system center. Numbers in circles identify the transducers.

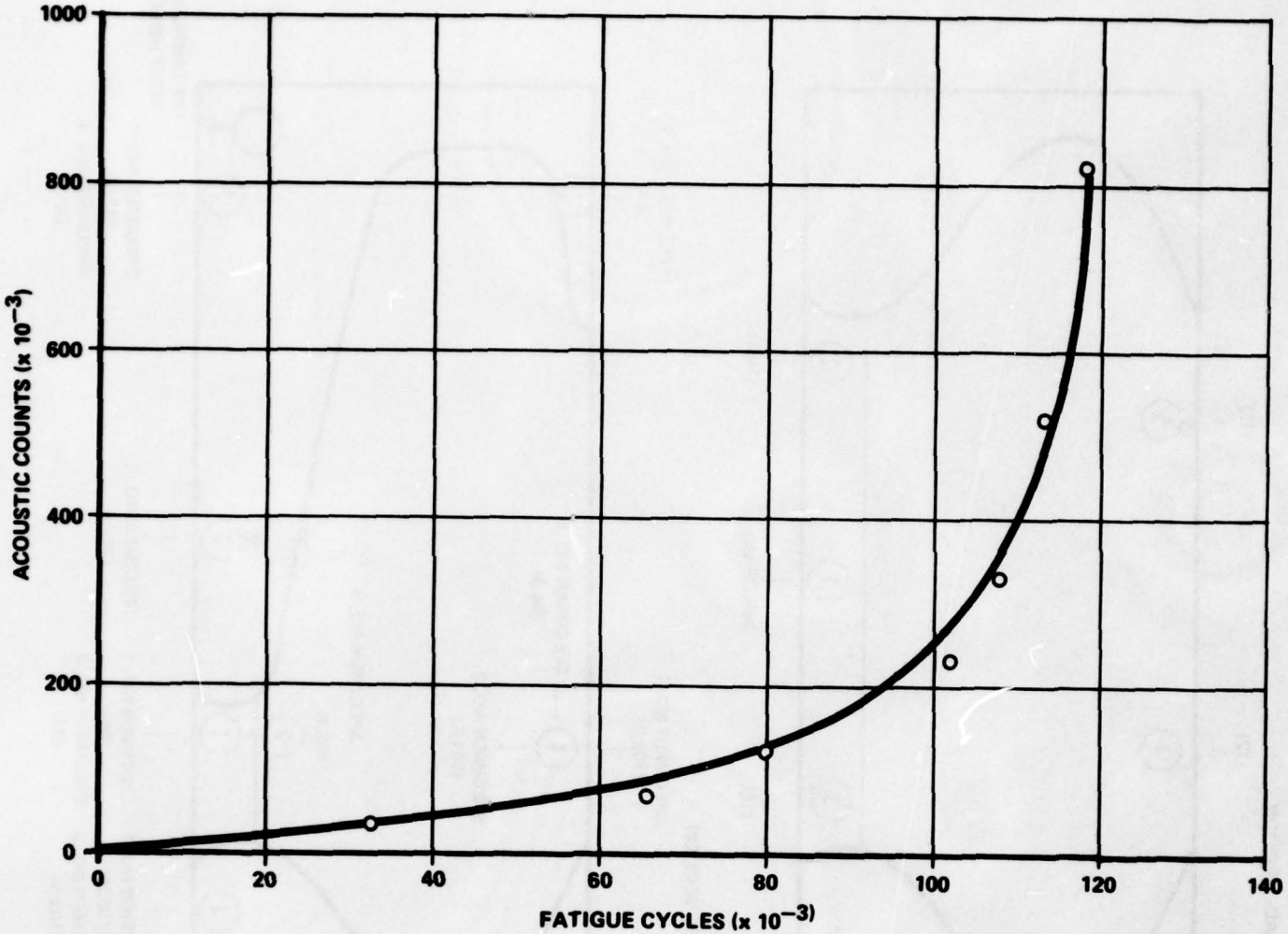


Figure 12 - Acoustic counts for 0.063-inch-thick aluminum (2024-T3) fatigue samples as a function of the number of cycles. Sample was fatigued in reverse bending at a stress of 45,000 psi.

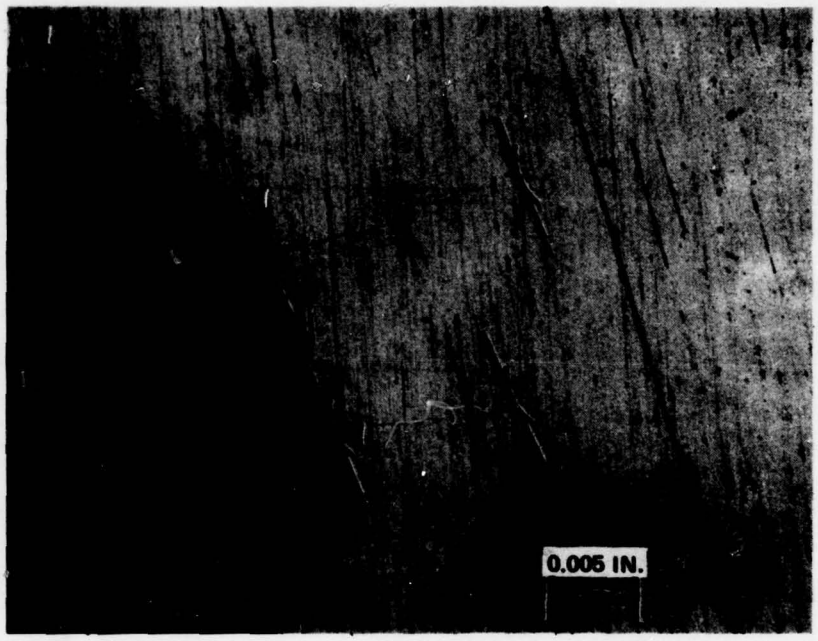


Figure 13 - Photomicrograph (X100) showing extent of cracking in aluminum fatigue sample after 118,000 cycles of reverse bending at a stress of 45,000 psig. This is the sample for which the acoustic emission curve is shown in Figure 12. Circular edge from which cracks emanate is 0.075-inch-diameter hole which was drilled in sample to serve as source for crack initiation.

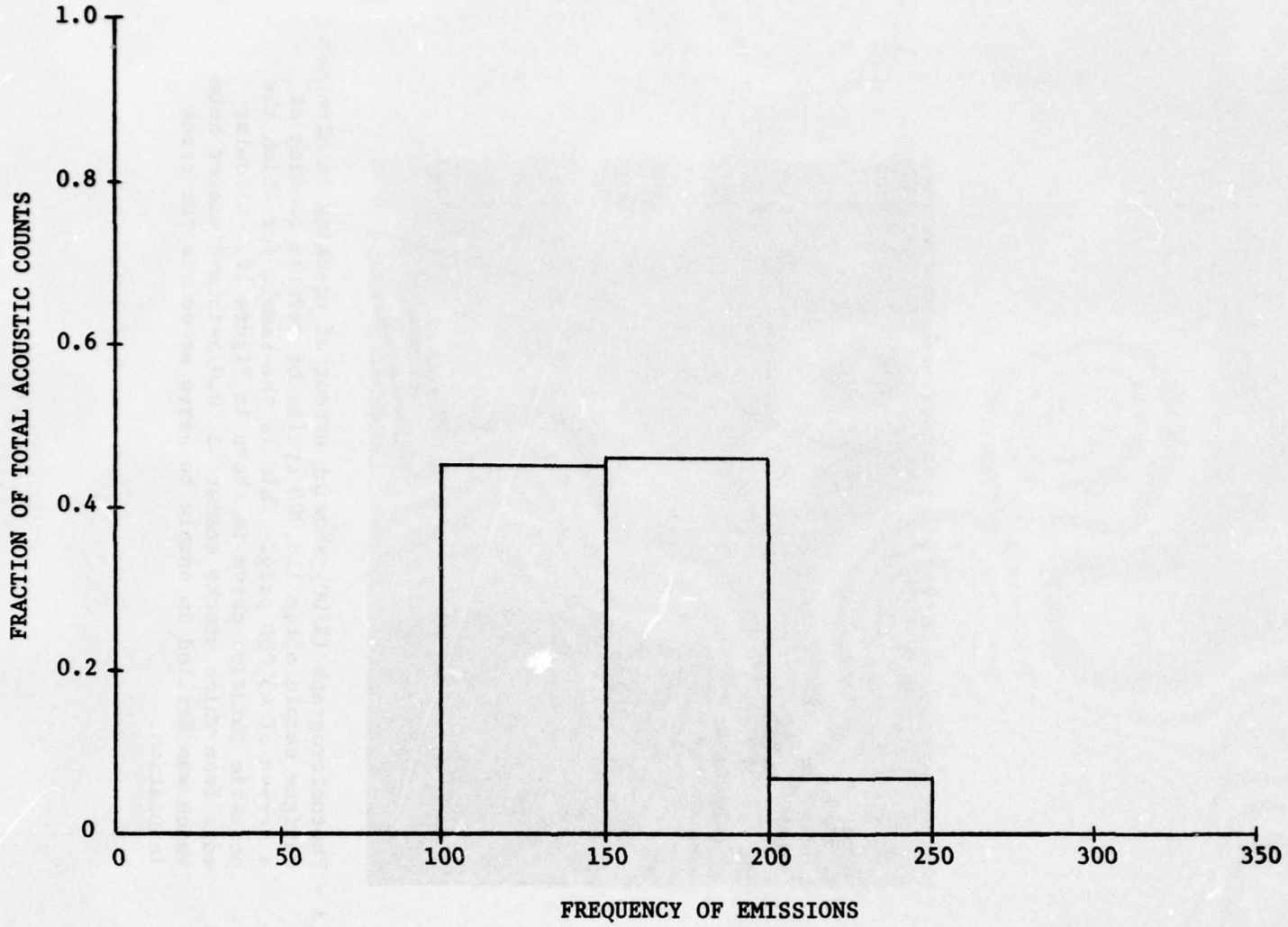


Figure 14 - Frequency distribution of acoustic emissions from aluminum (2024-T3) fatigue sample during reverse bending at 40,000 psi after 250,000 cycles.

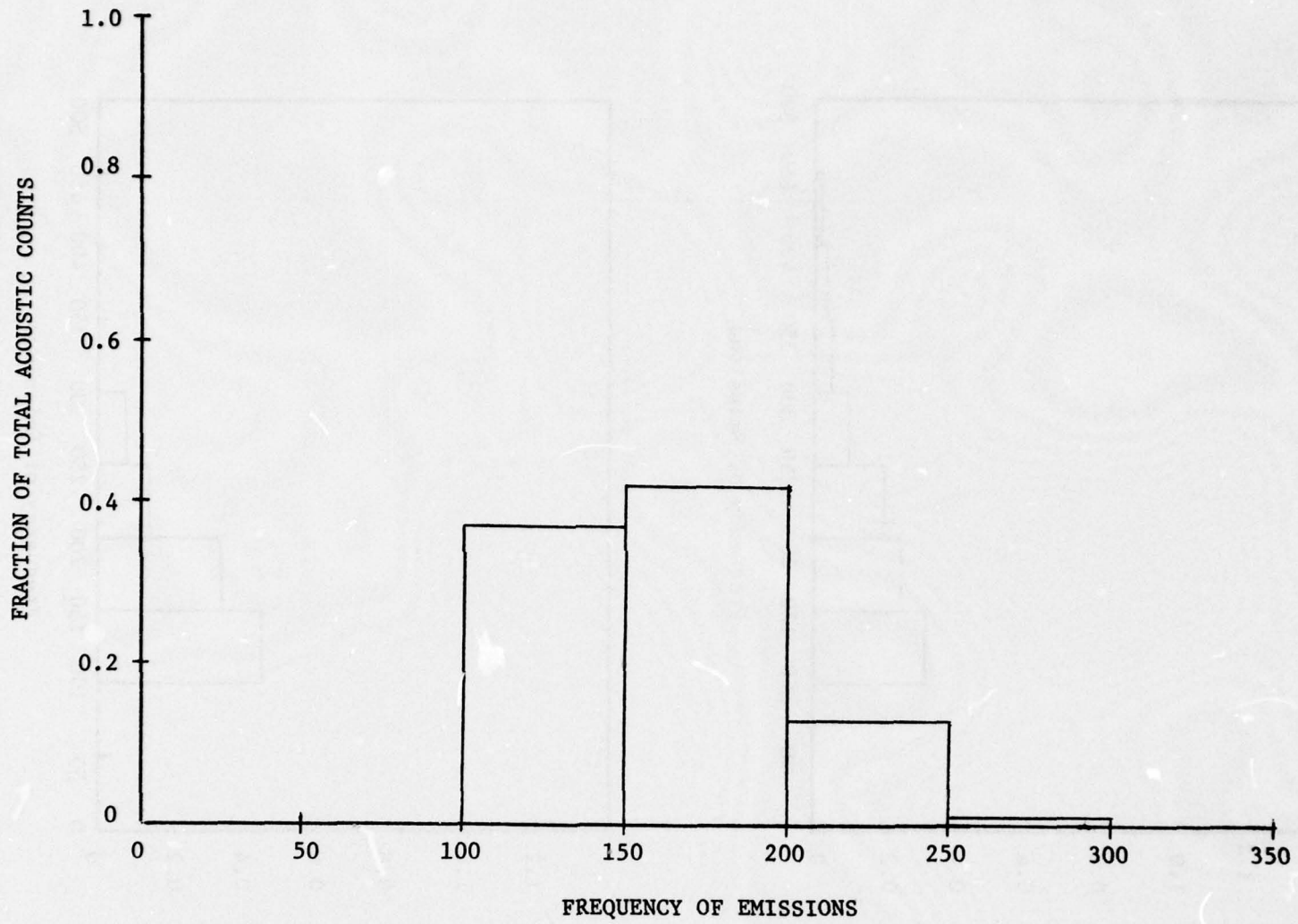


Figure 15 - Frequency distribution of acoustic emissions from aluminum (2024-T3) fatigue samples during reverse bending at 50,000 psi after 50,000 cycles.

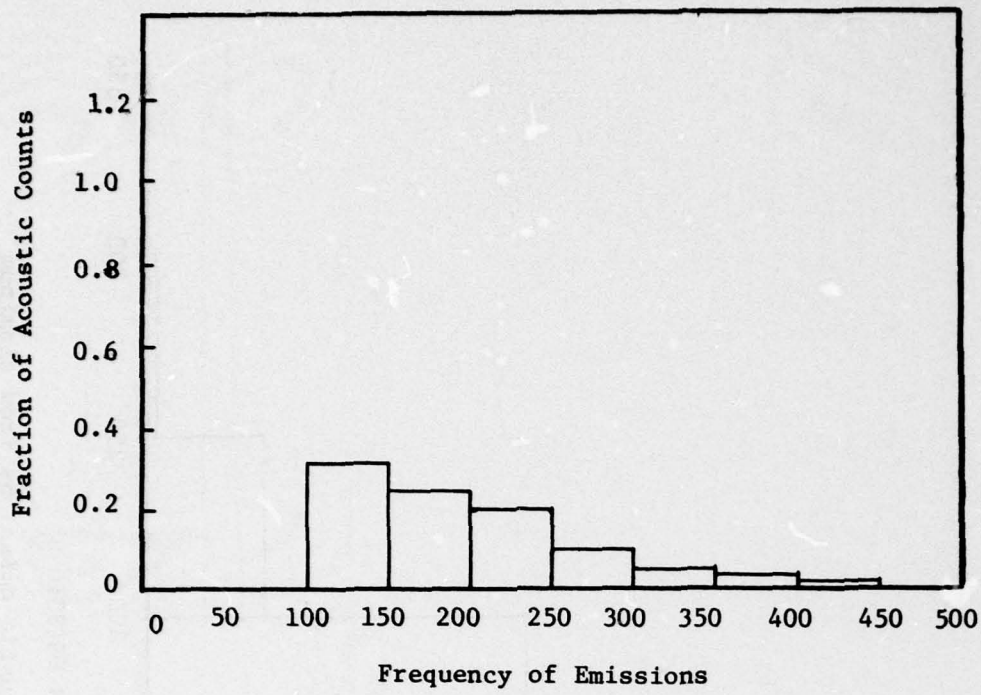


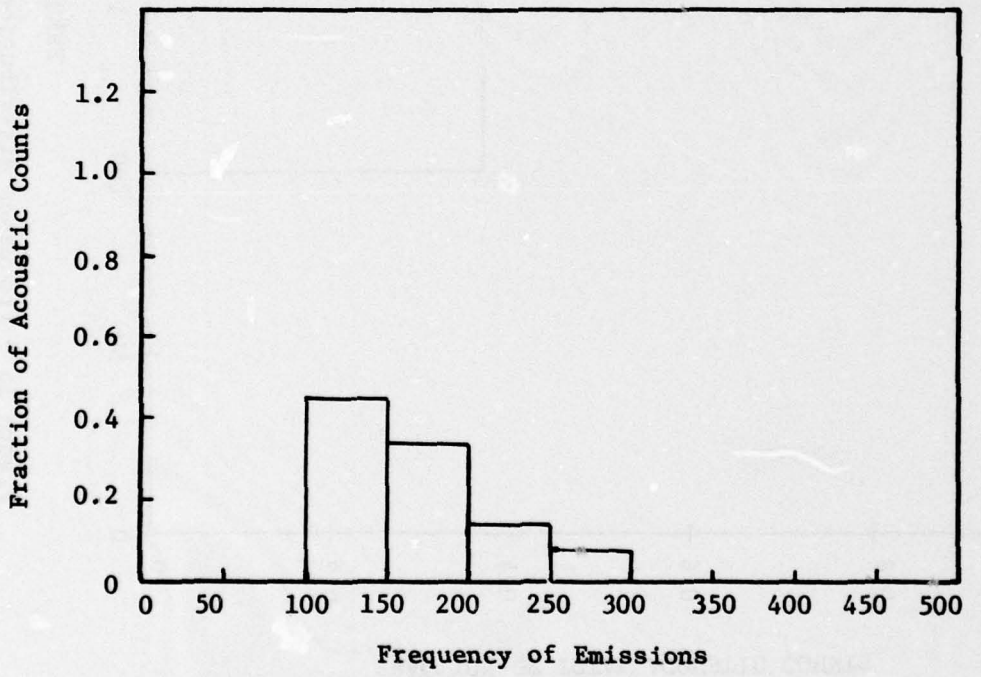


Figure 16 - Frequency distribution obtained with D 140B (below) and D 750B (above) transducers during fatigue test of 2024T3 aluminum sample. Sample was under maximum reverse bending stress of 30,000 psi at 340,000 cycles.

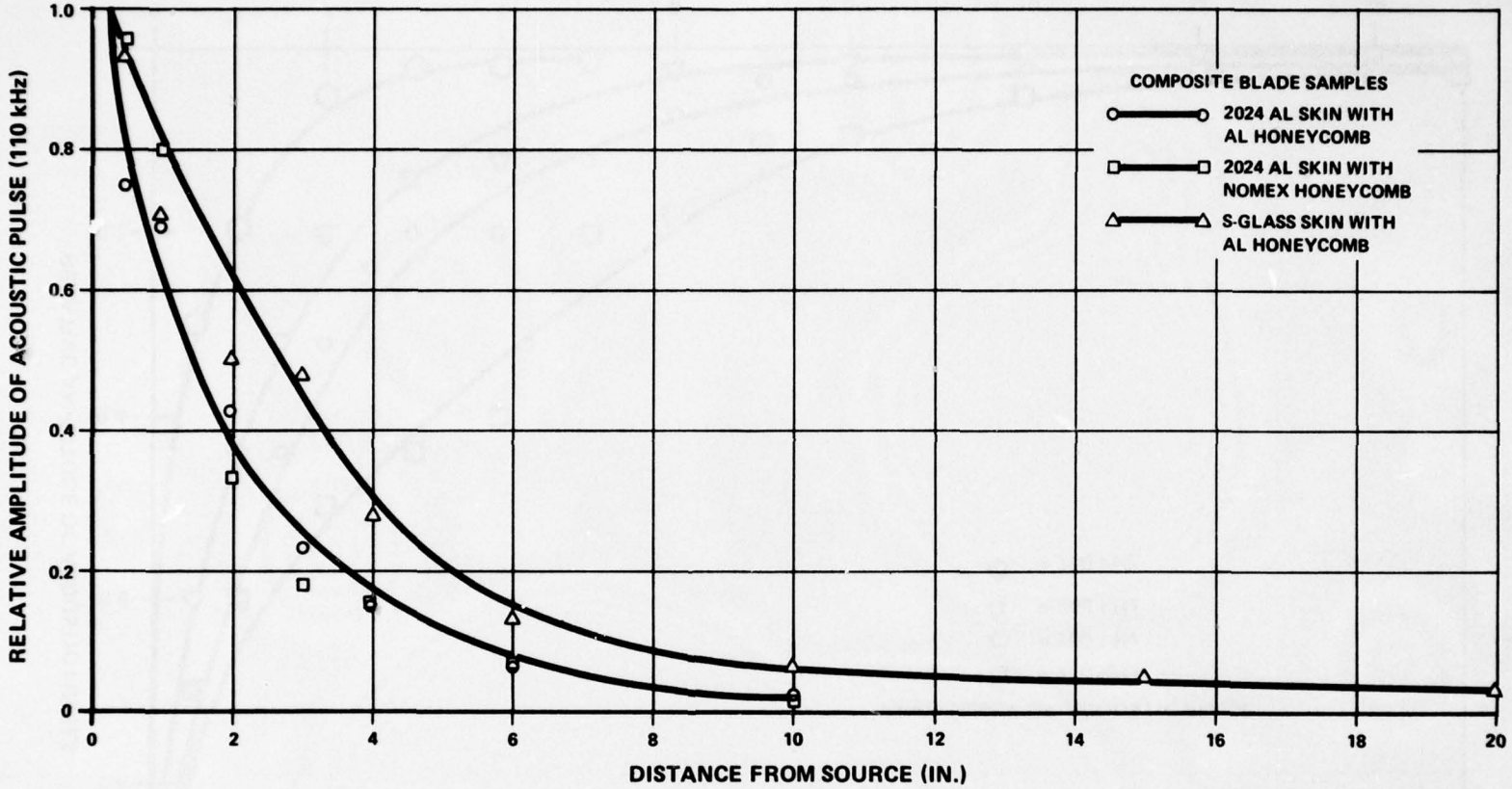


Figure 17 - Attenuation curve for blade composite samples. Simulated acoustic emission pulses were at a frequency of 110 kHz.

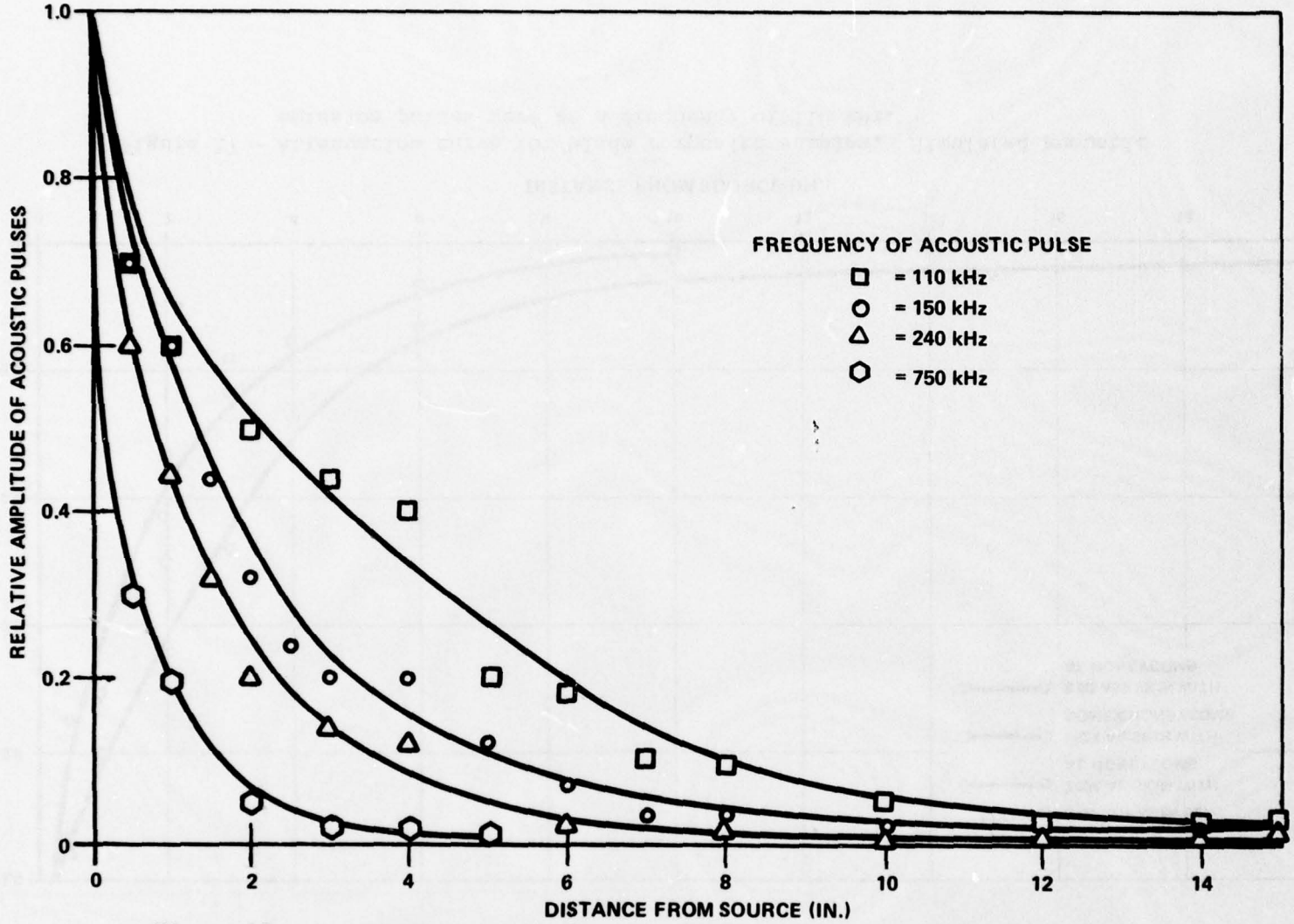


Figure 18 - Attenuation curves for the aluminum composite blade sample (2024-T3 Al skin/Al honeycomb) as a function of acoustic pulse frequency.

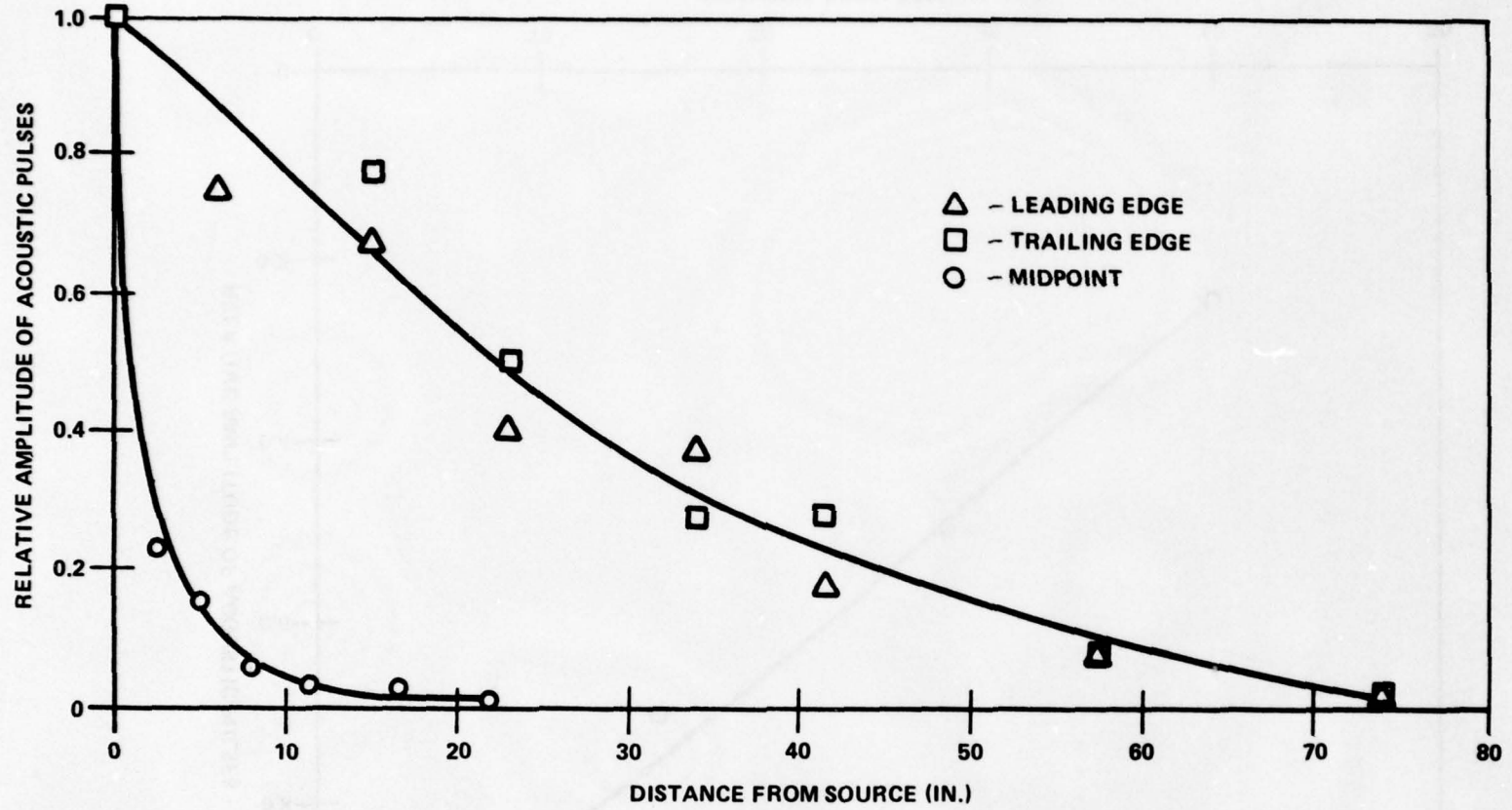


Figure 19 - Signal (150 kHz) attenuation along leading edge, trailing edges, and midpoint of Bell Model 214 helicopter rotor blade.

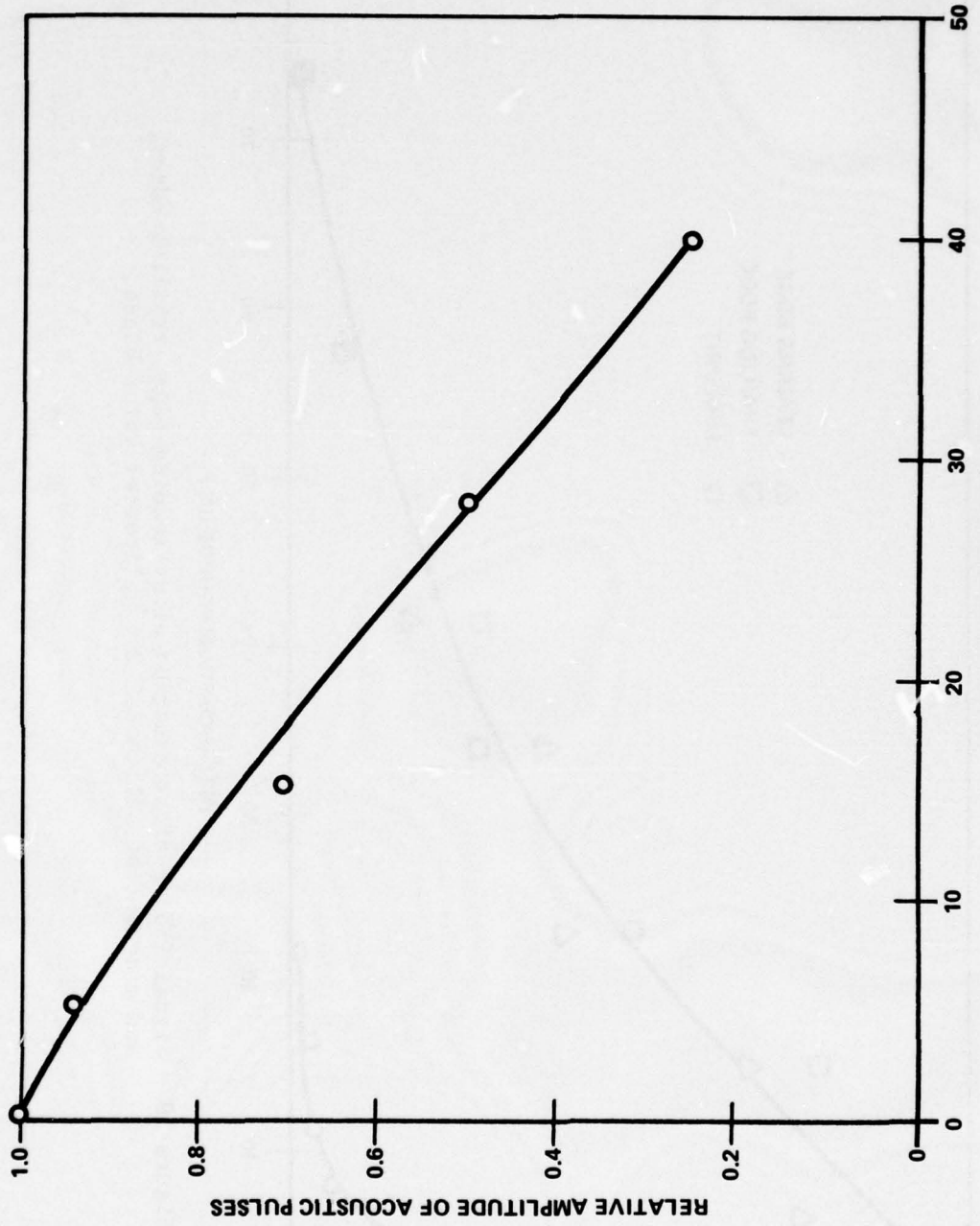


Figure 20 - Signal (150 kHz) attenuation along doubler section of Bell Model 214 helicopter rotor blade.

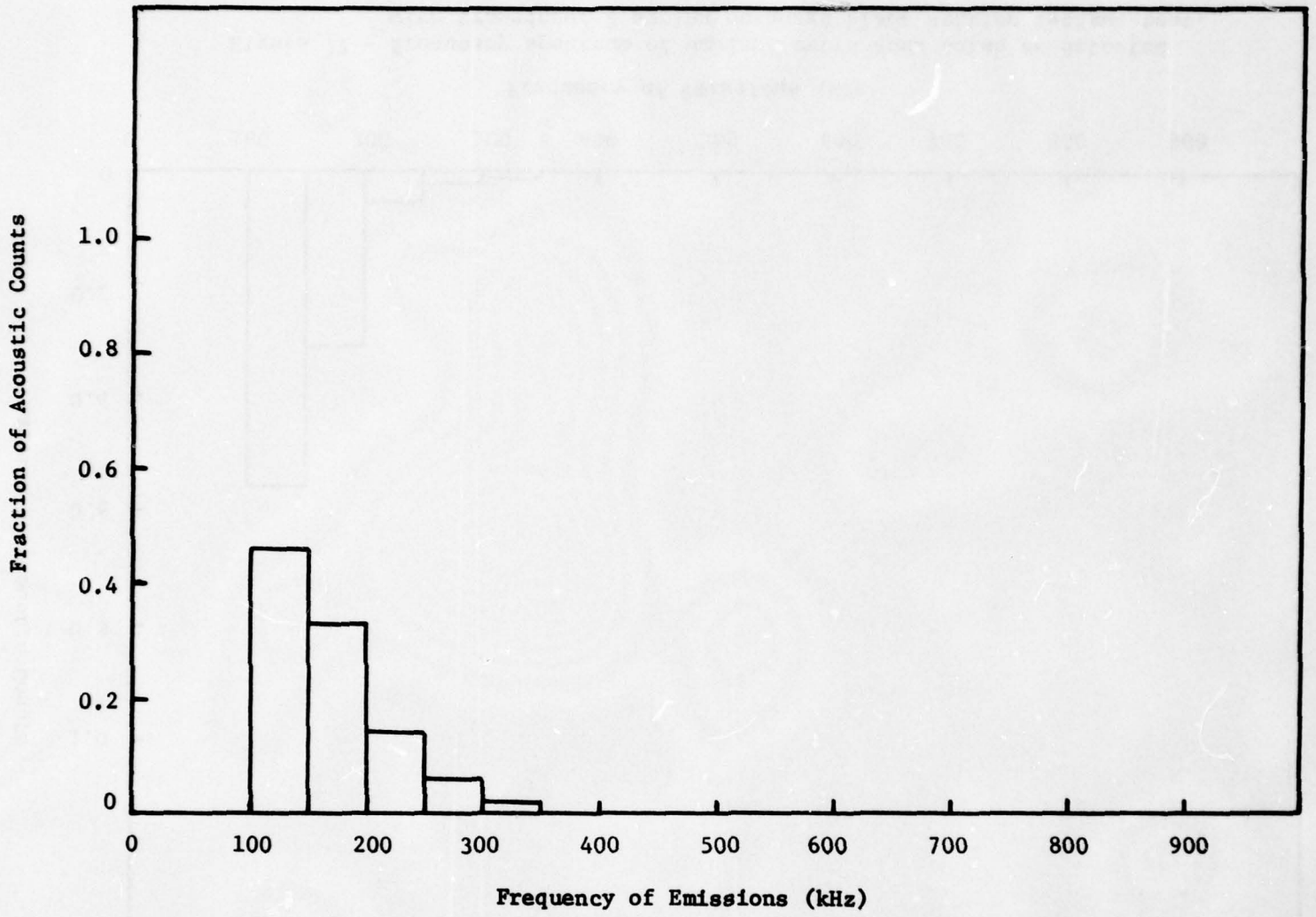


Figure 21 - Frequency spectrum of ambient extraneous noise as detected with transducer 1 during outboard blade section fatigue test.

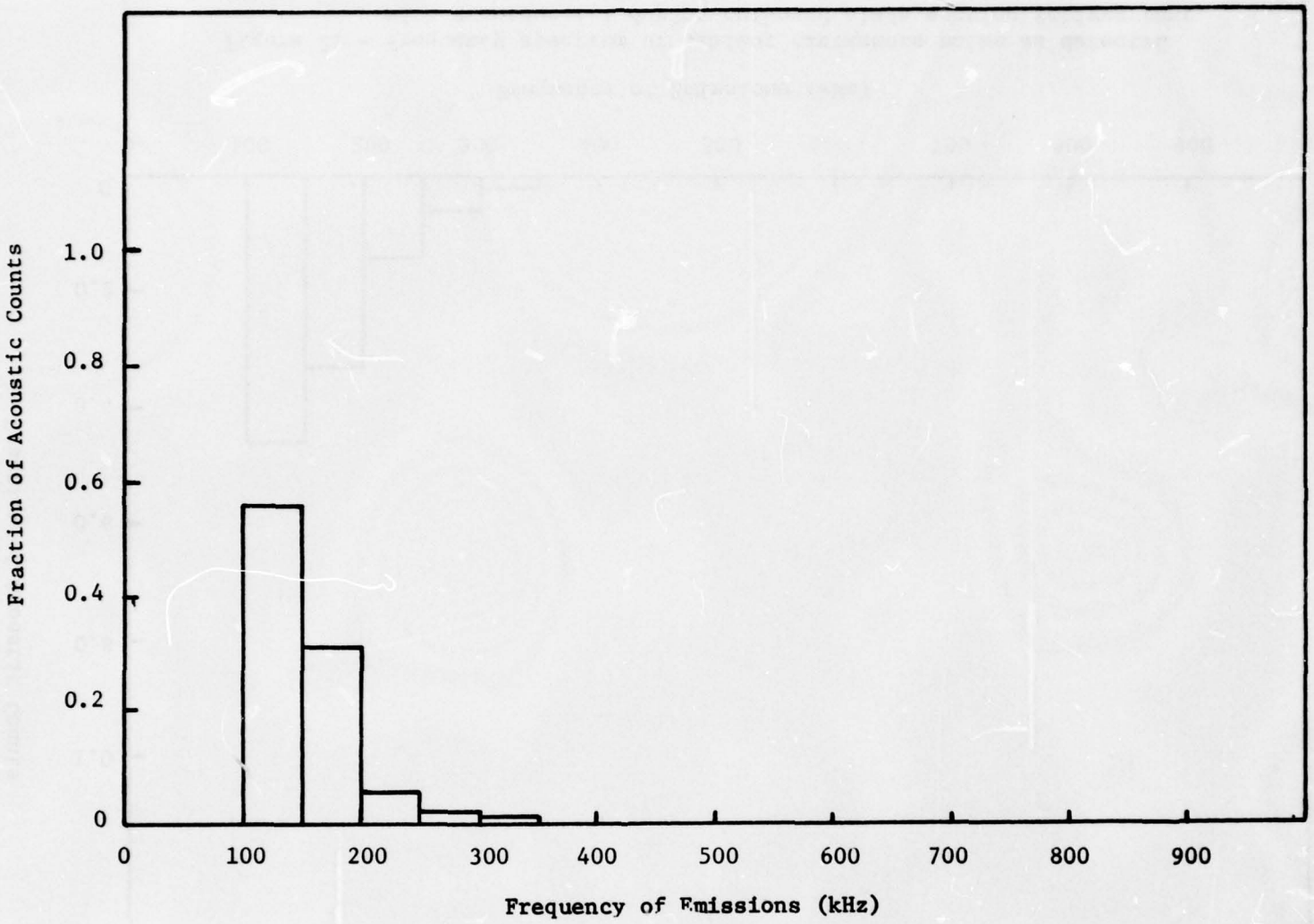


Figure 22 - Frequency spectrum of ambient extraneous noise as detected with transducer 2 during outboard blade section fatigue test.

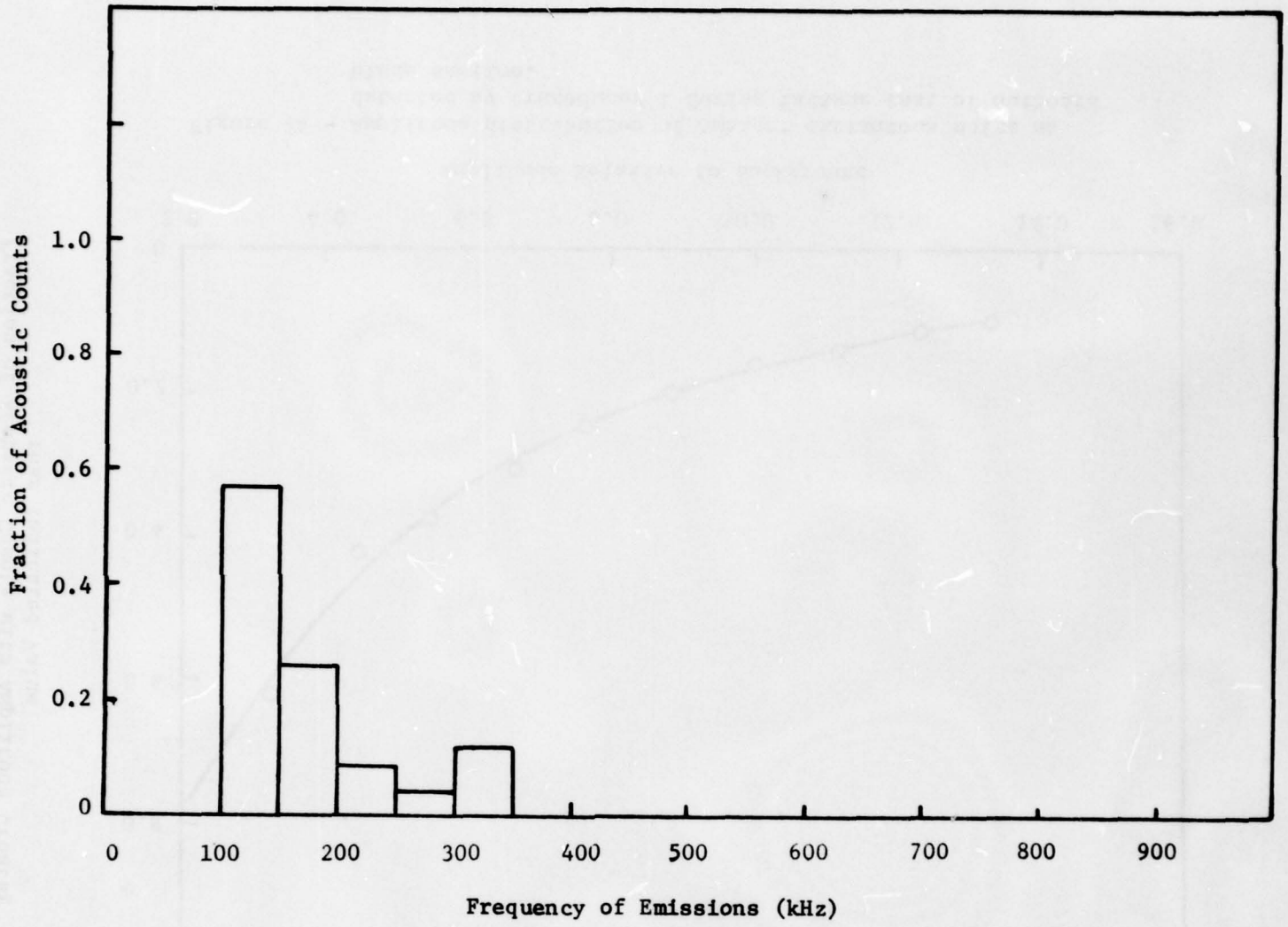


Figure 23 - Frequency spectrum of ambient extraneous noise as detected by transducer 3 during outboard blade section fatigue test.

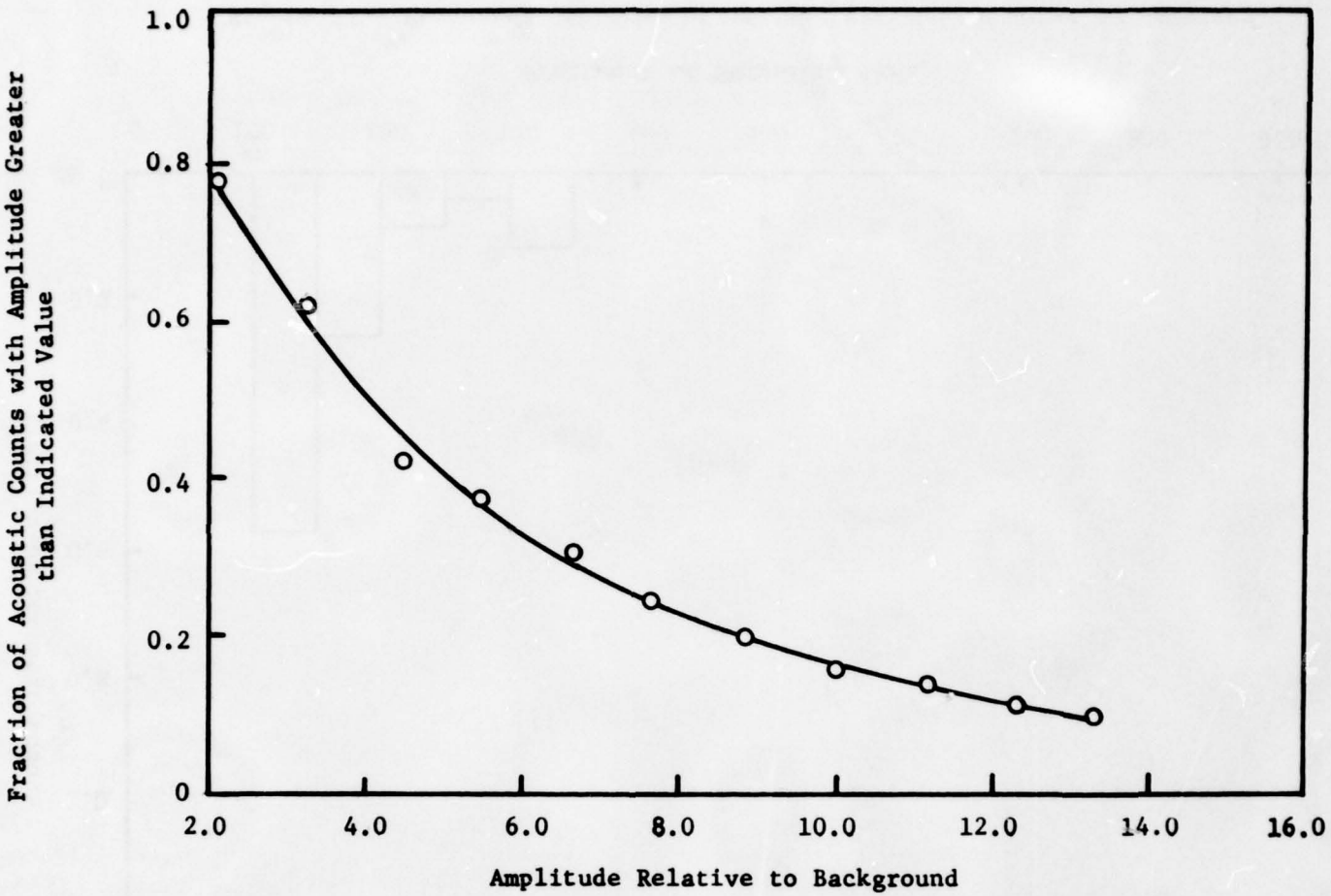


Figure 24 - Amplitude distribution of ambient extraneous noise as detected by transducer 1 during fatigue test of outboard blade section.

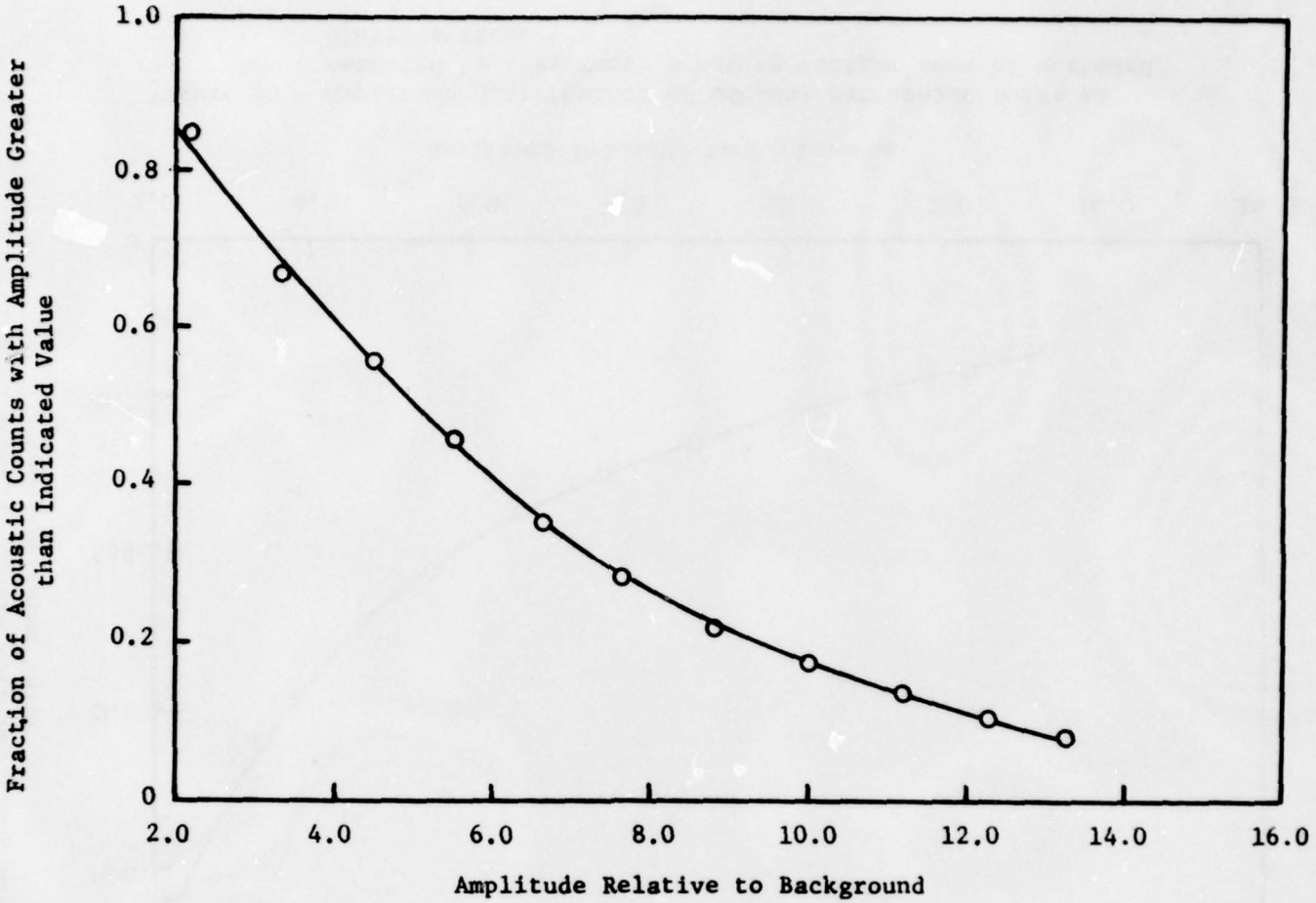


Figure 25 - Amplitude distribution of ambient extraneous noise as detected by transducer 2 during fatigue test of outboard blade section.

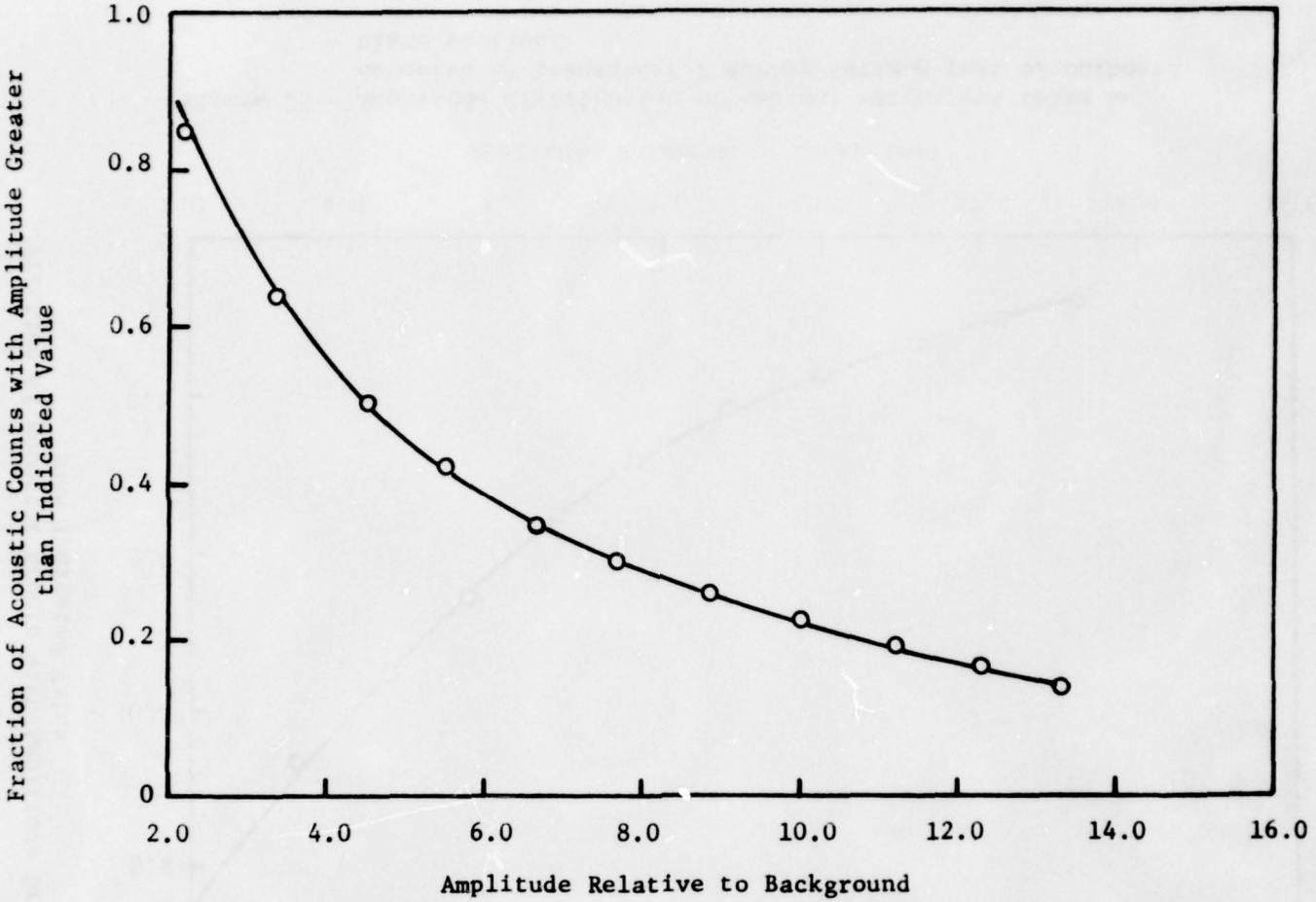


Figure 26 - Amplitude distribution of ambient extraneous noise as detected by transducer 3 during fatigue test of outboard blade section.

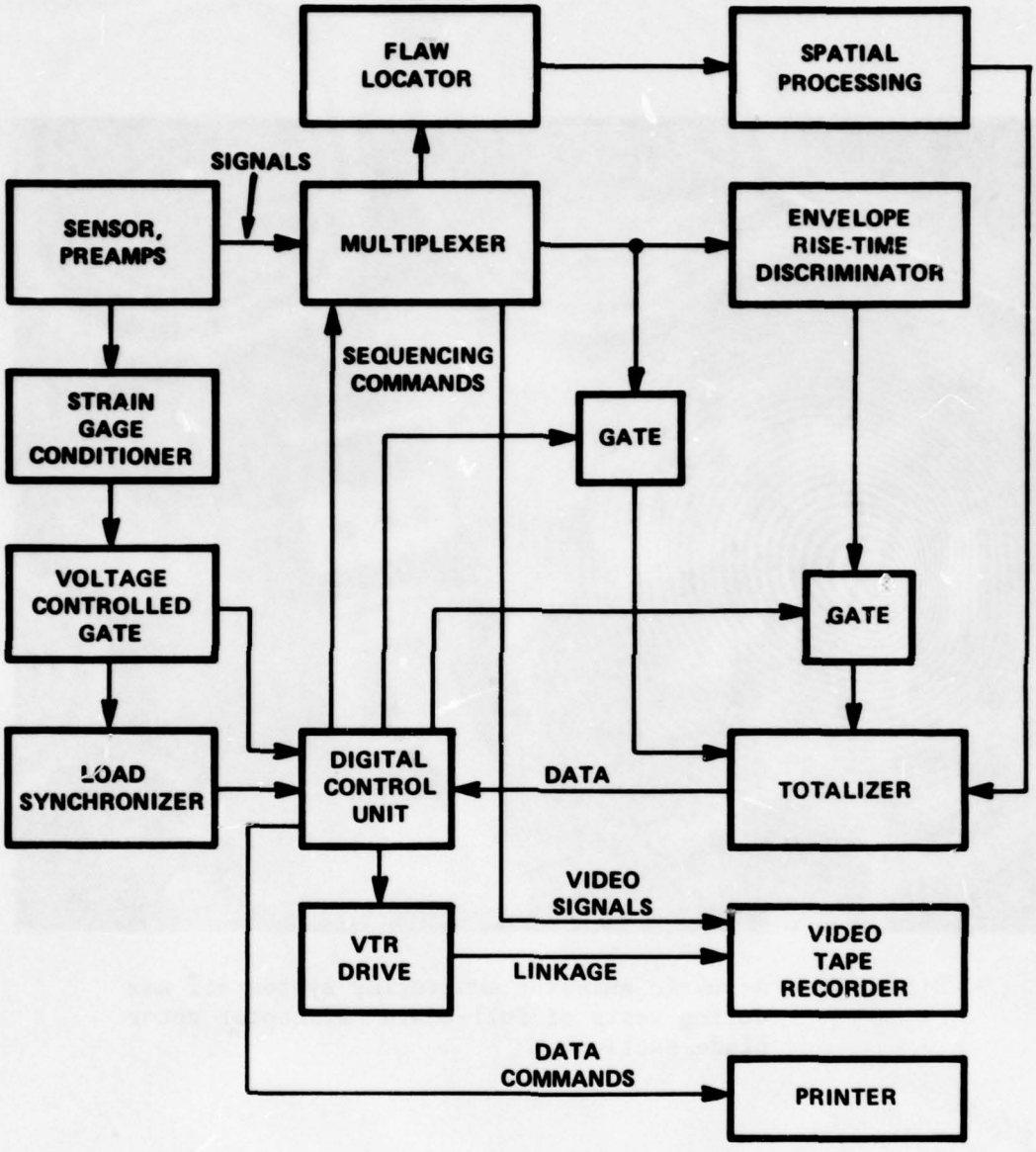


Figure 27 - Acoustic emission processing monitoring system.

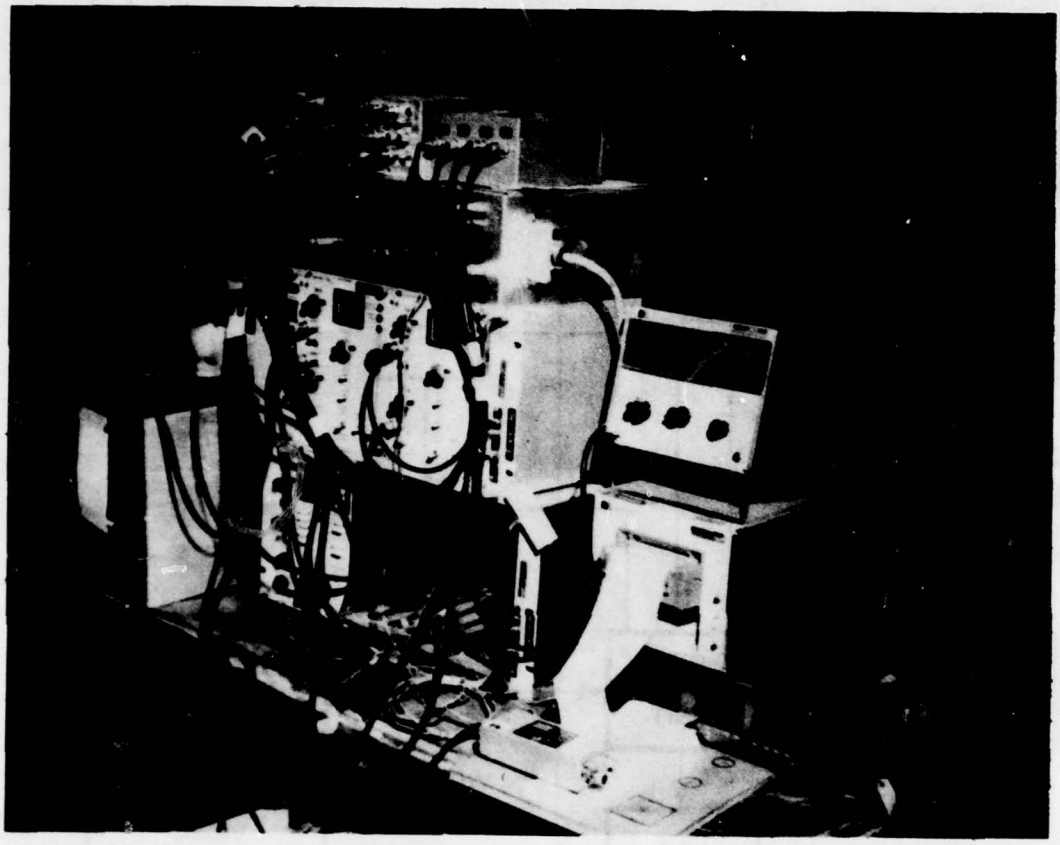

Figure 28 - Acoustic emission monitoring system for use during tests of full-scale helicopter rotor blade sections.

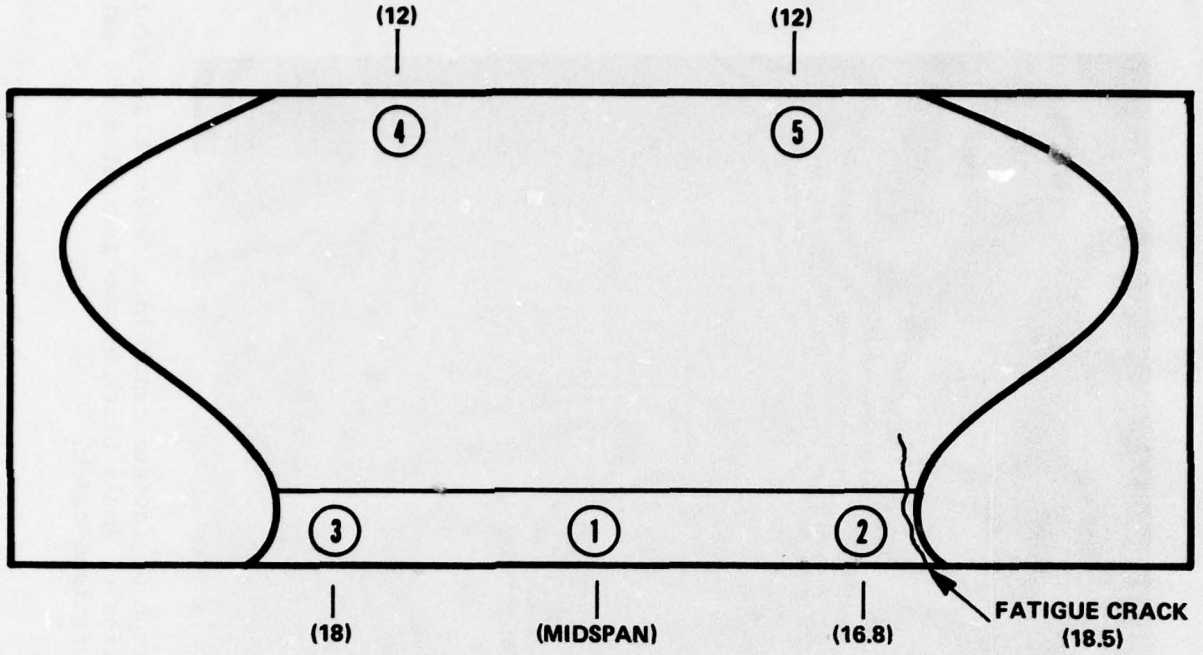


Figure 29 - Sketch showing location of fatigue crack in outboard blade section. Numbers in parentheses represent distance from blade midspan in inches. Numbers in circles identify transducer positions. Crack originated in spar and then progressed through upper side of blade.

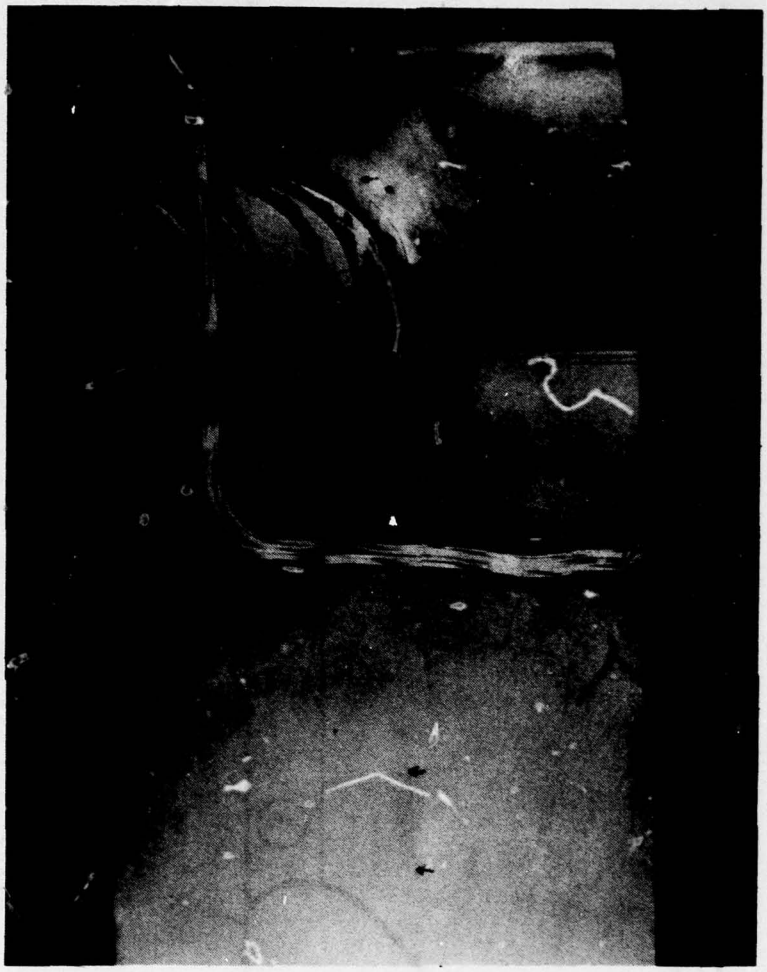

Figure 30 - Photograph of fatigue crack in outboard blade section. The series of small black arrows indicates the extent of the fatigue crack.

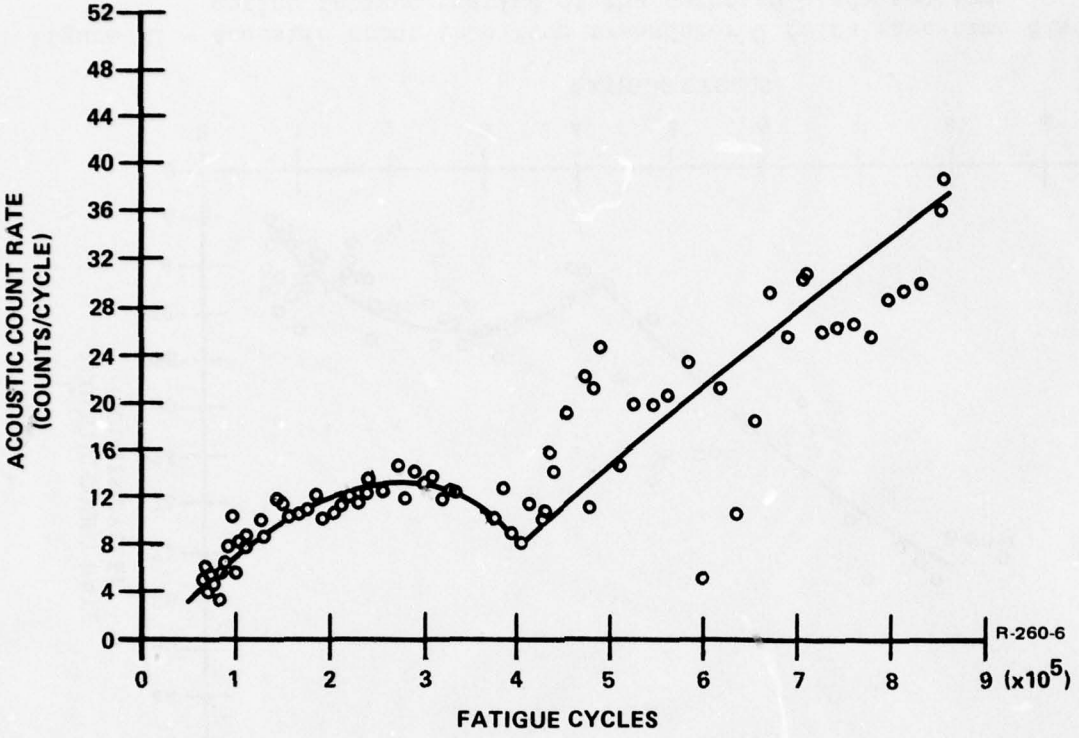


Figure 31 - Acoustic count rate from transducer 2 (with rise-time discrimination) during fatigue testing of the outboard blade section.

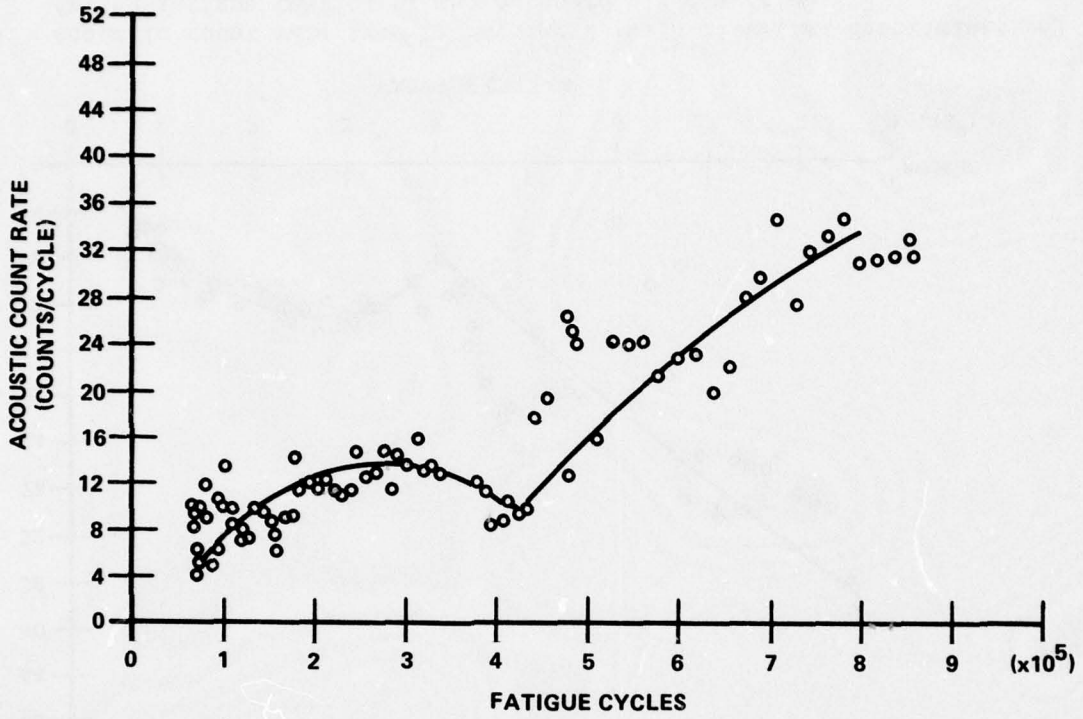


Figure 32 - Acoustic count rate from transducer 1 (with rise-time discrimination) during fatigue testing of the outboard blade section.

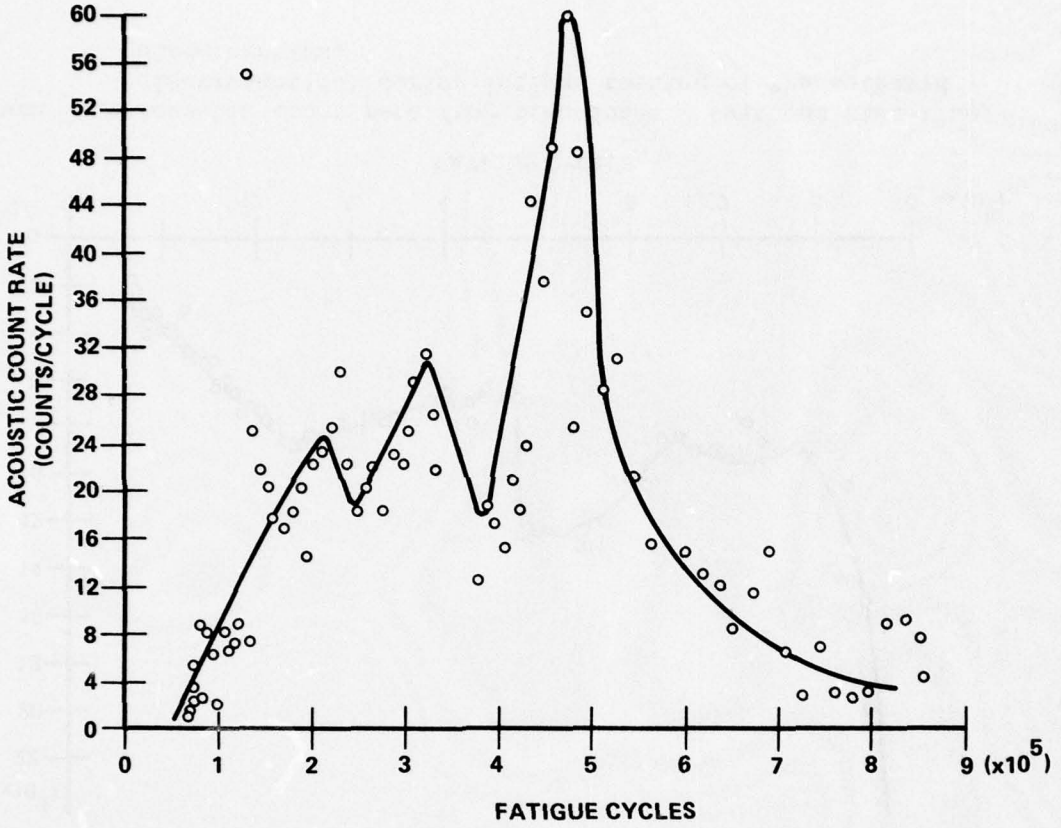


Figure 33 - Acoustic count rate from transducer 4 (with rise-time discrimination) during fatigue testing of the outboard blade section.

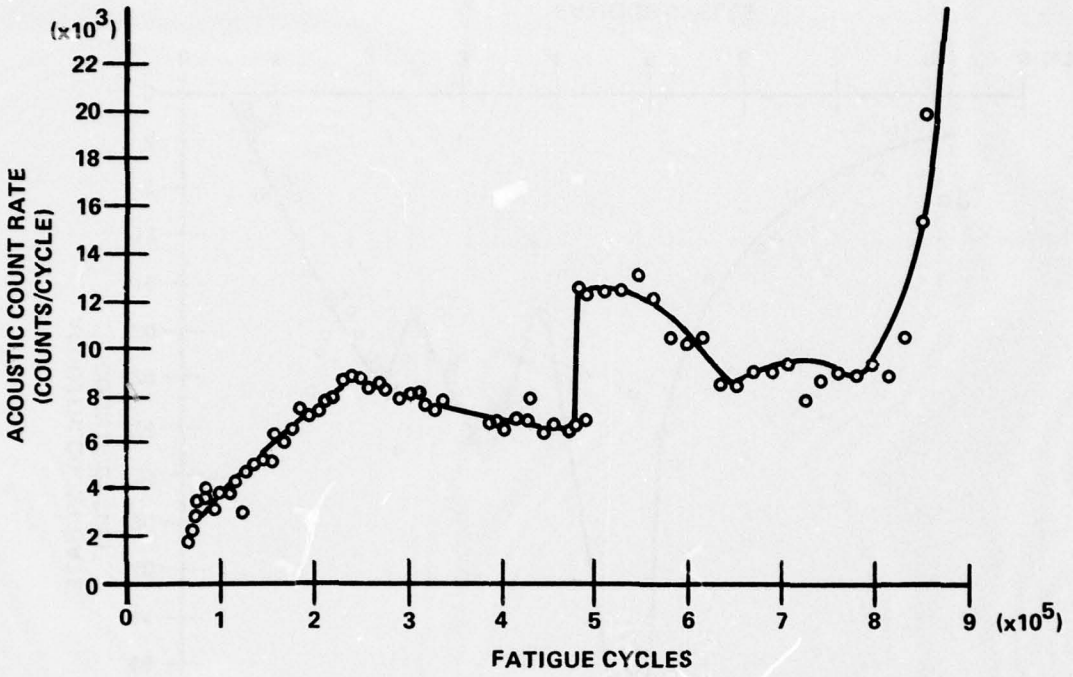


Figure 34 - Acoustic count rate from cransducer 2 (without rise-time discrimination) during fatigue testing of the outboard blade section.

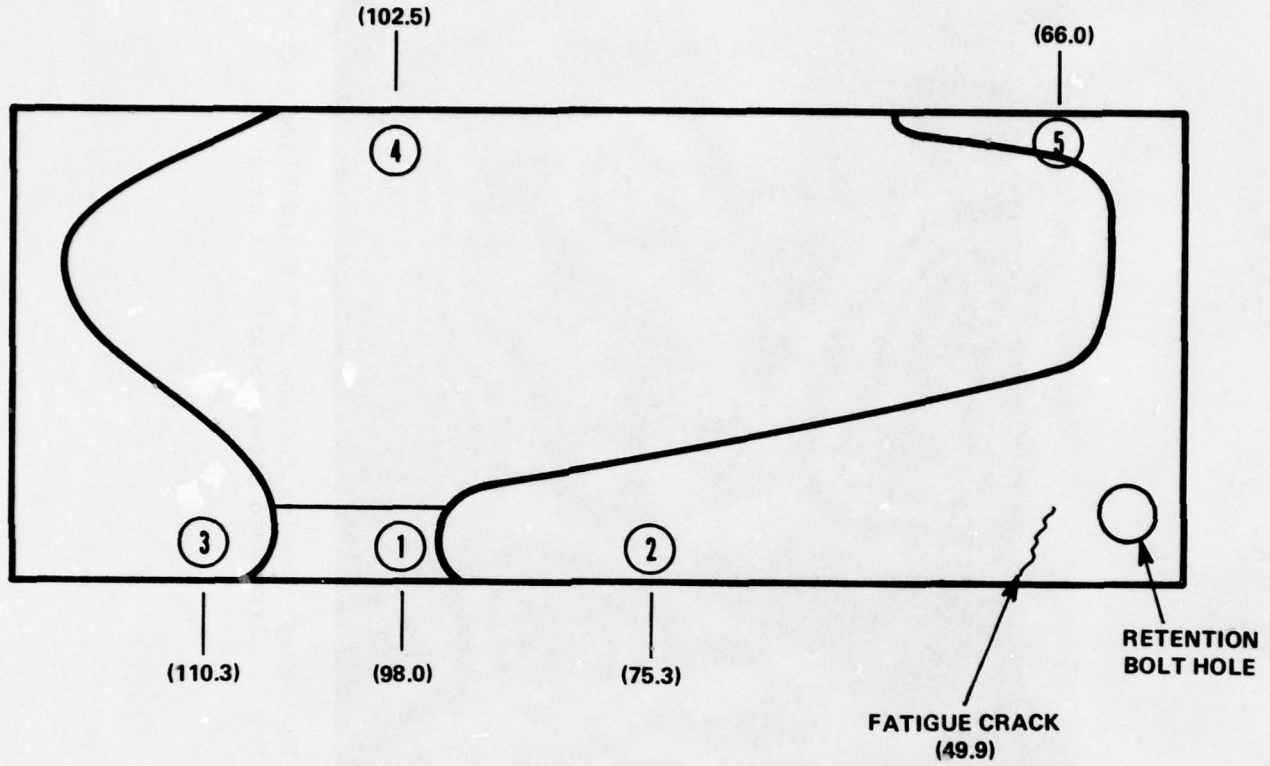


Figure 35 - Sketch showing location of fatigue crack in inboard blade section No. 1. Numbers in parentheses represent distance in inches from rotor system center. Numbers in circles indicate transducer positions. Sketch shows top view of blade; however, crack was located on underside of blade.

Figure 36 - Photograph showing failure in inboard blade section No. 1. Arrowhead shows location of origin.

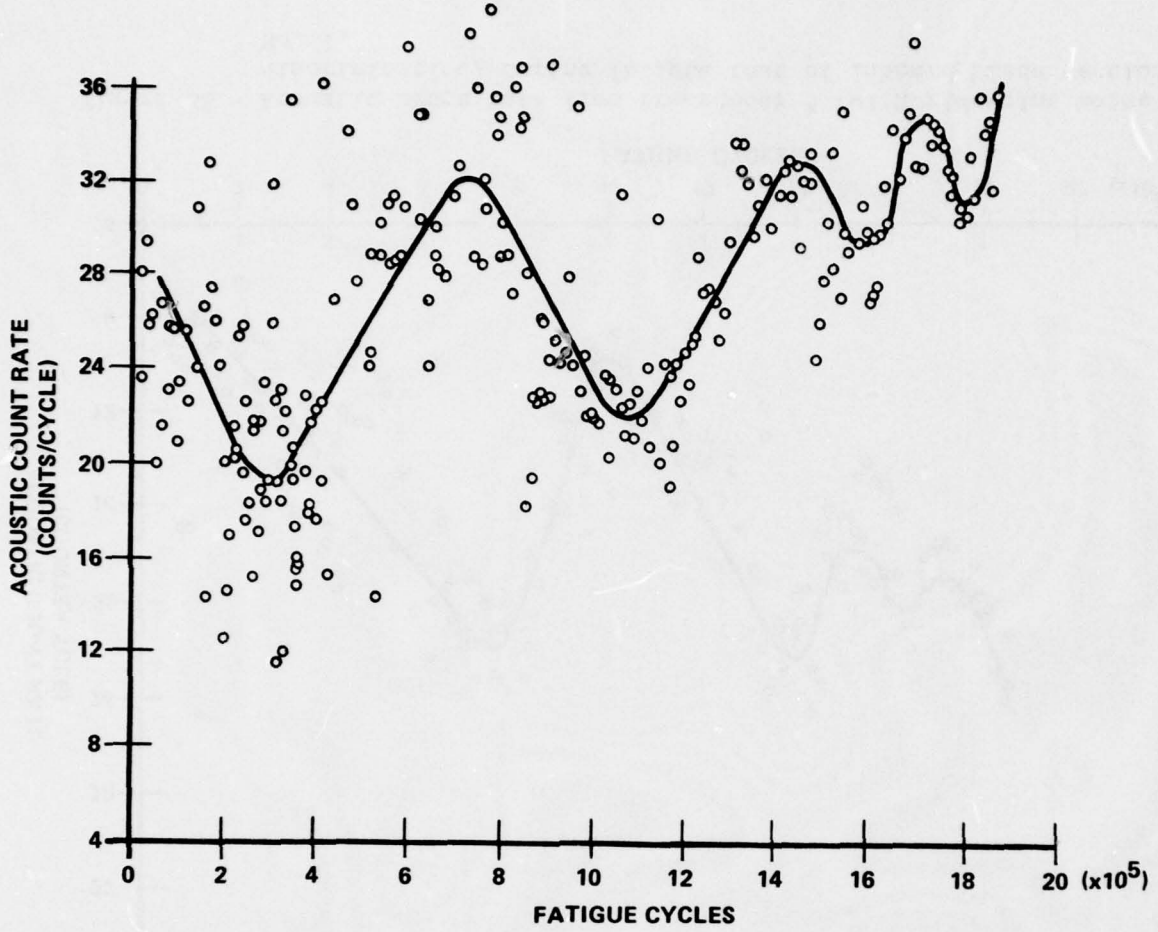


Figure 37 - Acoustic count rate from transducer 1 (with rise-time noise discrimination) during fatigue test of inboard blade section No. 1.

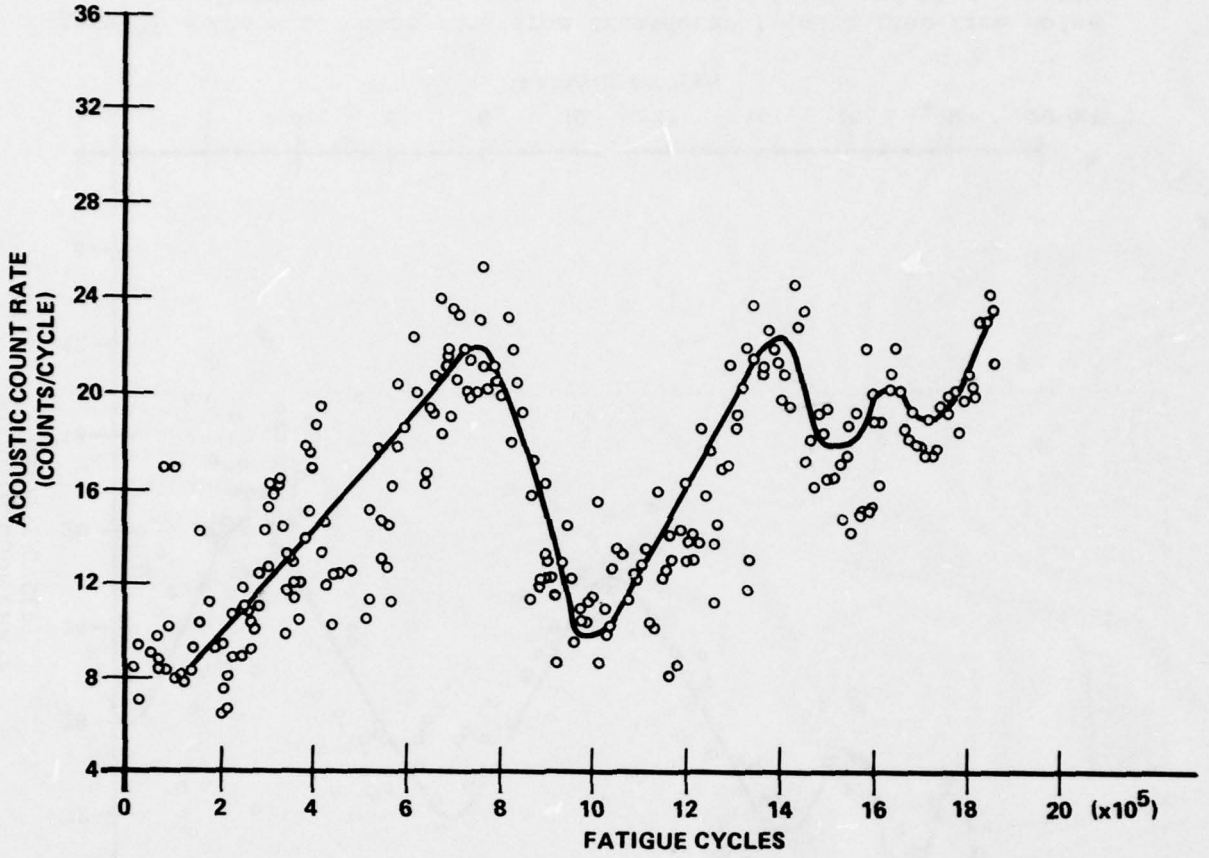


Figure 38 - Acoustic count rate from transducer 5 (with rise-time noise discrimination) during fatigue test of inboard blade section No. 1.

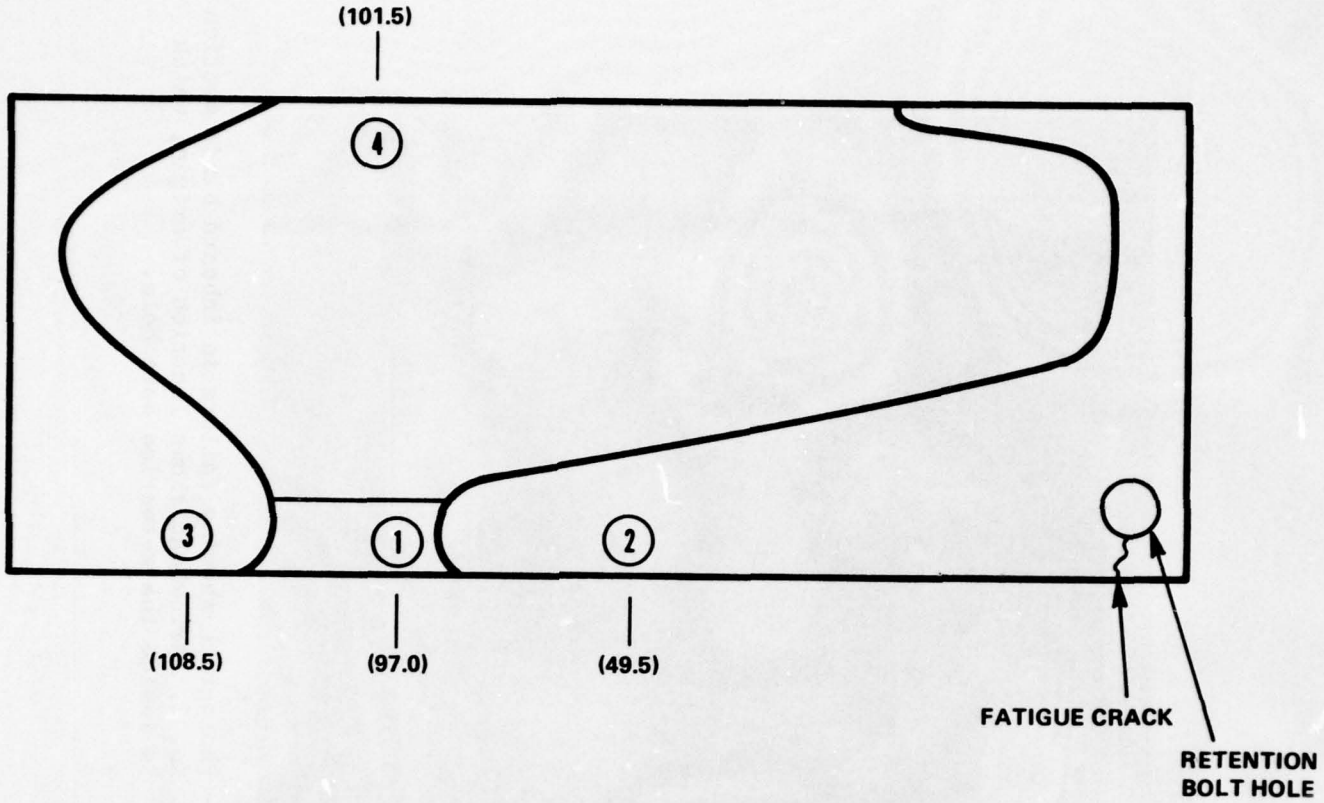


Figure 39 - Sketch showing location of fatigue crack in inboard blade section No. 2. Numbers in parentheses represent distance from rotor system center in inches. Numbers in circles indicate transducer positions. Sketch shows blade top view; however, crack was located on underside of blade.

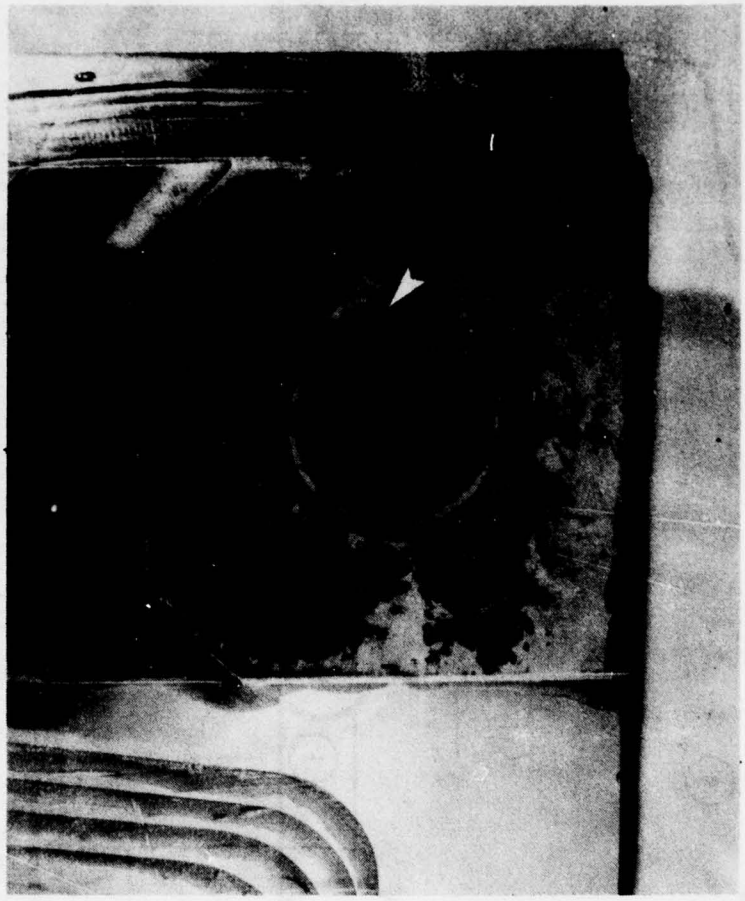

Figure 40 - Photograph showing failure in inboard blade section No. 2. Arrowhead shows location of origin, which is inside the retention bolt hole.

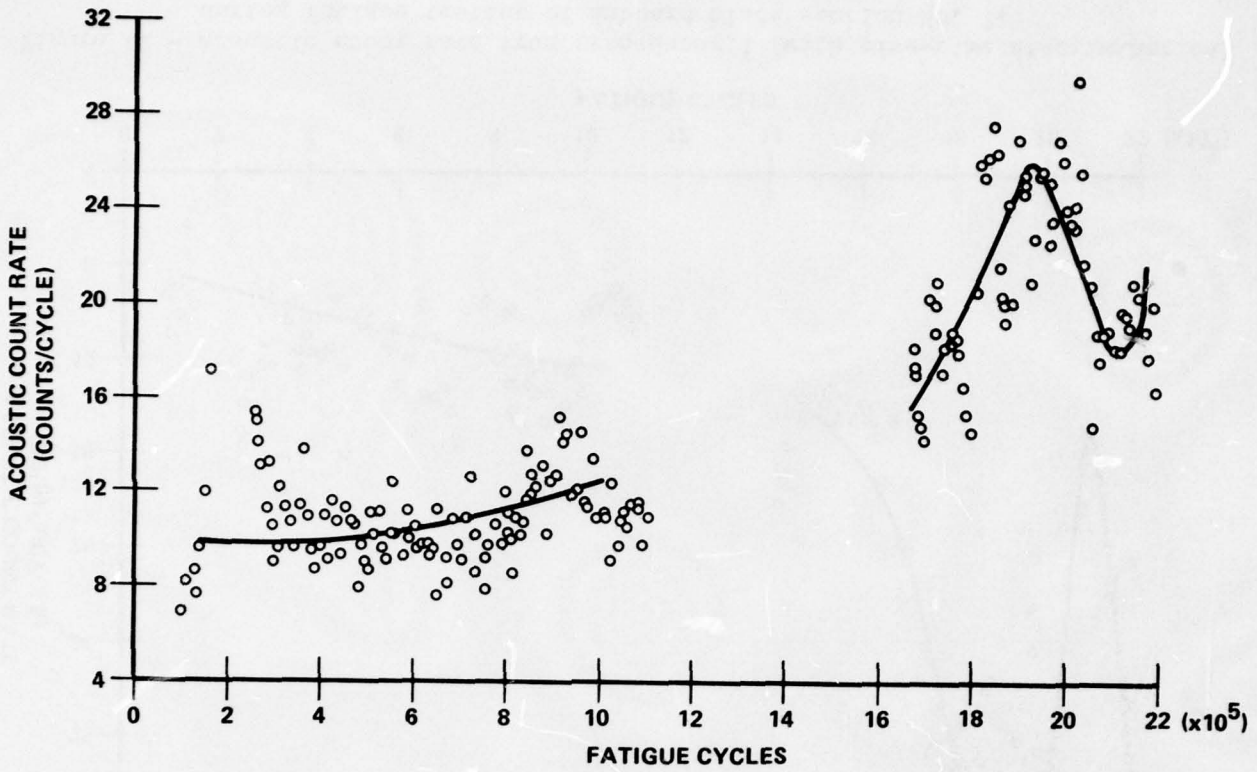


Figure 41 - Acoustic count rate from transducer 2 (with rise-time discrimination) during fatigue testing of inboard blade section No. 2.

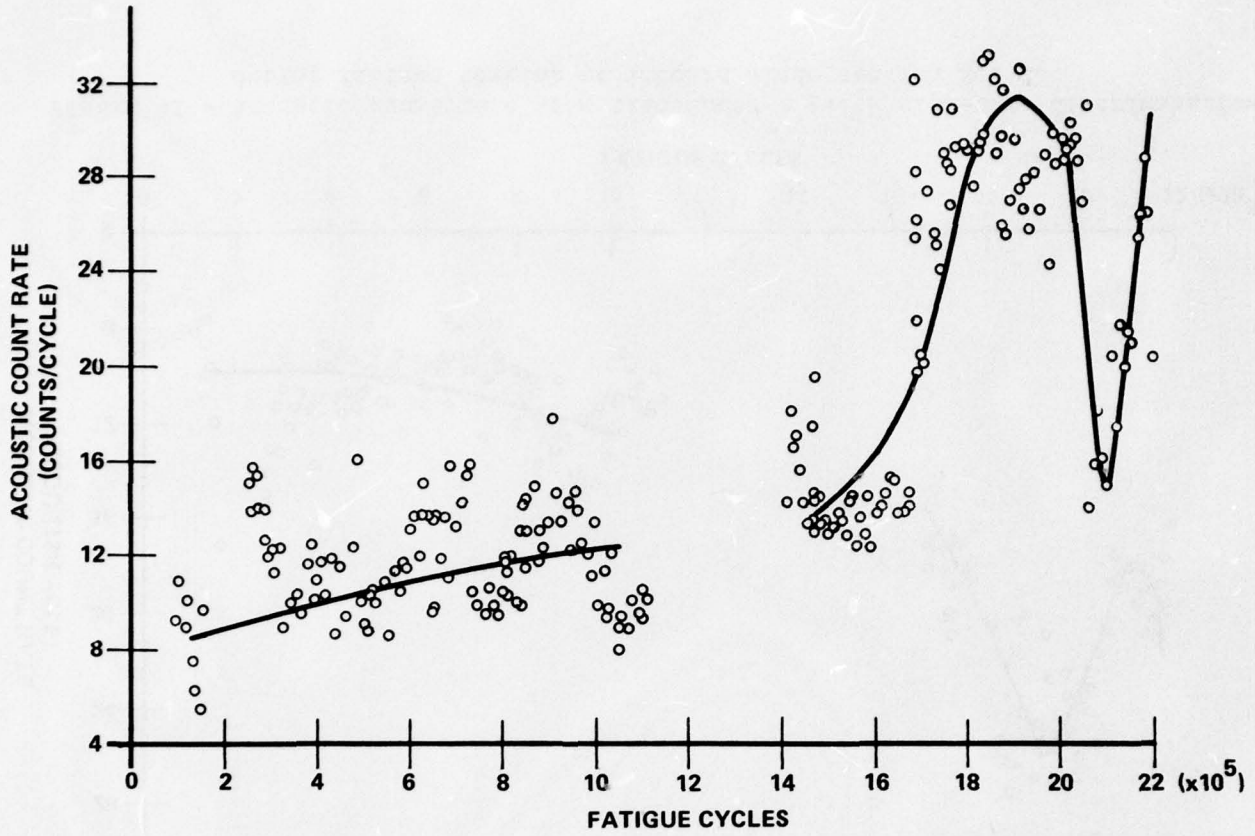


Figure 42 - Acoustic count rate from transducer 1 (with rise-time discrimination) during fatigue testing of inboard blade section No. 2.

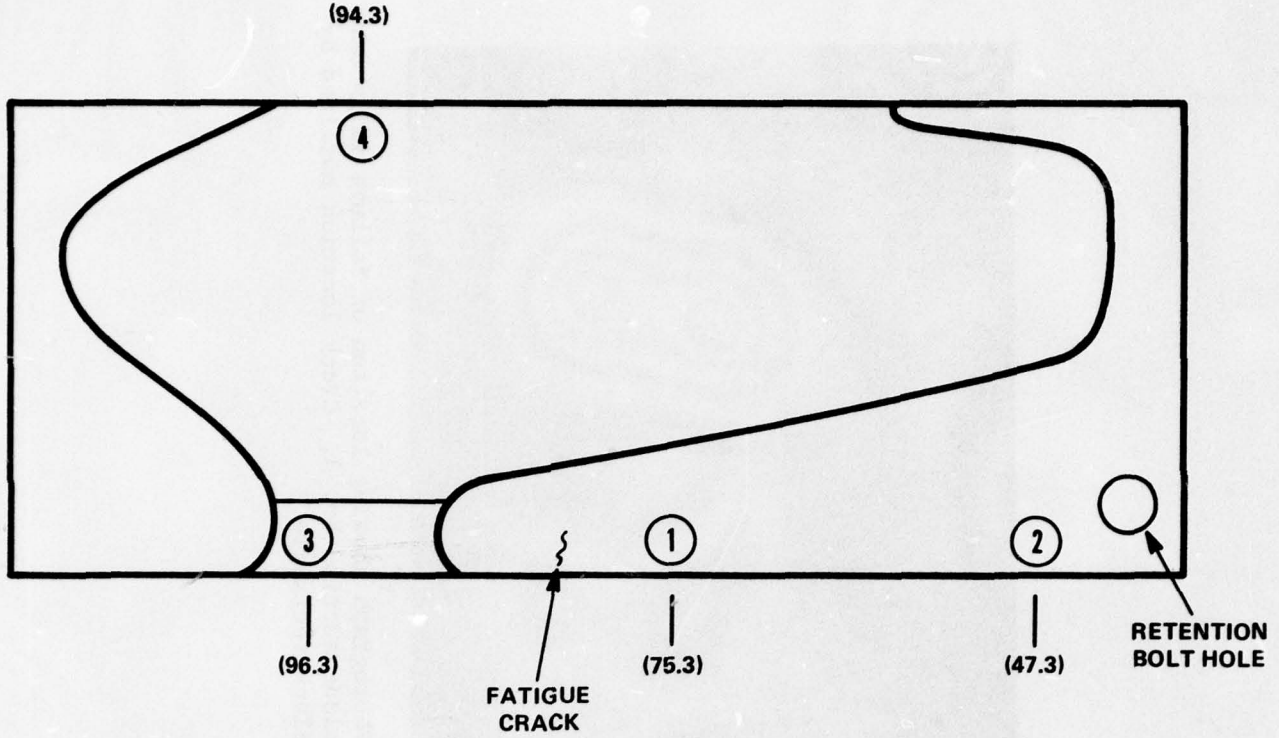


Figure 43 - Sketch showing location of fatigue crack in inboard blade section No. 3. Numbers in parentheses represent distance from rotor system center in inches. Numbers in circles indicate transducer positions. Sketch shows blade top view; however, crack was located on underside of blade.

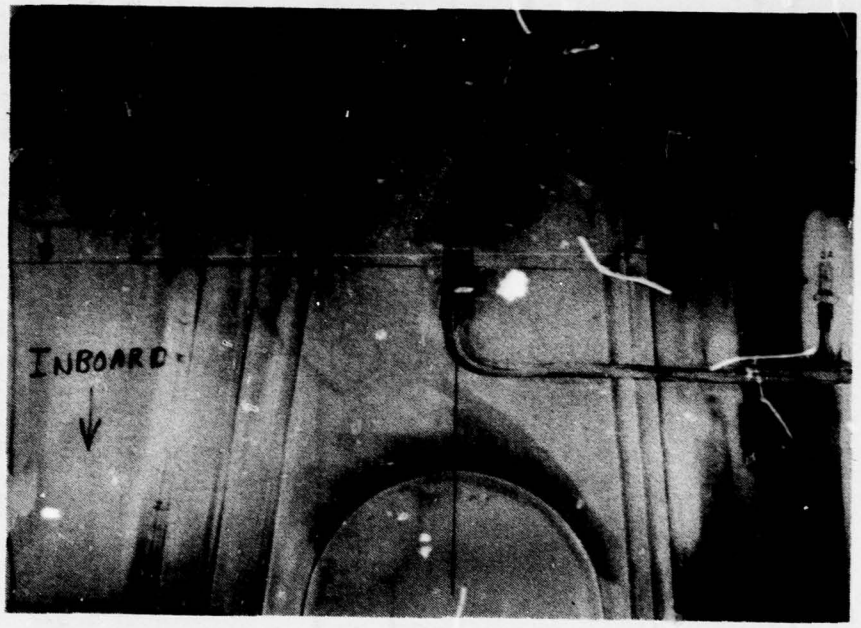


Figure 44 - Photograph showing location of failure in inboard blade section No. 3. Crack location outlined by black rectangle.

AD-A033 571 BENDIX RESEARCH LABS SOUTHFIELD MICH F/G 1/3
ACOUSTIC EMISSION INVESTIGATION - HELICOPTER ROTOR SYSTEM.(U)
NOV 76 R M RUSNAK, H C YEE, J K SEN DAAJ02-73-C-0066
UNCLASSIFIED RLD-7980 USAAMRDL-TR-76-11 NL

2 OF 2
AD A
033 571

END
DATE
FILMED
2-4-77
NTIS

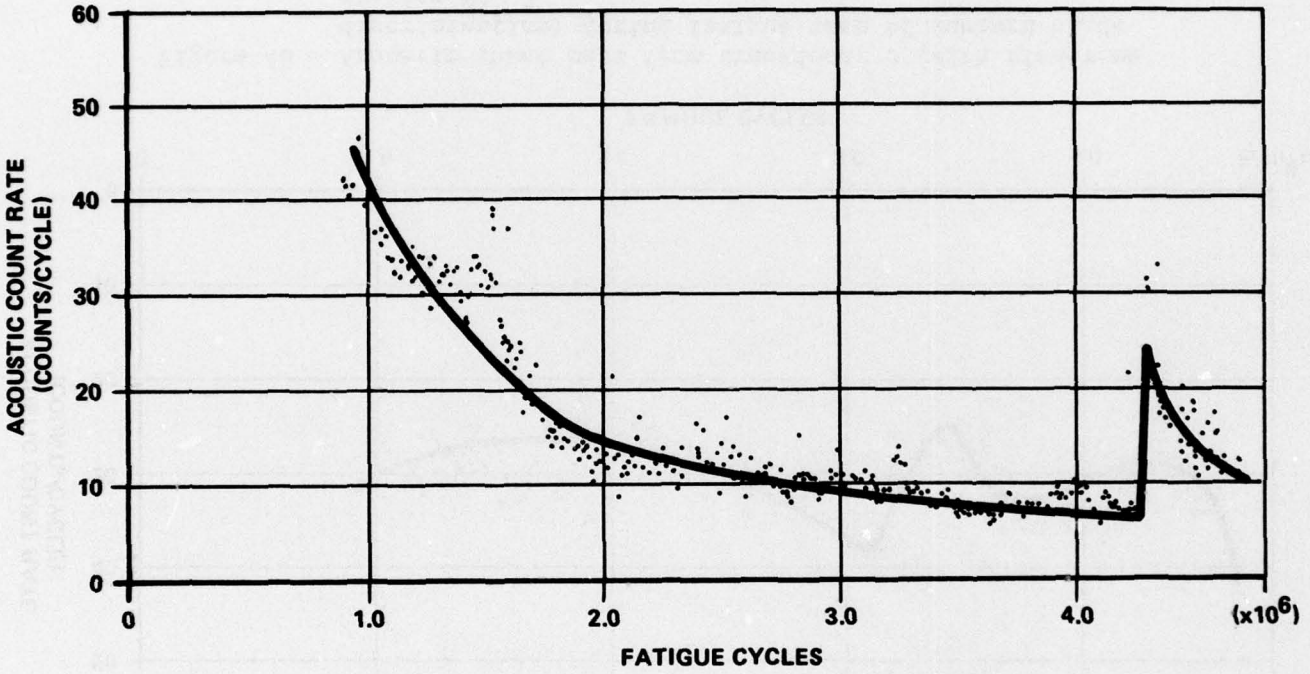


Figure 45 - Acoustic count rate from transducer 1 (with rise-time noise discrimination) during fatigue test of inboard blade section No. 3.

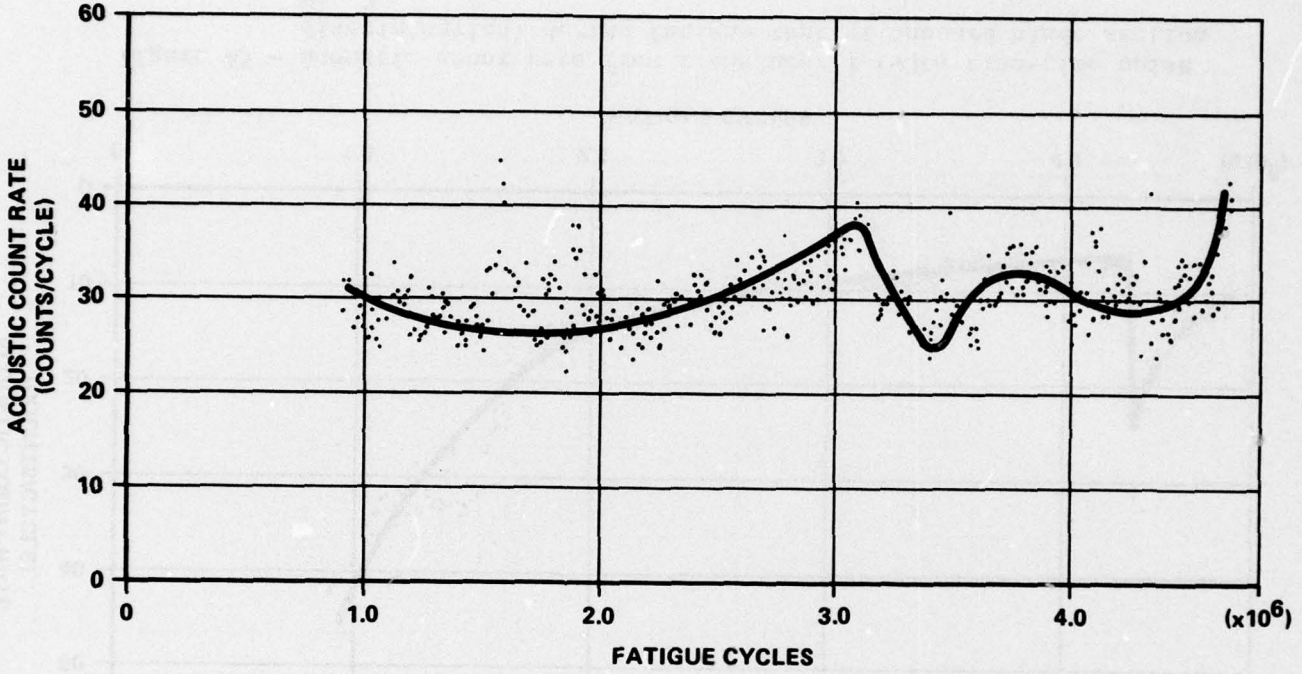


Figure 46 - Acoustic count rate from transducer 3 (with rise-time discrimination) during fatigue test of inboard blade section No. 3.

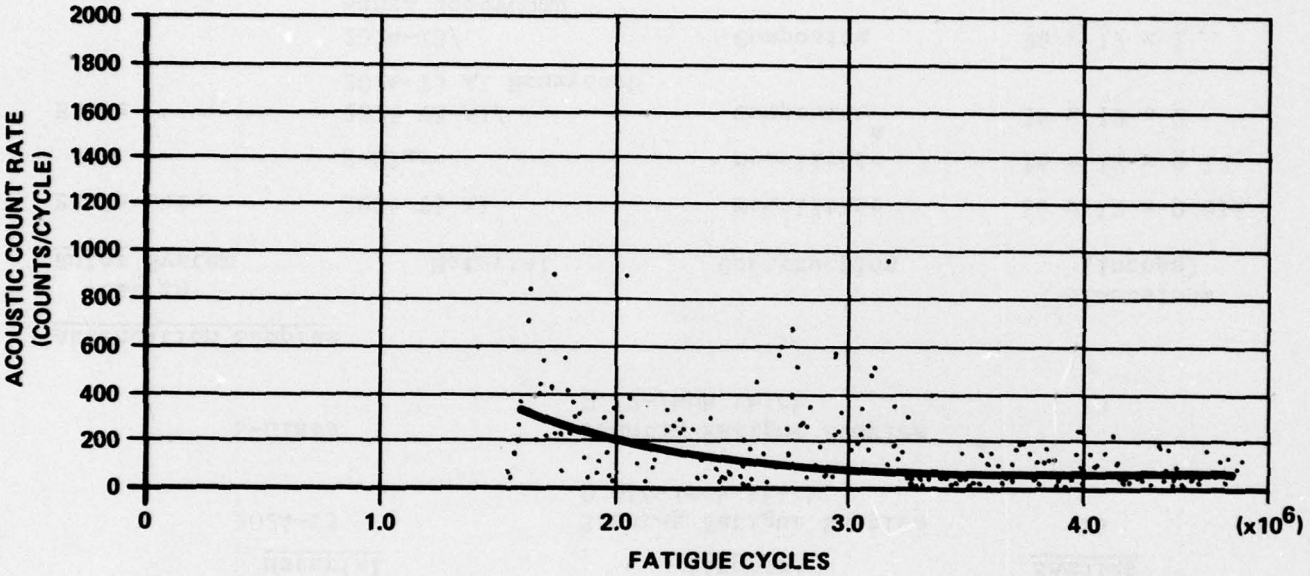


Figure 47 - Acoustic count rate from transducer 1 (with spatial gating noise discrimination) during fatigue test of inboard blade section No. 3.

TABLE 1

Fatigue and Attenuation Samples

**Fatigure Emission Samples (Skin Materials)**

| Material | Dimensions (inches) | No. of Samples |
|---|---|---|
| 2024-T3 | Sonntag Fatigue Samples 0.016-inch thick | 15 |
| S-Glass | Sonntag Fatigue Samples 0.12-inch thick | 15 |

**Attenuation Samples**

| Use in Rotor System | Material | Construction | Dimensions (inches) | No. of Samples |
|---|---|---|---|---|
| Blade Skin | 2024-T3 Al | Monolithic | 36 x 12 x 0.016 | 2 |
| | S-Glass | Monolithic | 36 x 12 x 0.12 | 2 |
| Blade | 2024-T3 Al/ 2024-T3 Al Honeycomb | Composite* | 36 x 12 x 2 | 2 |
| | 2024-T3/ Nomex Honeycomb | Composite | 36 x 12 x 1 | 2 |
| | S-Glass/ 2024-T3 Al Honeycomb | Composite | 36 x 12 x 1 | 2 |
| Grip | 7075-T73 Al | Monolithic | 36 x 12 x 3.0<br>36 x 12 x 0.75 | 1<br>1 |

* 1 sample with spar 1 inch from edge and 1 without spar.

TABLE 2

Conditions for Fatigue Testing of Full-Scale Rotor Blade Samples

| Blade Section | Percent of Level Flight Load | Cycles to Failure | Noise Discrimination Processing | Total Acoustic Emission System Gain (db) |
|---|---|---|---|---|
| Outboard (A2-00013) | 229 | 853,500 | Spatial Discrimination Rise-Time Discrimination (5 volts/millisec) | 90 |
| Inboard No. 1 (A2-00002) | 150 | 1,867,700 | Spatial Discrimination Rise-Time Discrimination (5 volts/millisec) | 90 |
| Inboard No. 2 (A2-00008) | 175 | 2,192,500 | Spatial Discrimination Rise-Time Distrimination (5 volts/millisec) | 86 |
| Inboard No. 3 (A2-00013) | 175 | 4,698,000 | Spatial Discrimination Rise-Time Discrimination (5 volts/millisec) | 86 |

TABLE 3

Summary of Acoustic Emission Signal Strength From
2024-T3 Aluminum and S-Glass Fatigue Samples

| 2024-T3 Aluminum | | S-Glass Epoxy Composite | |
|---|---|---|---|
| Maximum Stress in Reverse Bending (KSI) | Signal/Noise* | Maximum Stress in Reverse Bending (KSI) | Signal/Noise* |
| 30 | 10 | 15 | 3.1 |
| 40 | 10 | 20 | 6.5 |
| 45 | 19 | 25 | 13 |
| 50 | 7.5 | 28 | 6.0 |

*Noise reference is the electronic noise which exists in the acoustic emission instrumentation.

TABLE 4

Summary of Results, Rotor Sample Attenuation Measurements

| Sample | Attenuation at 1 Foot from Source (% of Source Location Signal Strength) | | | | Distance at Which Signal is 10% of Source Location Value (in.) | | | |
|---|---|---|---|---|---|---|---|---|
| | 110 kHz | 150 kHz | 240 kHz | 750 kHz | 110 kHz | 150 kHz | 240 kHz | 750 kHz |
| Al/Al Honeycomb | 3 | 2 | 1 | — | 7.8 | 5.2 | 3.7 | 1.6 |
| Al/Nomex Honeycomb | 3 | 2 | 1 | — | 5.0 | 4.2 | 2.8 | 1.5 |
| Al Sheet (2024-T3 0.016 in. thick) | 50 | 50 | 25 | 12 | >30.0 | >30.0 | >30.0 | >30.0 |
| S-Glass/Al Honeycomb | 8 | 3 | 8 | — | 8.3 | 7.3 | 11.7 | 2.0 |
| S-Glass Sheet (0.125 in. thick) | 10 | 8 | 18 | 1 | 12.0 | 9.3 | 20.0 | 5.3 |
| 7075-T73 Al | | | | | | | | |
| 36 x 12 x 0.75 | 30 | 35 | 48 | 14 | >34.0 | >34.0 | >34.0 | >34.0 |
| 36 x 12 x 3.0 | 42 | 36 | 40 | 20 | >34.0 | >34.0 | >34.0 | >34.0 |

Table 5

Attenuation in Rotor System Attachment Hardware

(Signal Frequency - 150 kHz)

| Hardware | Transducer Position | | Attenuation Factor* |
|---|---|---|---|
| | Transmitting | Receiving | |
| Blade/Grip Interface | 1 | 2 | 0.13 |
| Across Grip | 2 | 3 | 0.22 |
| Grip/Yoke | 3 | 4 | 0.11 |
| Across Yoke | 4 | 5 | 0.70 |
| Blade/Drag Brace Interface | 6 | 7 | 0.23 |
| Across Drag Brace | 7 | 8 | 0.06 |
| Drag Brace/Grip Interface | 8 | 9 | 0.50 |

*Ratio of detected signal amplitude to transmitted signal amplitude.

TABLE 6

Acoustic Emission Monitoring System Components

| Component | Identification | Function |
|---|---|---|
| Transducers | Dunegan D140B type | Detect acoustic signal |
| Preamplifiers | Dunegan 801P | Primary amplification of the acoustic signal |
| Digital Control Unit | Designed and built by Bendix Research Laboratories | Controls operating sequence timing and data transfer |
| Multiplexer | Designed and built by Bendix Research Laboratories | Steers system signals to appropriate processing; elements include electronic gates |
| Load Synchronizer | Designed and built by Bendix Research Laboratories | Synchronizes the operating sequences of the digital control unit to the stress cycle |
| Video Tape Recorder Drive | Designed and built by Bendix Research Laboratories | Provides electromechanical interface to operate video tape recorder |
| Voltage-Controlled Gate | Dunegan/Endivco Model 906A | Inhibits processing in selected parts of the stress cycle |
| Spatial Gating | Signal processor designed and built by Bendix Research Laboratories incorporated with two Dunegan Model 902 flaw locators | Inhibits processing of acoustic signals which originate outside selected region |
| Envelope Rise-Time Discriminator | Designed and built by Bendix Research Laboratories | Measures rise time of envelope of acoustic pulse and rejects signals having rise time less than selected value |
| Totalizer | Dunegan Model 301 (BRL modifications) | Counts oscillations of acoustic signal which exceed one volt threshold. Includes gain and bandwidth control. |
| Video Tape Recorder | Sony Video recorder, AV-3650 | Records acoustic signals on magnetic tape |
| Printer | Hewlett-Packard Digital Recorder Model 5055A | Prints acoustic counts and operational data |

TABLE 7

Transducer Location During Fatigue Testing of Full-Scale Helicopter Rotor Blade Sections

| | Transducer No. | From Midspan: Distance | Direction | Distance from Trailing Edge (Inch) | Remarks |
|---|---|---|---|---|---|
| Outboard | 1 | At Midspan | | 27.25 | --- |
| | 2 | 16.75 | Inboard | 26.75 | --- |
| | 3 | 18.0 | Outboard | 26.75 | --- |
| | 4 | 12 | Outboard | 1.50 | --- |
| | 5 | 12 | Inboard | 1.50 | --- |
| | 6 | -- | --- | -- | Dummy |

| | Transducer No. | Blade Station | Distance from Trailing Edge (Inch) | Remarks |
|---|---|---|---|---|
| Inboard No. 1 | 1 | 98.0 | 27 | --- |
| | 2 | 75.25 | 27 | No output |
| | 3 | 110.25 | 27 | --- |
| | 4 | 102.5 | 2 | ----- |
| | 5 | 66.0 | 2 | --- |
| | 6 | -- | -- | Dummy |

| | Transducer No. | Blade Station | Distance from Trailing Edge (Inch) | Remarks |
|---|---|---|---|---|
| Inboard No. 2 | 1 | 97.0 | 27 | --- |
| | 2 | 49.5 | 24.75 | --- |
| | 3 | 108.5 | 27 | No output |
| | 4 | 101.5 | 2.75 | --- |
| | 5 | -- | -- | Dummy |

| | Transducer No. | Blade Station | Distance from Trailing Edge (Inch) | Remarks |
|---|---|---|---|---|
| Inboard No. 3 | 1 | 75.25 | 26.5 | --- |
| | 2 | 47.25 | 24.0 | --- |
| | 3 | 96.25 | 27.0 | --- |
| | 4 | 94.25 | 1.5 | --- |

TABLE 8

Summary of Blade Section Tests

| Test Period | Blade Section | % of Normal Level Flight Load | Comment |
|---|---|---|---|
| March-April, 1974 | Outboard | 200 | Test was carried out to define noise environment. Sample did not fail. |
| June-July, 1974 | Outboard | 240 | Test was carried out to monitor noise and check out some of acoustic emission system components. Complete acoustic emission system was not available for this test. Sample did not fail under original test load. Additional tests were run at very high load (300% of normal level flight). Noise discrimination modules were not available for this test, so no meaningful results were obtained. |
| Sept.-Oct., 1974 | Inboard | 200 | Sample failed after only 315,000 cycles. Difficulties were experienced in coupling the acoustic emission system to fatigue test; therefore, no test results were obtained. |
| Oct.-Dec., 1974 | Inboard | 180 | Sample testing was delayed because of grip and machine failures. Sample failed after 800,000 cycles near retention bolt so that noise discrimination based on spatial gating was not effective because transducers could not be placed to discriminate in this region. No indication of impending failure was obtained from the acoustic emission monitoring. It was concluded that rise-time discrimination was not effective because it was set at too high a value, which rejected emissions from cracks as well as extraneous noise. Therefore, in following tests the value was changed from 10 to 5 volts/millisec for rise-time discrimination. |

TABLE 8

Summary of Blade Section Tests (Cont'd.)

| Test Period | Blade Section | % of Normal Level Flight Load | Comment |
|---|---|---|---|
| Dec., 1974 | Outboard | 300 | Sample failed at very low number of cycles, 265,000. Acoustic emission monitoring was not initiated until sample was within 10,000 cycles of failure. The delay in implementing the acoustic emission system was caused by difficulties in getting a good synchronizing signal from the fatigue machine. Consequently, no meaningful data were obtained. |
| Jan-June, 1975 | Inboard | 150 | Numerous failures of test machine components and grips prolonged the testing of this blade section. Failure was experienced after 1.87-million cycles and acoustic emission monitoring did give indications of impending failure. The fatigue crack formed on the bottom surface of the blade at the edge of the grip plate and propagated about 5 inches toward the trailing edge. The results of this test are given in detail in this report as inboard blade section test No. 1. Rise-time discrimination was effective but not spatial gating because of the location of the crack. |

TABLE 8

Summary of Blade Section Tests (Concluded)

| Test Period | Blade Section | % of Normal Level Flight Load | Comment |
|---|---|---|---|
| May, 1975 | Outboard | 230 | Sample failed after 850,000 cycles. Rise-time processing yielded acoustic emission curves which gave indication of impending failure. Spatial gating was not effective because of crack location. The crack originated in the spar about 19 inches inboard of midspan. It then progressed through the upper blade skin, the spar, and the leading edge abrasion strip. Detailed results of this test are presented in this report as the outboard test. |
| June-Aug., 1975 | Inboard | 175 | Sample failed after 2.2-million cycles. Acoustic emission system gave indications of impending failure. The crack originated on the grip plate at the retention bolt hole and progressed to the leading edge and through the spar. Detailed results of this test are reported as inboard test No. 2 in this report. |
| Sept.-Dec., 1975 | Inboard | 175 | Sample failed after 4.7-million cycles. Acoustic emission data gave no indication of impending failure either with spatial gating or rise-time noise discrimination. The failure consisted of a crack about 3.5 inches long which was confined mainly to the abrasion strip of the blade. The fact that the crack was somewhat smaller than those formed in preceding tests or that it was located in a non-load-bearing region of the blade may be the reason for lack of detection. Detailed results of this test are reported as inboard test No. 3 in this report. |